TIME AND LENGTH DEPENDENT AIRWAY SMOOTH

MUSCLE MECHANICAL PROPERTIES

A THESIS

SUBMITTED TO THE FACULTY OF GRADUATE STUDIES

UNIVERSITY OF MANITOBA

IN PARTIAL FULFILLMENT OF THE REQUIREMENTS

FOR THE DEGREE OF

DOCTOR OF PHILOSOPHY

By

©   Chun   Y.   Seow

DEPARTMENT OF PHYSIOLOGY

UNIVERSITY OF MANITOBA

WINNIPEG, MB. CANADA

JANUARY, 1989

Canada

TIME AND LENGTH DEPENDENT AIRWAY SMOOTH
MUSCLE MECHANICAL PROPERTIES

BY

CHUN Y. SEOW

A thesis submitted to the Faculty of Graduate Studies of
the University of Manitoba in partial fulfillment of the requirements
of the degree of

DOCTOR OF PHILOSOPHY

©   **1989**

ABSTRACT

The series of experiments described in this thesis were aimed at elucidating the mechanisms underlying some of the phenomena observed in smooth muscle contraction. Emphasis was placed on characterizing smooth muscle stiffness, maximum shortening velocity, force-velocity relations and internal "viscous" force as functions of muscle length and contraction time. Supramaximal electrical stimulation was used to elicit contraction. Muscle stiffness was measured using both force-perturbation and load-clamping methods; maximum velocity was obtained using the method of zero-load clamp or extrapolating from force-velocity (F-V) data obtained using quick-release technique. The major findings and conclusions from the experiments were: a) Maximum force extrapolated from the F-V data [$P_o(t)$] was greater than the directly measured isometric force [$P_o'(t)$] during contraction, however, $P_o(t)$ was less than $P_o'(t)$ during relaxation, and the two were equal at the plateau of contraction. The observation can be explained in terms of negatively strained crossbridges or/and viscous element in parallel with the contractile element. b) Hill's constants a and b were in fact functions of time. Analysis suggested that a/b was an index of internal resistance that reduced shortening velocity of unloaded muscle, and it was found to increase progressively during contraction. c) There was a transient increase in stiffness of the series elastic component (SEC) of muscle during contraction, and it

coincided with the transient increase in zero-load velocity. This suggested that the transient myosin phosphorylation not only increased the cycling rate of the crossbridges, but also the number of attached bridges. d) The maximum shortening velocity of muscle at optimum muscle length varied with time, but the minimum length at which velocity diminished to zero was time independent, suggesting that the amount of shortening probably was determined by some noncontractile component of the muscle. e) Stiffness of the SEC increased as muscle length decreased. This increase was inversely proportional to the SEC length itself, suggesting that the series elasticity of smooth muscle may stem from the non-overlap portion of the thick and thin filaments.

ACKNOWLEDGEMENTS

TABLE OF CONTENTS

INTRODUCTION

Many aspects of our understanding of smooth muscle contraction has been derived from our knowledge about striated muscle contraction. The presence of a highly organized repeating sarcomeric pattern in striated muscle has greatly facilitated our understanding of the mechanism of muscle contraction. Without it, the formulation of the filament-sliding, crossbridge-cycling model of muscle contraction (H. E. Huxley and Hanson, 1954; A. F. Huxley, 1957) would require much more imagination. Studies of smooth muscle mechanics have never enjoyed the credibility of striated muscle studies because of the absence of a well-defined repeating sarcomeric pattern, despite the fact that respectable mechanical data can be obtained from it. In recent years, however, evidence has begun to accumulate to suggest that if tissue preparation and fixation are carried out under appropriate conditions, thick filaments can be seen in large numbers and appear highly organized in smooth muscle (Somlyo et al, 1973). Electron microscopy of portal vein smooth muscle cell by Somlyo et al (1984) showed clearly that the crossbridges originating from the thick filaments attached to the thin filaments. Light microscopic pictures of smooth muscle cells treated with antimyosin fluorescent antibodies (Groschel-Stewart et al, 1975) revealed a very striking cross-striation pattern similar to that observed in striated muscle, indicating that sarcomeres probably exist in smooth muscle. Cooke et al (1986) were

able to resolve skinned amphibian smooth muscle cells as fibrils containing F-actin and myosin filaments and adjacent cytoplasmic dense bodies, containing α-actinin and actin. By electron microscopy, they showed that the fibrils were linked axially through actin filaments to the dense bodies, structures thought to be equivalent to the Z-discs in striated muscle. The arrangement of these two structures provided the essential features of a sarcomere to the contractile elements. They also found that during contraction the axial movements of dense bodies were uniform, and the dense bodies were not simply displaced passively during contraction because the extent of radial movements was less than would be expected for the observed increase in cell diameter. The ultrastructural evidence helps to explain the qualitative similarities in mechanical properties, such as length-tension and force-velocity relations, observed in both smooth and striated muscles. The more direct evidence for the existence of functional crossbridges, however, came from studies on tension transients initiated by photolysis of caged ATP in portal vein smooth muscle by Somlyo et al (1987). They showed that the mechanical transients accompanying the actomyosin crossbridge cycle present in striated muscle (Goldman et al, 1982) were also present in smooth muscle.

Most of the studies on smooth muscle mechanics were done on multicellular preparations. There are few studies in which single cell preparations were used (Warshaw and Fay,

1983; Warshaw et al, 1987). Findings in single cell studies are mostly comfirmatory to the findings in multicellular preparations. However, single smooth muscle cell does possess some unique mechanical features. For instance, the series elasticity in single taod stomach smooth muscle cell seems to reside mostly in the crossbridges (Warshaw and Fay, 1983), where as in multicellular smooth muscle preparations a significant portion of the series elasticity is extracellular, and may represent the elasicity of the connective tissue matrix external to the muscle cell (Mulvany and Warshaw, 1981; Hellstrand and Johansson, 1979; Meiss, 1979). Despite the short comings associated with the multicellular preparations, careful analysis of their mechanical behavior still permits us to interpret the experimental observations in terms of the activities of the contractile aparatus, specifically, the crossbridges (Hellstrand and Johansson, 1979; Uvelius, 1979; Meiss, 1978; Meiss, 1982; Cox, 1978; Dillon et al, 1981; Herlihy and Murphy, 1974; Johansson, 1973; Kamm and Stull, 1986; Siegman et al, 1976; Gunst, 1986).

The above dicussion is necessary for establishing the validity of describing smooth muscle contraction in the light of striated muscle and the model of sliding filament and cycling crossbridge. To help us understand better the results and discussions presented in this thesis, some of the contraction theories are described in the following sections.

I. Striated Muscle Contraction Models

A. F. Huxley's 1957 model stems from the evidence for independent force generators operating cyclically in muscle contraction. There are two particularly important pieces of evidence supporting the model. One is the observation that isometric tetanic tension is proportional to the extent of actin-myosin overlap (Gordon et al, 1966), the other is the evidence that the speed of unloaded shortening is independent of actin-myosin overlap (Huxley and Julian, 1964). If the crossbridges are assumed to be independent force generators, they must inevitably operate on a cycle of attachment, force development, and detachment, on purely geometric grounds. The relative sliding motion between thick and thin filaments in each half sarcomere can exceed 0.5 μm, however, the maximum range of crossbridge rotation is only a small fraction of the entire length of the myosin molecule of 0.2 μm. Therefore the crossbridges have to go through many cycles of attachment and detachment in a single contraction. The 1957 model assumes that a crossbridge can exist in one of the two states: attached and detached. It also supposes that a crossbridge splits an ATP when it passes in sequence through the states. The crossbridge exerts force on the thin filament only when attached. The amount of force exerted changes if the thick and thin filaments are displaced with respect to each other. The force (F) is assumed to be proportional to the displacement (x). The distance between sites on the actin filament to

which the crossbridge can attach is assumed to be large enough that only one such site at a time is "within range" of the crossbridge. The model also supposes that the rate constants for the transition between the states are functions of x. The functions are chosen such that the crossbridges attach more rapidly at positive values of x than at negative values while the converse is true for detachment. This asymmetry causes shortening and the development of force. Huxley's 1957 model is basically mathematical in nature, and is founded on two equations:

$$dn(x)/dt = [1-n(x)]f(x)-n(x)g(x) \qquad [1]$$

and

$$F = kx \qquad [2]$$

where n(x) is the probability that an arbitrarily chosen crossbridge, whose displacement is x, is attached; f(x) and g(x) are functions of x and represent the rate constants for attaching and detaching processes, respectively; F is the force exerted by a crossbridge and k is a constant characterizing the elasticity of the crossbridge. Equation [1] and [2] can be solved, with the appropriate assumptions and boundary conditions, to predict the mechanical and energetic behavior of a muscle, such as crossbridge distribution (both positively and negatively strained bridges) for isotonic shortening, tension development, rate of energy liberation, force-velocity curve and even the discontinuity in the slope of that curve for lengthening. The phenomenon of muscle yielding at large velocity of

stretch and the Fenn effect (Fenn, 1924) can also be predicted from the model.

One major difficulty with the 1957 model is that it predicts a much higher rate of energy liberation for rapidly shortening muscle than the rate that is actually observed. Also the model makes no prediction on the mechanical events during rapid transients, such as those observed during a quick-release in length. Huxley suggested in 1973 that crossbridge attachment may take place in two stages. The first stage does not lead to the development of force and is readily reversible without ATP being split. The second stage does lead to force development and ATP splitting and its reversal is negligible. Evidence from X-ray diffraction studies (H. E. Huxley, 1979) and high-frequency stiffness measurements (Cecchi et al, 1982) did suggest that crossbridge may attach to the thin filament before tension is developed. Huxley and Simmons (1971a) proposed a mechanism to explain the rapid recovery of tension after a quick length step. They suggested that it results from a change in the distribution of attached crossbridges between a small number of states without any attachment or detachment. In their model, the crossbridge consists of two parts joined by a hinge. The tail part contains an undamped spring, as in the 1957 model. The crossbridge head can attach to actin at a number of different angles and because of the presence of the spring it can move between these different positions, without detaching, and without relative

movement of the actin and myosin filaments. The force exerted by the bridge, the same as the force in the spring, now depends on two variables: the relative movements of the filaments and the rotation of the bridge head.

The model of Eisenberg and Greene (1980) incorporates the ATP hydrolysis and the associated release of products (from the crossbridge) into the crossbridge cycle. Structural studies suggest that crossbridges bind to actin at an angle of about 45° in the absence of ATP (rigor). In relaxed muscle, the bridges appear to extend from the myosin filament at an angle of 90°. In the Eisenberg-Greene model it is assumed that the release of inorganic phosphate (P_i) from the myosin head is necessary for the crossbridge to enter the strong binding state (45° state), and rapid release of ADP from the head is only possible when the crossbridge is at the 45° conformation. It is when ADP is released that ATP can bind to the myosin head and start a new cycle. If the crossbridge is prevented from cycling to the 45° state, ADP release will be slow and the strained crossbridge will exert force on the thin filament. One line of evidence supporting the model comes from studies with the ATP analog, AMP-PNP (adenyl-5'-yl imidodiphosphate) (Marston et al, 1976). It has been shown that AMP-PNP can actually cause a muscle fiber to lengthen slightly, an effect that would occur if AMP-PNP were to cause the crossbridges to rotate from a 45° angle to a 90° angle. Weakly bound crossbriges have been detected (Brenner et al, 1982) and

their structure appears to be different from the strongly bound bridges that occur in the absence of ATP.

II. Smooth Muscle Contraction Models

Regulation of smooth muscle contraction is different from that of striated muscle. However, at the crossbridge level, the mechanism of crossbridge cycling that involves ATP hydrolysis and the subsequent products release seems to be the same for both muscles. Activation of actomyosin ATPase activity in smooth muscle requires phosphorylation of the 20,000 dalton molecular weight myosin light chain (LC20) (Sobieszek and Small, 1977) by myosin light chain kinase which is in turn activated by binding to calcium-calmodulin complex (Dabrowska et al, 1978). Also dephosphorylation of attached crossbridges produces the so called "latch" bridges (Dillon et al, 1981), that are characterized by their low cycling rate and hence the ability to maintain tension at low energy cost.

The smooth muscle contraction model proposed by Hai and Murphy (1988) hypothesizes two types of crossbridge interactions: 1) cycling phosphorylated (or "normally cyling") crossbridges and 2) noncycling dephosphorylated (or "latch") crossbridges. Detailed kinetics for the "normally cycling" bridges were not delineated in the model of Hai and Murphy, but presumably they are the same as those proposed for striated muscle. But for a "latch" bridge to go through a cycle, according to Hai and Murphy (1988), it has to

detach, and then the myosin has to be phosphorylated (becoming a "normally cycling" bridge again) and then dephosphorylated while still attached to actin.

A spatial-temporal model of smooth muscle contraction was proposed by Rasmussen et al (1987). According to this model, spatial separation of calcium function contributes to temporal separation of distinct phases of the muscle contraction. The initial transient rise in cytosolic calcium concentration is thought to be responsible for activation of a subset of phosphoproteins that could include the LC20, resulting in the formation of the cycling phosphorylated crossbridges. The sustained phase of smooth muscle contraction, on the other hand, is brought about by the interaction of calcium with diacylglycerol, to cause the association of protein kinase C with the plasma membrane. Activation of protein kinase C in turn phosphorylates another subset of phosphoproteins, including some cytoskeletal proteins, and somehow prolongs the contraction in the absence, or reduced phosphorylation of myosin light chain. The exact mechanism by which the sustained contraction is maintained by protein kinase C dependent protein phosphorylation is unknown. However it is suggested that phosphorylation of cytoskeletal proteins would somehow change the mechanical properties of the cytoskeleton, and result in maintenance of force without or with little participation of the crossbridges (Rasmussen et al, 1987).

None of the contraction models described above is proven perfect and can account for all the experimental facts observed. This is probably truer for smooth muscle models than for striated. However, the models have made invaluable contributions to our understanding of muscle contraction. One of my favorite quotations is from the article "Facts and theories about muscle" by Douglas Wilkie: "Facts and theories are natural enemies. A theory may succeed for a time in domesticating some facts, but sooner or later inevitably the facts revert to their predatory ways. Theories deserve our sympathy, for they are indispensable in the development of science. They systemize, exposing relationship between facts that seemed unrelated; they establish a scale of values among facts, showing one to be more important than another; they enable us to extrapolate from the known to the unknown, to predict the results of experiments not yet performed; and they suggest which new experiments may be worth attempting. However, theories are dangerous too, for they often function as blinkers instead of spectacles. Misplaced confidence in a theory can effectively prevent us from seeing facts as they really are" (Wilkie, 1954).

III. Background to the Present Studies

The series of experiments described in this thesis represent an effort to elucidate the true mechanism of smooth muscle contraction. The experiments were concentrated on characterizing some of the previously unexplored aspects

of smooth muscle contraction. Particular attention was paid to identifying variables that would affect the results and thus the conclusion of the experiments.

a) Conceptual mechanical model of muscle

Fig. 1A depicts idealized tension and length records of a quick-release experiment. Before the quick release, the muscle is developing a tetanic force P_o. After the release, it is no longer held at constant length but at constant force P. Fig. 1B depicts a four-component conceptual model of muscle. The components are defined functionally; their possible anatomical counterparts in the muscle is speculated in Discussed section. The parallel elastic component (PEC) acts in parallel with the part of the muscle which generates force, the contractile element (CE). Together the PEC and the series elastic component (SEC) account for the passive tension properties of muscle. In our multicellular preparation that consisted of smooth muscle cells embedded in extracellular connective tissue matrix, the properties of PEC may reflect the mechanical features of this connective tissue matrix. The intermediate filaments that make up the cytoskeleton inside the cells (Somlyo et al, 1984; Wang and Ramirez-Mitchell, 1983) are also candidates for the anatomical counterparts of PEC. The source of series elasticity represented by SEC in a multicellular muscle segment is more complicated and controversial. In skeletal muscle, it seems that the major source of the series compliance is associated with the crossbridges (Bressler and

Clinch, 1975; Ford et al, 1981). Warshaw and Fay (1983) suggest that in single smooth muscle cells the series compliance stems mainly from the crossbridges also. In multicellular preparation, however, a significant portion of the SEC is extracellular (Mulvany and Warshaw, 1980). Although in most experiments the investigators take great care to eliminate damage to the muscle preparation, almost inevitably the two ends of the muscle strip that connect to the measuring device are "crushed". The crushed ends will introduce series compliance to the preparation. In striated muscle, the striation provides a convenient way for devices that follow striation image or the laser diffraction pattern to monitor the true length change of the contractile element, in the presence of stray compliance. In smooth muscle there are no distinct regular cellular features that could provide reliable markers to indicate the movement of the contractile element. One alternative to solve this problem is to use external markers put on the surface of the smooth muscle to provide estimation of the relative movement of small segment of the muscle (Uvelius, 1979; Warshaw et al, 1987). Quick-release experiments may be interpreted to provide direct evidence of the existence of a SEC, as shown in Fig. 1A. The rapid change in length which accompanies the sharp change in load is consistent with the mechanical definition of a spring, that is, the force in a spring is purely a function of length. It is assumed that the CE is damped by a viscous element (VE) and cannot change its

length instantaneously. The quick elastic recoil after quick-release, therefore, is thought to stem entirely from the SEC. The observation that muscle develops its greatest force when the speed of shortening is zero led Hill (1922) to propose that stimulation always brings about development of this maximum force, but that some of the force is dissipated in overcoming an inherent viscous resistance if the muscle is shortening. He suggested that the CE should be in parallel with the VE as depicted in Fig. 1B, in which the viscous element is represented by a "dashpot" that reacts to length change with a damping force of magnitude proportional to the rate of the length change. It is generally believed now that the force-velocity behavior of a muscle is not governed by the simple "mechanical dashpot", but rather (or mainly) by biochemical reactions that control the rate of energy release and therefore the mechanical properties. Nevertheless the model, like the one shown in Fig. 1B, has proven very useful in calculating the pure mechanical features of muscle working against a load.

b) Velocity-force-time and velocity-length-time relations

The "latch" bridge phenomenon observed in smooth muscle contraction from different perspectives in the laboratories of Murphy (Dillon et al, 1981), Siegman (Siegman et al, 1976), Uvelius (Uvelius, 1979), and Stephens (Stephens et al, 1986) suggests that to characterize smooth muscle velocity-force and velocity-length relations, one extra dimension has to be added - that is, time (after onset of

stimulation). The "time" variable probably reflects the time course of change in phosphorylation and dephosphorylation of certain subset of proteins during smooth muscle contraction. The time dependent velocity-force and velocity-length relations are quantitatively described in the Results section.

c) Stiffness of the series elastic component

Stiffness of the SEC of muscle is thought to be directly proportional to the number of attached crossbridges (Bressler and Clinch, 1975; Cecchi et al, 1982; Ford et al, 1981; Ford et al, 1986; Huxley and Simmons, 1971b; Julian and Sollins, 1975; Kamm and Stull, 1986; Meiss, 1978). To correctly use the SEC stiffness as an index of the number of attached crossbridges, however, all other variables that influence the stiffness have to be identified, and their relations with the stiffness have to be characterized. In smooth muscle one important question to be asked is: How does the SEC stiffness change with time? This question is dealt with in detail in this thesis.

In skeletal muscle the series elasticity seems to stem predominantly from the crossbridges (Bressler and Clinch, 1975; Ford et al, 1981), therefore the SEC stiffness is directly proportional to the number of attached crossbridges and the former varies in the same manner as tension does with respect to length (Ford et al, 1981). Will the same relationships among stiffness, force and length be observed in smooth muscle? The SEC length at maximum isometric

tension for various types of smooth muscle varies somewhere from 7% to 20% of the optimum muscle length (Herlihy and Murphy, 1974; Johansson, 1973; Lundholm and Mohme-Lundholm, 1966), whereas in skeletal muscle it is less than 1% (Sugi and Kobayashi, 1984; Woledge et al, 1985). It is possible that most of the series compliance in smooth muscle, unlike that in skeletal muscle, is of non-crossbridge origin. If that is the case then stiffness would not necessarily vary in the same manner as isometric tension does with respect to length (for a detailed discussion on this point, see Ford et al, 1981), and the estimation of the number of attached crossbridges using stiffness measurement in smooth muscle would require extra precaution. The effect of muscle length on SEC stiffness in smooth muscle is examined in detail in this thesis.

METHODS

a) Preparation of muscle strip

Mongrel dogs were anesthetized by i. v. injection of 30 mg/kg body weight of pentobarbital. This was followed by rapid removal of the cervical trachea via a mid-line incision and intracardiac injections of saturated KCl solution to sacrifice the animals. Each trachea was placed immediately in a beaker of ice-cold, aerated Krebs-Henseleit solution of the following composition (millimolar): NaCl, 115; $NaHCO_3$, 25; NaH_2PO_4, 1.38; KCl, 2.51; $MgSO_4-7H_2O$, 2.46; $CaCl_2$, 1.91; dextrose, 5.56. With the connective tissue carefully removed under a dissecting microscope, a strip of muscle was cut from the trachea. The strips used in the experiments possessed an average length of 7 mm, an average weight of 2 mg, and a width of 0.5 mm. One end of the strip was connected to the lever by a highly non-compliant (7-0 silk) surgical thread. The average compliance of the thread was about 0.003 mm/mN. The force range used in the experiments is far less than the yield strength of the thread, therefore no permanent deformation of the thread occured, and no hysteresis was found during the loading and unloading of the thread. The other end of the strip was fixed in the muscle bath by a clamp. The bath containing Krebs-Henseleit solution was aerated with a 95% O_2-5% CO_2 mixture which maintained a PO_2 of 600 torr, a PCO_2 of 40 torr and pH of 7.4 at a temperature of 37 °C. The strip was equilibrated in the bath for 2 hrs. During this time it was

stimulated every 4 min electrically by 17 V, 60 Hz alternating current applied to platinum electrodes that were positioned on each sides of the muscle. Since stimulation of the muscle was through release of acetylcholine from the cholinergic nerve endings in the preparation, the variation in the amount of acetylcholine released could affect the mechanical response of the muscle. However, electrical stimulation elicited about 90% of the maximum tension elicited by direct membrane depolarization using high potassium solution, and also this electrical response was quite constant with respect to the maximum high potassium response, one can conclude that the neural component of the preparation does not contribute to the variation of the mechanical responses described in this thesis. The duration of stimulation was 10 s which was also the contraction time for the muscle (to reach isometric tension plateau). An steady state was achieved when muscle developed a steady tetanic tension upon stimulation. The optimum muscle length, l_o, was obtained by varying the preload (and hence the length) of the muscle strip, and measuring the isometric tetanic tension. The length that was associated with the development of maximum isometric tension (P_o) was identified as l_o. The preload associated with l_o was about 10% of P_o. Tension was normalized to the muscle's cross-sectional area. The area was determined by dividing the muscle volume (wet muscle density was assumed to be 1.0 g/cm^3) by its optimum length. In dissecting the muscle, caution was taken to

minimize the mechanical damage of the tissue, especially the two ends of the muscle strip. The series stray compliance of the preparation was much less than 1% of l_o.

b) Data acquisition

The instantaneous force and displacement produced by the muscle were recorded with the use of an electromagnetic lever system. The lever was fashioned from magnesium and attached by epoxy cement to a coil suspended in a strong magnetic field provided by a permanent magnet. This system possessed a total compliance of 0.2 μm/g and a total equivalent moving mass of 225 mg. The equivalent mass of the lever was 40 mg. The system was originally designed by Brutsaert et al (1971) for use in studies of cardiac muscle mechanics. The thread connecting the muscle strip to the lever had a non-linear force-length relationship. Therefore after each experiment the force-length curve of the connecting thread was obtained by applying force to the thread and measuring the corresponding elongation. The curve was later used to correct the experimental data. The frequency response of the lever system was 450 Hz. Signals from the lever system were digitized by an analog-to-digital (A/D) converter, and the digital signals were fed to a HP9836 computer that analyzed and plotted out data in both graphical and numerical forms. The maximum sampling frequency of the recording system was 1000 Hz.

c) Force-velocity measurement

Shortening velocity at different loads was obtained using the load clamp method (Fig. 2). The time at which the muscle was released was controlled by a timer, or in other words time was a controlled variable in the experiments. Since load clamps were applied to isometrically contracting muscle, the length variable was fixed at l_o. The lever oscillation at the onset of a load clamp was critically damped, since over- or underdamping of the lever would reduce the velocity measured. Damping in the lever system was provided electronically by differentiating and inverting the displacement signal and adding this negative velocity signal to the original displacement signal through an adjustable resistor that controlled the degree of damping. Shortening velocity of the muscle was measured right after the quick-release, when the rapid elastic recoil of the muscle was replaced by a steady shortening velocity of the CE. Force-velocity data were fitted by Hill's hyperbolic equation:

$$V = b(P_o-P)/(P+a) \qquad [3]$$

where V is the shortening velocity of muscle; P_o is the maximum isometric tension; P is the load on muscle; a and b are the constants. To fit the F-V curve to the data, a combination of iteration and least-square best-fit method were employed (Seow and Stephens, 1986).

The validity of using Hill's equation on smooth muscle is worthy of some discussion. The equation is usually used to describe the F-V relations in tetanized, isolated

striated muscle. It is now regarded as empirical and used only because it is mathematically simple and also fits the experimental data well. In striated muscle it appears that fundamentally only one type of force, or shortening-generating mechanism (the crossbridge), is active throughout the entire time course of a contraction (i.e., the F-V relationship is time independent). In smooth muscle, as mentioned in the Introduction, the F-V characteristics change with time. Therefore the velocity predicted by the Hill equation should not be a function of load alone, but also of time. Therefore a more generalized Hill equation (at least for smooth muscle) should more correctly be:

$$V(P,t) = b(t)[P_o(t)-P)]/[P+a(t)] \qquad [4]$$

where $a(t)$, $b(t)$ and $P_o(t)$ are functions of time, and can be obtained from fitting the F-V data with Eq. 4.

d) Maximum isometric tension obtained from F-V curve and
   direct measurement from isometric myogram

The maximum isometric tension extrapolated from a F-V curve is found at the intersection of the force-axis and the hyperbolic F-V curve (Fig. 3). It can be defined as the isometric tension developed by the muscle when the shortening velocity of the CE is zero. This maximum tension is designated here as P_o.

Directly measured isometric tension from an isometric myogram does not always represent the isometric tension developed by the muscle when shortening velocity of CE is zero, therefore it is designated here as P_o'. Force

generated by the CE is transmitted through the SEC. In an isometric contraction, although the muscle does not shorten externally, internal movement of the muscle components must occur due to the compliance of the SEC. This internal movement will affect the instantaneous external force output (isometric tension) of the muscle. Only at the plateau of contraction (when $dP/dt=0$) does P_o' equal P_o. At the ascending and descending phases of contraction, because the shortening velocity of CE is not zero (and hence $dP/dt=0$), P_o and P_o' should be different. The quantitative difference between P_o and P_o' during the entire time course of contraction and relaxation was examined by comparing the maximum force computed from the F-V curve (P_o) at different points in the time course, to the directly measured isometric tension (P_o') at the same time point. F-V data were obtained by applying load clamps to muscle during isometric contraction. For a single F-V curve, the time at which the load clamps were applied was fixed (Fig. 2), therefore the effect of time on shortening velocity (Dillon et al, 1981) was held constant. A family of such F-V curves were obtained at different points in time during the course of isometric contraction and relaxation, and from the curves the function $P_o(t)$ was obtained. The function $P_o'(t)$, on the other hand, was obtained from direct measurement of the isometric tension curve at time t.

e) Measurement of "internal resistance" to shortening

In the following discussion of F-V relations, the time variable is omitted temporarily for simplicity's sake.

From experimental observations it is clear that the larger the force-step (P_o-P) in quick-release, the greater the subsequent shortening velocity. In other words, the force-step is proportional (but not necessarily directly proportional) to shortening velocity, or $(P_o-P) \propto V$. We can equate the two by putting in a "constant" of proportionality α :

$$(P_o-P) = \alpha V. \qquad [5]$$

The equation is true only when the velocity is constant with respect to time. If $dV/dt=0$, then the inertial force of the muscle has to be considered. Buchthal and Rosenfalck (1957) have shown that the magnitude of the inertial force in contracting isolated muscle is negligible. Our calculation based on some preliminary data revealed that the value of the inertial force ranged from zero to 10^{-5} mN/mm². Therefore the inertial force could be neglected without introducing a significant error. If shortening velocity is measured under certain conditions such that the change in velocity is entirely due to the change of load on muscle, then a hyperbolic F-V curve is usually obtained, and α is found to be a linear function of load (P). If we arbitrarily define the linear function as

$$\alpha = (P+a)/b \qquad [6]$$

where a and b are constants, the equation $(P_o-P) = \alpha V$ becomes Hill's equation $[(P_o-P) = V(P+a)/b]$. The term

(P+a)/b possesses the same unit as the coefficient of viscosity. Although the simple mathematical manipulation does not prove the existence of a viscous force, the analysis shows that a decrease in muscle shortening velocity is always associated with an increase in the value of the term (P+a)/b, provided that the force-step is the same. Therefore in a hyperbolic F-V relation, the "internal resistance" to shortening can be represented by (P+a)/b. If the muscle is shortening under zero load (P=0), the internal resistance is a/b. The constants a and b were obtained from the F-V curve that best fitted the experimental data.

Because the constants a and b are actually functions of time, that is, a(t) and b(t), and because the isotonic load (P) is a controlled variable and hence time independent, the term (P+a)/b is essentially a function of time. The physiological factors that could possibly affect the values of a and b during smooth muscle contraction will be discussed later.

f) Measurement of series elasticity as a function of time

Both Voigt and Maxwell models (Woledge et al, 1985) can be used in analyzing the mechanical behavior of the muscle. Since in the experiments the muscle was never stretched beyong its optimum length (l_o), the parallel elastic component (PEC) of the muscle had little effect on the experimental results. Under the circumstances, the model presented in Fig. 1B (a modified Voigt model) is a more convenient and straightforward one to use in the data

analysis. The tension-extension (T-E) curve of the SEC was obtained by releasing the muscle during isometric contraction to various isotonic loads (Fig. 4A), and measuring the elastic recoils (SEC lengths). The SEC length under zero load was arbitrarily defined as zero. The extension of the SEC under a given afterload was determined by subtracting the length of the elastic recoil under the afterload from that obtained with zero afterload. A family of the T-E curves was obtained at different points in time during isometric contraction. The stiffness (or elasticity) of the SEC was obtained from the slope of the T-E (or stress-strain) curve of the muscle.

The T-E curve of the SEC of resting muscle was obtained by releasing the muscle from its l_o or resting tension to various afterloads without stimulating the muscle (Fig. 4B). The passive response of the muscle to a force step was qualitatively similar to the active response and consisted of a rapid elastic recoil and a slow shortening phase. The T-E curve for the SEC of muscle in rigor (Fig. 4B) was obtained in the same way as in resting muscle except the muscle was incubated in the bath containing zero-glucose Krebs-Henseleit solution bubbled with 95% N_2-5% CO_2 gas mixture for 1 h. Electrical stimulation was applied every 4 min during incubation. A slight rise in resting tension and diminished isometric tension indicated a rigor or near-rigor state. The muscle could recover to a near normal state when incubated again in normal Krebs-Henseleit solution aerated

with 95% O_2-5% CO_2 gas mixture. Again, the passive response of the muscle in rigor to a force step was qualitatively similar to the response of active normal muscle and consisted of a rapid elastic recoil and a slow phase (Fig. 4). The shortening velocity in the slow phase of resting and rigor muscle was much less (at least 40 times less) than that of an active muscle. The production of rigor and the associated ATP concentration in tracheal smooth muscle has been described in detail by Bose (1984).

The present study and others (Bressler and Clinch, 1975; Herlihy and Murphy, 1974; Stephens and Kromer, 1971; Warshaw and Fay, 1983) show that stiffness of SEC is a function of load (on muscle). In fact, it can be shown that the stiffness is linearly related to the load. A formula widely used to describe the relation is of the form:

$$d\sigma/d\varepsilon = E_o + A\sigma \qquad\qquad [7]$$

where σ is the stress in muscle, ε is the strain of the SEC (normalized to l_o), $d\sigma/d\varepsilon$ is the stiffness, E_o is the initial elastic modulus, and A is the slope of the linear stiffness-stress curve. By arbitrarily defining that $\varepsilon = 0$ when $\sigma = 0$, Eq. 7 can be integrated to give

$$\sigma = (E_o/A)(e^{A\varepsilon} - 1) \qquad\qquad [8]$$

Eq. 8 describes the stress-strain relationship of the SEC, and it was used in this study to fit the experimental data. The computer was used to perform the two-dimensional (A, E_o) search for the minimum deviation of the experimental data from the curve described by Eq. 8.

g) Measurement of velocity as a function of length

The zero-load velocity (V_o) was obtained by measuring the slope of the displacement curve right after a quick-release to zero-afterload. The load clamp was critically damped. The "zero-load" the muscle was released to was in fact a finite load of 0.2 mN (about 0.4% of P_o), which was partially counter-balanced by the weight of the thread connecting the muscle to the lever. Muscle length at the moment the muscle was released was controlled indirectly by the load on the muscle. The isotonic loads used in the experiments ranged from 5% to 100% P_o, which correspoded to a length range of about 50% to 100 % of l_o (Fig. 5).

h) Measurement of stiffness as a function of length and time

Continuous measurement of stiffness ($\Delta P/\Delta L$) was made by applying small force perturbations (ΔP) to an isotonically contracting muscle and measuring the amplitude of the resulting displacement perturbations (ΔL) (Fig. 6). The force perturbation the muscle subjected to was a train of rectangular force waves varying from 0 to about 4 mN (10% of P_o), with a frequency of 10 Hz. Length oscillation was critically damped. The reason square wave force perturbation was used instead of a sinusoidal one (which is used by most investigators when they apply length perturbations to isometrically contracting muscle) was that the step change of force quick-released and stretched the muscle and thus revealed the corresponding quick length transient (the elastic response) that represented the change in the SEC

length (Fig. 6C). Force perturbation did not reduce the degree of activation of the muscle. This was concluded from experimental observations that the displacement curve of the muscle under a load of 2 mN could be superimposed on the mean displacement curve of the same muscle under force perturbations ranging from 0 to 4 mN at a perturbation frequency of 10 Hz (Fig. 6B). Also the maximum isometric tension (P_o) after the perturbation was not reduced. However, if a force perturbation amplitude greater than 20% of P_o was used, the shortening ability of the muscle was reduced, probably due to disruption of the crossbridge attachments by large force steps. Ideally a small amplitude of force perturbation should be used. But if the amplitude is too small, the resulting small length perturbation can not be accurately measured. In our experiments, an amplitude of 10% P_o was used. The force perturbation method enabled us to measure the stiffness continuously in a single isotonic contraction. The 10 Hz perturbation frequency enabled us to make measurements of the stiffness ($\Delta P/\Delta L$) 20 times per second. For smooth muscle, because of the relatively long time course of contraction, this perturbation frequency was adequate to give a "continuous" function of the SEC stiffness with respect to time. Stiffness of the SEC was obtained by dividing the force perturbation amplitude (ΔP) by the corresponding change in SEC length (ΔL). The compliance of the thread and the lever system was taken into account when measuring the SEC length.

In an isotonic contraction, at least two variables are involved: length and time. To eliminate the latter and address oneself purely to the effect of length on stiffness, stress-strain curve for SEC was obtained at 4 different muscle lengths. All the curves were obtained by quick-releasing and quick-stretching the muscle at 10 s after contraction (Fig. 7). In an isometric contraction of canine tracheal smooth muscle, it takes about 10 s for the muscle to reach maximum tension. The muscle length, immediately prior to the application of the load clamps, was controlled by the isotonic load. A lighter load would allow the muscle to shorten more before the load clamp came on, and vice versa. The amount of rapid elastic length response after quick-release or quick-stretch was taken as the change in the length of the SEC. The SEC length under zero load was arbitrarily defined as zero. For quick-release, the extension of the SEC under a given afterload was determined by subtracting the length of the elastic recoil under the afterload from that obtained with zero afterload. For quick-stretch, the extension of the SEC under a given afterload was determined by adding the length of the elastic length transient under the afterload to the length of the elastic recoil obtained with zero afterload. The T-E data were fitted with Eq. 8 described earlier. The onset of the load clamp was controlled by a digital timer which triggered the release or stretch of the muscle at a preset time. The timer

also controlled the onset and duration of stimulation of

muscle.

RESULT

a) Isometric tension from F-V curve and isometric myogram

Results for this section are summarized in Fig. 8 and Table 1. Fig. 8 shows the isometric tension curve [$P_o'(t)$] and the curve representing the extrapolated maximum force [$P_o(t)$] from the F-V curve. The coefficients of determination (r^2) for the 41 curves that best-fitted the F-V data were all greater than 0.9. During the experiments $P_o'(t)$ changed slightly from one contraction to another. To obtain a set of F-V data about 5 contractions were required. Therefore the mean value of $P_o'(t)$ was used for comparison with $P_o(t)$. To ensure that $P_o(t)$ statistically did not belong to the same population as that for $P_o'(t)$, Nair's (Kennedy and Neville, 1976) method was used to prove that $P_o(t)$ value was an outlier to the population of $P_o'(t)$ values. $P_o(t)$ value at 10 s (Table 1) was an exception in that it was not judged as an outlier by the Nair's criterion. Also values of $P_o'(t)$ and $P_o(t)$ from 6 experiments were not different from each other (Student's paired t-test) at 10 s. At other times, however, they were all significantly different from each other (Student's paired t-test). The value of $P_o(t)$ was greater than that of $P_o'(t)$ during contraction and was less during relaxation. The two were equal at the plateau of contraction where $dP/dt=0$. This is reflected in the left-shift of $P_o(t)$ curve compared to $P_o'(t)$ curve (Fig. 8).

b) Time dependent F-V characteristics

To show the time dependency of the F-V characteristics,
F-V curves were obtained at 1-s intervals during the course
of isometric contraction. Fig. 9 shows one typical F-V curve
obtained early in contraction (2 s) and the other obtained
at the plateau phase of contraction (8 s). On comparing the
8-s to the 2-s curve, a significant increase in the value of
a (+75%) was found, although the change in b was small (
-4.3%). The maximum zero-load velocity (V_o) dropped by 30%
from 2 to 8 s. Statistical analysis of the two groups (n=5)
of data obtained at 2 and 8 s showed that there was a highly
significant difference (p<0.005) between the values of a at
2 and 8 s, whereas there was no significant difference for
values of b (see Table 2). For values of P_o, V_o, and a/P_o at
2 and 8 s, also see Table 2.

F-V curves were obtained at 1-s intervals from 1 to 12
s. The mean values of a and b obtained from 5 experiments
(±SE) are shown in Fig. 10. The values of a remained
relatively low during the first 2 s of contraction, then
increased rapidly for the next couple of seconds. The rate
of increase then decreased, and the curve reached a maximum
at about 10 s. In contrast, b remained relatively constant
with time at a value of about 0.081 l_o/s.

Mean plots (n=5, mean±SE) of V_o and P_o vs. time are
shown in Fig. 11. There was a transient increase in V_o.
Maximum V_o occurred about 2 s after stimulation.

A mean plot (n=5, mean±SE) of the value of a/b is shown
in Fig. 12; a/b progressively increases with time.

c) Time dependence of series elasticity

As mentioned earlier, the stiffness (or elasticity) of the SEC, when properly measured, can be used as an index of the number of attached crossbridges. Typical stress-strain curves of the SEC from a single experiment are shown in Fig. 13. Eq. 8 was used to fit the experimental data. The constants A and E_o associated with the best-fitting curve were obtained for each SEC. It was found that the SEC stress-strain curves were different at different times after stimulation, although each of them can be fitted with an exponential curve with roughly the same goodness of fit (Fig. 13). The SEC of the muscle in rigor was the stiffest; the resting muscle was the most compliant. At 0.5 s after stimulation, before the isometric tension was detected, the stiffness of the SEC increased significantly ($p < 0.05$) (Fig. 14 and Table 3).

Stiffness of the SEC is broken down into two components according to Eq. 7: one is the initial elastic modulus E_o which is stress independent; the other is $A\sigma$, which depends on stress (σ) linearly. Both components are plotted in Fig. 14. To compare the stiffness of the SEC's, the magnitude of the stress in the SEC has to be specified. However, because the stress-independent stiffness (E_o) is relatively small and remains quite constant throughout contraction (Fig. 14), the only parameter that determines the stiffness at any stress level is the constant A. Constant A therefore is an index of the stiffness that excludes the effect of stress in

the SEC. Constant A as a function of time is shown in Fig. 14; it represents the time variation of the SEC stiffness. Here the value of A is multiplied by a constant stress value of 22.2 mN/mm² (10% of P_o, see Table 3) so that the relative values of E_o and $A\sigma$ can be compared. It should be realized that, if different stress levels were used, the shape of the $A\sigma$ curve would be the same but the magnitude would be different. A typical isometric tension-time curve [$P_o'(t)$] is also shown in Fig. 14 to indicate the time course of contraction.

The constants E_o, A and P_o' (directly measured isometric tension) of the four muscle strips from four dogs used in the experiments are shown in Table 3.

From the results presented in Figs. 13 and 14, and Table 3, it was clear that the stress-strain curves of the SEC obtained at different times were different. The stiffness of muscle in rigor state was much higher than that at resting state. The stiffness of normal muscle during contraction varied significantly with time but within the limits of the stiffness of muscle in rigor and that at resting state. The constants (from Eq. 8) that characterized the stress-strain curves (A, E_o) behaved differently with respect to time. Constant A was time dependent (or phasic) but constant E_o did not change with time.

d) Velocity-length-time relations

The velocity-length data shown in Figs. 15 and 16 were obtained from "raw" data similar to the one shown in Fig. 5

in Methods. The data were fitted with a parabolic function
of the form:

$$V_o(l) = V_{max}\{1-[(1-l)/(1-l_{min})]^2\} \tag{9}$$

where V_{max} was the maximum shortening velocity or zero-load
velocity at l_o [i.e., $V_{max}=V_o(l_o)$] and l_{min} was the length
of the maximally contracted muscle under zero load or the
minimum muscle length. l was expressed as percent of l_o, and
therefore l_o was unity. The coefficients of determination
(r^2) for the curves in Figs. 15 and 16 were all >0.94
($p<0.05$). Because of the close fit, for any given values of
V_{max} and l_{min} the parabolic equation was sufficient to
define the V_o-l curve. For this reason the parameters V_{max}
and l_{min} were emphasized in this part of study. The values
for each of the 8 experiments are listed in Table 4. Note
that V_{max} varied with time, whereas l_{min} was time
independent, as shown in Fig. 16. The maximum value of the
parabolic function V_{max} varied from second to second, but
the x-axis intercept of the function remained the same. The
results clearly indicated that the unloaded shortening
velocity was length dependent.

e) Stiffness-length-time relations

In this part of the present studies the experiments
were divided into two groups. One measured the stiffness
change during an isotonic contraction and relaxation using
the force-perturbation technique. The other measured the
stiffness change with respect to muscle length by obtaining
the stress-strain curves of the SEC at different muscle

lengths 10 s after onset of stimulation. For the first group

of data, the mean values (n=5) of the muscle length and the

SEC stiffness as functions of time are plotted in Figs. 17

and 18. Fig. 17 shows the function during contraction,

whereas Fig. 18 shows the functions during relaxation. The

data for displacement were obtained from raw data such as

the ones shown in Fig. 6 (in Methods). Displacement of

muscle at a particular point in time was taken as the mean

value of the upper and lower limits of the amplitude of the

length perturbation curve at that time. Muscle length was

calculated by subtracting the amount of displacement from

l_o. Stiffness at a particular point in time was obtained by

dividing the ΔP, which remained the same throughout

contraction (Fig. 6), by the corresponding ΔL at that time.

During contraction, stiffness increased as the muscle

shortened (Fig. 17). During relaxation, the decrease in

stiffness preceded that of muscle lengthening and also

stiffness decreased as the muscle lengthened (Fig. 18).

For the second group of data, the SEC stiffness was

obtained by measuring the slope of the stress-strain curves

(Fig. 19). The curves were obtained from raw data such as

the ones shown in Fig. 7. Because the stress-strain curves

were not linear, a stress level of 5% P_o was chosen for

calculating the stiffness (Fig. 20) for it to be comparable

to that in the first group of data. In the first group,

stiffness was estimated by applying a force perturbation

varying from 0 to 10 % of P_o. 5% P_o was the mean value of

the force perturbation amplitude. The "constant-stress stiffness" shown in Fig. 20 (solid line) was calculated from Eq. 7 (in Methods). The constants A and E_o were obtained by curve fitting. The σ was set to equal to 5% P_o. If different values for σ were used to calculate the stiffness, this stiffness vs. length curve would remain basically the same shape but shift up or down (without rotation) depending on the value of σ used. The constant-stress stiffness could also be obtained by drawing a tangent line over the stress-strain curve at the 5% P_o stress level and measuring the slope of the tangent line.

The relationship between constant-stress stiffness and the SEC length (L) was examined by plotting the reciprocal of the SEC length against the stiffness. The SEC lengths were obtained by measuring the amount of strain at 5% P_o from data such as the ones shown in Fig. 19. Assuming that the increase in SEC stiffness at short muscle length was due to a decrease in the SEC length itself, then, when other variables such as stress and time were held constant, the reduction in SEC length during shortening should linearly relate to the increase in the apparent stiffness. In other words, $d\sigma/d$ is inversely proportional to L. Fig. 20, inset, shows that stiffness and 1/L are indeed linearly related. The reciprocal of SEC length was plotted as a function of muscle length in Fig. 20 (dashed line). Stiffness and 1/L varied with muscle length in a very similar fashion.

Fig. 21 shows the change in stiffness during isotonic contraction and relaxation, as a function of muscle length (solid line). The curves were obtained from data shown in Figs. 17 and 18. Note that the time variable was not held constant. Therefore, part of the changes in stiffness was due to time variation, which could be related to the variation of the number of attached crossbridges. The stiffness vs. muscle length curve shown in Fig. 20 was redrawn in Fig. 21 (dashed line) for purpose of comparison. Note that the dashed line was obtained with time variable held constant.

Table 5 summarizes the results from the second group of data. It lists, for each experiment, the values of P_o, muscle lengths, and the corresponding SEC lengths (at 5% P_o), constants A and E_o, and the coefficients of determination (r^2) for curve fitting (for obtaining A and E_o), the correlation coefficients for E_o and $1/L$ values. The values of A and E_o associated with each of the four muscle lengths were significantly different from one another ($p<0.05$) according to the t-test.

DISCUSSION

The basics of airway smooth muscle mechanics, namely, the classical length-tension and tension-velocity relations, have been thoroughly documented (Stephens et al, 1969; Stephens, 1970). This thesis deals with some novel aspects of mechanical properties of the muscle. Although the general subject area of this thesis is on the mechanical aspects of airway smooth muscle contraction, the specific problems dealt with in this thesis are not concentrated on a single issue, therefore an integrated discussion of the problems is difficult. Each group of experiments therefore will be discussed separately. One general comment, however, can be made based on the experimental results is that the unique structural and regulatory features of smooth muscle are reflected in the mechanical properties of the muscle, which are distinctively different from those of striated muscle despite the common belief that the basic mechanism of contraction (filament-sliding and crossbridge-cycling) is the same for both muscles. Experimental results that in any way related to the mechanical properties of smooth muscle, therefore, have to be interpreted in a way that accounts for all the special features of smooth muscle.

Most of the material presented in this thesis is already published (Seow and Stephens, 1986; Seow and Stephens, 1987; Seow and Stephens, 1988; Seow and Stephens, 1989). For more comprehensive information, readers are

referred to the original papers which are included in this thesis as appendices.

a) Isometric tension generated by the contractile element

Muscle, especially smooth muscle, is a very "popular" tissue used in physiological, pharmacological and biochemical studies because of the important functions it serves in the organism, and also because the cell response is relatively easy to elicit and record. Isometric tension is often used in such studies to indicate the degree or intensity of the cell response because tension, especially isometric tension, can be measured accurately with the use of a relatively inexpensive strain gauge. But what does the measured isometric tension tell us about the contractile activity of the cell? This question is not only important to muscle physiologists, but also to pharmacologists, biochemists and other scientists who use muscle tissue in their studies.

The isometric tension curve $[P_o'(t)]$ or myogram indicates the time course of tension registered, by a force transducer, at the two ends of an isometrically contracting muscle. It is generally accepted that force generated by the CE, the actomyosin crossbridges, is transmitted to the outside media through a functionally defined series elastic component (SEC), which could reside in the crossbridges or other intra- or extracellular components of the muscle (Hellstrand and Johansson, 1979; Mulvany and Warshaw, 1981; Warshaw and Fay, 1983). In an isometric contraction,

although the muscle does not shorten externally, internal
movement of muscle components must occur due to the
compliance of the SEC. This internal movement will tend to
reduce the instantaneous external force output of the
muscle. A. V. Hill (1922) was the first to recognize this
problem. Based on the observation that maximum muscle force
developed only when the speed of shortening is zero, Hill
proposed that the contractile element (or pure force
generator) was in parallel with a viscous element (VE) (Fig.
1) and he defined the pure force generator as the "active
state". The model (Fig. 1) predicts that the externally
measured isometric tension does not always reflect the
active state of the muscle. The external isometric tension
equals the tension produced by the pure force generator only
at the plateau of contraction where internal shortening is
absent (dP/dt=0). Extensive efforts have been made in an
attempt to elucidate the active state of muscle contraction.
Gasser and Hill (1924) suggested that by quick-stretching
(the SEC of) the muscle in the early phase of contraction,
the active state could be revealed. Ritchie (1954) and Edman
(1970) examined the time course of active state in a single
twitch by releasing the muscle to a shorter isometric length
at different times after a single stimulus, and by
identifying all the points on the curves where dP/dt=0 they
were able to delineate the rise and fall of the active
state. The "active state" hypothesis as originally proposed
by A. V. Hill is, however, controversial (Inbar and Adam,

1976; Jewell and Wilkie, 1958; Jewell and Wilkie, 1960), and
is now regarded only as a qualitative parameter of muscle
activity. The present study is not intended as a "revisit"
to "active state". The possibility that the externally
measured force does not always equal the force produced by
the contractile element, has its practical implications.
Studies that attempt to correlate isometric tension with
other parameters such as myosin phosphorylation, or aequorin
luminescence, have to first make sure that the isometric
tension is indeed a direct reflection of the mechanical
activity of the contractile apparatus and not a distorted
reflection due to internal movement occuring in isometric
contraction. The concept of "active state", for what it is
worth, probably is more applicable to smooth muscle than to
striated muscle. In skeletal muscle, it appears that most of
the series compliance of muscle is in the crossbridges
themselves (Bressler and Clinch, 1974; Ford et al, 1981).
The internal movement occurring during an isometric
contraction of skeletal muscle therefore mainly involves
straining of the crossbridges. In smooth muscle the SEC is
much more compliant than that of skeletal muscle (Hellstrand
and Johansson, 1979; Mulvany and Warshaw, 1981; Warshaw and
Fay, 1983). The source of the series compliance is believed
to be of both intra- and extracellular origins. The internal
movement occurring during an isometric contraction of smooth
muscle therefore is likely to involve filament sliding, or
internal shortening. If this is true, then the "isometric"

tension recorded during the rising and falling phases of isometric contraction cannot be regarded as isometric tension. In the present study, true isometric tension $[P_o(t)]$ is defined as the tension produced by the muscle when the velocity of the CE is zero. $P_o(t)$ is represented by the maximum tension (where $V=0$) of the F-V curve obtained at time t.

The validity of using the F-V curve to obtain the force generated by the CE needs to be discussed here. In the quick-release protocol (Fig. 2), after the rapid elastic length transient, the slower phase that follows represents shortening produced by the CE. Because the afterload (P) is constant in the protocol, $dP/dt=0$. Therefore the length of the SEC is constant (with respect to time) after the release. The shortening trace recorded therefore indicates the true length change (or velocity) of the CE. Every point in the F-V curve indicates the true velocity of the CE shortening under the corresponding load (including the zero velocity point). The maximum force that corresponds to zero velocity of CE therefore is the true isometric tension $[P_o(t)]$.

If indeed the reason underlying the difference between $P_o(t)$ and $P_o'(t)$ is internal movement of CE, then how does the CE movement cause tension decrease? In connection with the "active state" hypothesis, Hill (1922) proposes that stimulation always brings about development of maximum isometric tension, $P_o(t)$, even when the muscle is

shortening. However, some of the force is dissipated in overcoming a viscoelastic resistance if shortening occurs and therefore cannot be detected by external measurement. In this "viscoelastic" model, the force-velocity characteristics of muscle is thought to be due to the presence in muscle a "dashpot" that resists length change with a force whose magnitude is proportional to the speed of shortening. Because the F-V relationship in muscle is not linear, therefore the "constant" of proportionality (or the coefficient of viscosity of the dashpot) is a function of force (or velocity). This "viscoelastic" model is now discarded mainly because it fails to explain the Fenn effect (Fenn, 1924). Although it is not likely that a viscous element is totally responsible for the F-V characteristics of the muscle, complete absence of viscous force in contracting smooth muscle has yet to be proven. Viscous force is ubiquitous in any physical system that involves relative movement of solid and fluid. The interior of a muscle cell during contraction resembles such a system. The magnitude of the viscous force that is likely to be present in tracheal smooth muscle contraction, however, is not known.

Another explanation is provided by A. F. Huxley's 1957 model which predicts that the distribution of the attached crossbridges is velocity dependent. The number of positively strained crossbridges diminishes as the shortening velocity of the CE increases. The developed force diminishes still

faster because because some crossbridges which attached in the positive force region are carried by the sliding motion into the negative force region before detaching (formation of negatively strained crossbridges). This could account for the diffference observed between $P_o'(t)$ and $P_o(t)$. The existence of negatively strained crossbridges in smooth muscle is suggested by Somlyo et al (1986). Using the method of photolysis of caged ATP in skinned smooth muscle, they showed that the negatively strained crossbridges probably caused the initial transient tension increase upon laser photolysis of caged ATP in preshortened rigor muscle.

During the descending (relaxation) phase, the discrepancy of $P_o'(t)$ and $P_o(t)$ can also be explained by the 1957 model. During isometric relaxation, the CE is being stretched (by the SEC). This will put additional stress on the positively strained crossbridges, resulting in a higher measured isometric tension, $P_o'(t)$, than that predicted from the F-V relations, $P_o(t)$, that represents the true force generated by the CE at time t, when the velocity of CE is zero.

The latch bridge described by Dillon et al (1981) is another candidate that could be the cause of the observed muscle behavior. Latch bridges, by virtue of their slow intrinsic cycling rate, could impede the cycling rate of other normally cycling bridges. However, the experimental protocol used here is not suitable for testing this hypothesis because, at the plateau of contraction where

latch bridges are expected to form in a large number, the CE's movement is minimal. Therefore even with the latch bridges present, without CE movement, their impeding effect cannot be seen.

The observed difference between $P_o'(t)$ and $P_o(t)$ probably is due to a combination of the above mentioned mechanisms and may be some other unknown mechanisms. The emphasis of the present study is not placed on unravelling the mechanisms but rather on characterizing the functions $P_o'(t)$ and $P_o(t)$ in a quantitative way. To do that we first had to make sure that the isometric tension just before onset of load clamp $[P_o'(t)]$ did not vary too much from contraction to contraction. If the recorded isometric tension showed signs of deterioration during experiment, extra time was allowed for the muscle to recoup before the next measurement was made. Because only about 5 measurements were required for each F-V curve, it was possible to limit the variation of $P_o'(t)$ to within a 5% range. Without first showing statistically [Nair's method (Kennedy and Neville, 1976)] that the value of $P_o(t)$ (from the best-fitting curve) and the values of $P_o'(t)$ (from several contractions) belonged to different populations, attempting to show (using the paired t-test) that the value of $P_o(t)$ and the mean value of $P_o'(t)$ are different, would be meaningless.

As mentioned in the Introduction, the mechanical model shown in Fig. 1B is ideal for analyzing the pure mechanical features of muscle contraction. In an isometric

contraction, the forces counter-balancing the force generated by the CE are the external force $[P_o'(t)]$ applied through the SEC and internal "viscous" force stemming from the VE (Fig. 1B). Inertial force is small and can be neglected (Seow and Stephens, 1986). An expression for the relationship among the forces is:

$$P_o(t) = P_o'(t) + \delta \qquad [8]$$

where δ is the difference between force generated by CE and the external force. During the rising phase of an isometric contraction when internal shortening of the CE is occurring, according to the model (Fig. 1B) the "viscous" internal force has to be added to the externally measured isometric force to obtain the force produced by the CE [i.e., $P_o(t) = P_o'(t) + \delta$]. During relaxation when internal lengthening of the CE is occuring, however, the "viscous" force has to be subtracted from the externally measured isometric force to obtain the force generated by the CE [i.e., $P_o(t) = P_o'(t) - \delta$]. At the plateau of contraction the VE does not offer any resistance because there is no internal movement, and therefore external isometric tension equals the tension generated by the CE. The internal force (δ), therefore changes sign and magnitude depending on the direction and magnitude of the force applied to the VE of the muscle.

The difference between values of $P_o(t)$ and $P_o'(t)$ was substantial during the initial phase of contraction (Table 1). Therefore studies that attempt to compare the time course of isometric tension development to other parameters

such as myosin light chain phosphorylation, have to be
cautious. The true isometric tension developed by CE [$P_o(t)$]
has to be used in such comparison, instead of the external
isometric force [$P_o'(t)$], because the latter is strongly
influenced by the stiffness of the SEC (which could reside
extracellularly) and does not reflect directly the activity
of the contractile apparatus.

b) Time dependent F-V characteristics of the CE

The model shown in Fig. 1B was used in the last section
to describe the mechanical properties of muscle in isometric
contraction. It can also be used to describe muscle in
isotonic contraction. Eq. 8 used in the last section can
also be modified and used for isotonic contraction:

$$P_o(t) = P + \delta \qquad\qquad [9]$$

where P, which replaces $P_o'(t)$ in Eq. 8, is the external
isotonic load applied through SEC. When the internal
"viscous" force δ (whose magnitude is strongly velocity-
dependent) is replaced by the term $V(P+a)/b$, Eq. 9 becomes
Hill's equation (Eq. 3). Hill's equation, therefore, can be
understood as the balance between internal force, external
force and the force generated by the contractile apparatus.

Another way of analyzing the F-V data was presented in
Methods: The force step (P_o-P) and the corresponding
velocity (V) was related through a "constant" of
proportionality (α). By defining α appropriately
[$\alpha=(P+a)/b$], Hill's equation was obtained. Though the two
approaches may superficially seem different, they all stem

from the same model shown in Fig. 1B. As pointed out earlier, the model is only good for analyzing pure mechanical responses of muscle, so are the equations. Nevertheless they are extremely useful in analyzing experimental results.

The experimental results indicated that the F-V characteristics changed with time (Fig. 9-12, Table 2). To analyze those changes in a more insightful way, Eq. 5 and Eq. 6 $[(P_o-P)=\alpha V; \alpha=(P+a)/b]$ are used. The change in curvature of the F-V curve with respect to time (Table 2 and Fig. 12) can now be interpreted as the result of an increase in internal force with time that impeded the shortening velocity. This internal force could be, as discussed earlier, the formation of "latch" bridges, the change in viscous force, the redistribution of attached, possitively and neagtively strained, crossbridges (i.e., the change in $f(x)$ and $g(x)$ with time in Huxley' 1957 model), or a combination of the above factors, or, some still unknown factors. One immediate consequence resulting from the above finding of the time dependency of the F-V parameters is the invalidation of the conventional isotonic afterloaded method for obtaining F-V curve, because with isotonic afterloaded method the time variable is not held constant.

c) Time dependent series elasticity

Continuous measurement of the SEC stiffness in an isometric contraction using small sinusoidal length perturbations and measuring the amplitude and phase of the

resulting tension perturbations (Cecchi et al, 1982; Kamm and Stull, 1986) is not applicable to the present study because load on the SEC is not held constant during the measurement. (The load on the SEC in an isometric contraction is the isometric tension). With the use of such measurements it is found that the stiffness at plateau of contraction is higher than that early in contraction. If we were to conclude on this basis that more crossbridges were attached at the plateau phase than they were early in contraction, it would be erroneous. Because the stiffnesses were obtained at different portions of the non-linear stress-strain (or T-E) curve, they cannot be compared. To compare the SEC stiffness, either stress or strain of the SEC has to be specified. It is clear from Fig. 14 that the magnitude of E_o is relatively small and remains quite constant throughout contraction. This makes possible another way of comparing the SEC stiffness, which is to compare the slope of the stiffness-stress curves (the constant A in Eq. 7).

In tracheal smooth muscle, constant A is not a constant with respect to time, however (see Fig. 14), nor is isometric tension constant throughout the time course of contraction. The continuous measurement of the SEC stiffness using high-frequency length perturbations therefore involves a changing value of A with time and a changing isometric tension with time, and it can be described by a modified Eq. 7: $d\sigma/d\varepsilon = E_o + A(t) \cdot P_o'(t)$, where $A(t)$ is a time function

of constant A. The instantaneous isometric tension $P_o'(t)$ is the load on the SEC when the muscle is contracting isometrically. By plotting the dynamic stiffness $[E_o + A(t) P_o'(t)]$ and the isometric tension $[P_o'(t)]$ vs. time (Fig. 22), it can be found that there is a shift to the left of the stiffness curve compared with the isometric tension curve. This seems to suggest that the development of stiffness precedes the development of isometric tension. Similar results have been found in skeletal muscle (Cecchi et al, 1982; Ford et al, 1986) and smooth muscle (Dillon and Murphy, 1982; Kamm and Stull, 1986). Their interpretation is that a long-lived state exists between crossbridge attachment and force generation. Our experiment seems to confirm the existence of such a state in our preparation, because at 0.5 s after the onset of stimulation, while no development of isometric tension can be observed, there is a significant increase in the SEC stiffness estimated by the value of $E_o + A\sigma$ (Student's t test, $p < 0.05$). However, the shift to the left of the stiffness curve cannot be totally explained by the existence of the long-lived crossbridge state. Mathematically speaking, it is the time dependence of constant A that prevents the superimposition of the stiffness and isometric tension curves. If we assume that A is constant with respect to time, then the continuous (or dynamic) stiffness $[E_o + A \cdot P_o'(t)$; note that function $A(t)$ here is assumed to be a constant with respect to time; that is, A] is proportional to the isometric tension, and by

plotting the two curves and selecting the "proper" scales, the two curves can be made to superimpose. Therefore it is the behavior of the function A(t) that determines how the stiffness curve is going to differ from the isometric tension curve. In the experiment it is the fact that the value for A(t) is greater early in contraction compared with the A(t) value at the plateau of contraction that results in the left-shift of the stiffness curve. What could the function A(t) represent physiologically then?

As mentioned earlier, since the value of E_o is relatively small and time independent, constant A directly reflects the SEC stiffness (at any stress level), which could be directly related to the number of attached crossbridges. Therefore the left-shift of the stiffness curve could partly be due to the fact that the number of attached crossbridges is greater early in contraction than that at plateau.

It is interesting to note that the zero-load velocity of the muscle (Fig. 14, dashed line) and the constant A vary in a very similar manner with time. The peak velocity and peak stiffness both occur at 2 s after stimulation. Dillon et al (1981) found that both shortening velocity and phosphorylation of myosin light chain (LC20) varied in a similar manner with time. Kamm and Stull (1986) also obtained similar results in bovine tracheal smooth muscle. These findings together with the present results [that showed stiffness (constant A) and zero-load velocity varied

in a similar way with time] suggest that myosin phosphorylation, maximum shortening velocity, and stiffness (or number of attached crossbridges) of smooth muscle are intimately related.

Stiffness of the SEC during contraction falls within the limits of the stiffness of resting muscle and that of muscle in rigor (Fig. 13 and Table 3). This is in agreement with the X-ray diffraction studies of striated muscle in which it is found that "the changes in structure that occur when a relaxed muscle is activated are in the direction of those changes that occur when a relaxed muscle goes into rigor" (Squire, 1981). Studies on the rate of oxygen uptake in tracheal smooth muscle (Stephens and Skoog, 1974) indicate that early in contraction the oxygen uptake rate is more than three time higher than that in plateau phase. This seems to support the notion that the number of active crossbridges is greater early in contraction. Of course the high oxygen uptake rate could also be the result of the high crossbridge cycling rate early in contraction [according to Eisenberg and Hill (1985)].

d) Velocity-length-time relations

In skeletal muscle (single fiber) there seems to be a length range over which the shortening velocity is relatively constant. Edman (1979) reported that this range was from 1.65 to 2.7 µm of the sarcomere length. In cardiac muscle this range is somewhat smaller (Brutsaert et al, 1971). Under normal physiological conditions, skeletal and

cardiac muscle are probably operating in or near the constant-velocity length range. In smooth muscle, a physiological working length range is hard to define. In airway and vascular smooth muscle, from a pathological point of view, it is the behavior of the muscle near l_{min} that seems to be important. [Asthma and essential hypertension in animal models seem to be associated with an increased ability of the smooth muscle to shorten (Antonissen et al, 1979; Kepron et al, 1977; Packer and Stephens, 1985).] Although in real life smooth muscle probably never shortens under zero load and therefore never reaches l_{min}, there are data to suggest that a muscle can shorten more under a finite load also possesses a shorter l_{min} (Antonissen et al, 1979; Seow, 1989). This study focused on the velocity behavior that was length dependent at short muscle lengths. However, the relatively length-independent shortening velocity near l_o could be seen in both Figs. 15 and 16.

Although the parabolic equation $V_o(l) = V_{max}\{1-[(1-l)/(1-l_{min})]^2\}$ is purely empirical, it helps in simplifying the data analysis and in constructing V_o-l curves out of the V_{max} and l_{min} data. The fact that the V_o-l curve was smooth and continuous and not like that reported by Edman (1979), which consisted of a linear ascending phase and a flat plateau, probably was because our muscle preparation was multicellular. The asynchronous contraction of the individual cells and the effect of the non-muscle components in the preparation, such as connective tissues, could

"smooth out" the V_o-l curve. However, that does not exclude the possibility that the lack of a length-independent velocity region in smooth muscle is due to a more fundamental difference in the structure of the contractile apparatus. The recent finding that smooth muscle shortens in a corkscrew-like fashion (Warshaw et al, 1987) suggests that the contractile apparatus is helically oriented within the cell. The effect of this helical arrangement on the velocity-length relations needs further investigation. The behavior of the curve beyond l_o was not examined; therefore a plateau for the curve at $l > l_o$ is not excluded.

The fact that a parabolic curve fits the V_o-l curve implies that the change in V_o due to the change in l (dV_o/dl) is linearly related to the deviation of the muscle length from its optimum (l_o-l). That is, $dV_o/dl \propto (l_o$-l$)$. By putting in a constant of proportionality and integrating the differential equation (providing that $V=0$ when $l=l_{min}$ and expressing all the lengths as fractions of l_o), a parabolic function of the same form as the one we used to fit the V_o-l data, can be obtained.

The factors that cause the drop in the shortening velocity at $l < l_o$ could be many. One well observed phenomenon is shortening inactivation. This has been described in skeletal (Taylor and Rudel, 1970), cardiac (Brutsaert et al, 1971; Jewell and Blinks, 1968) and smooth muscles (Stephens et al, 1984). This inactivation can be alleviated by increasing the extracellular calcium concentration. A

reduced tension due to shortening inactivation could affect the shortening velocity. This may sound contradictory to Huxley's 1957 model. However, if the muscle shortens to such an extent that it compresses its internal structures, which in turn creates an internal load on the contractile apparatus, then the zero load will no longer be so, although the external load is zero. Under such circumstances, a reduced tension will result in a reduced shortening velocity. An internal viscoelastic load in actively shortening cat papillary muscle was well described by Chiu et al (1982). A reduced tension at short muscle lengths, due to the muscle operating on the ascending phase of the muscle's length-tension curve, could also reduce the shortening velocity if there is an internal load. A recent study by Gunst (1986) on the effect of length history on contractile behavior of tracheal smooth muscle showed that the initial muscle length and the shortening process per se affected the rate and magnitude of force redevelopment. This suggests that different velocity-length-time surfaces would be obtained if contraction started at different initial lengths. In this study, contraction always started at l_o.

In contrast to V_{max}, l_{min} is relatively time independent. This probably indicates that the maximum amount of shortening produced by a muscle is largely determined by the physical properties of passive components of the muscle whose mechanical properties do not change with time, but not the state of the contractile apparatus. However, the

interaction of actin with myosin may be relatively inhibited because of the deformation of the cytoskeletal protein network and the packing of the filaments at short muscle length. In this case, the real factor that determines l_{min} would still be the non-contractile component of the muscle. Changes in l_{min} associated with pathological changes in smooth muscle function such as those found in canine asthmatic and rat essential hypertension models (Antonissen et al, 1979; Kepron et al, 1977; Packer and Stephens, 1985) therefore probably involve alterations in non-contractile components of the muscle, such as cytoskeletal proteins.

The time dependence of smooth muscle shortening velocity has been described earlier. Although controversies still exist as to the cause of this time dependency, one explanation proposed by Dillon et al (1981) is the formation of the so called "latch" bridges that impede the shortening velocity.

Unloaded shortening velocity of muscle is generally regarded as an index of the maximum intrinsic crossbridge cycling rate. However, many non-mechanical factors such as pharmacological or biochemical ones, can affect this cycling rate. To study their effect, one should make allowances for the dependency of shortening velocity on length and time, especially when isotonic contractions are involved. To give the reader an integrated view, a 3-dimensional plot of the velocity-length-time surface is shown in Fig. 23. Given time and muscle length, a corresponding zero-load velocity can be

found on the surface. The surface is therefore particularly useful in predicting the time behavior of unloaded shortening velocity in isotonic contractions.

e) Stiffness-length-time relations

The main finding in this part of the studies was that the SEC stiffness of canine tracheal smooth muscle increased as muscle length decreased. The increase in stiffness was not likely due to an increase in the number of attached crossbridges, because no evidence has been found in either smooth or striated muscle to indicate that the number of attached crossbridges increased as muscle shortens below l_o. On the contrary, evidence gathered from length-tension studies (Close, 1972; Edman, 1966; Ramsey and Street, 1940) indicated that tension decreased at short muscle lengths, suggesting that the number of attached crossbridges decreased when muscle shortened below its optimum length.

One possible explanation for the observed increase in stiffness at short lengths is that the part of the muscle structure that constitutes the SEC becomes shorter when muscle shortens. The ultrastructure of smooth muscle is not as well revealed as that for skeletal muscle. However, as mentioned earlier, it is generally believed that the sliding filament mechanism also is responsible for smooth muscle contraction (Somlyo et al, 1984). This implies the existence of overlap (between thick and thin filaments) and non-overlap zones in smooth muscle. Could this non-overlap zone be part of the SEC in smooth muscle? Compared to smooth

muscle, the non-overlap zones in skeletal muscle seem to contribute little to the series compliance (Bressler and Clinch, 1975; Ford et al, 1981; Julian and Morgan, 1981). The SEC of skeletal muscle is also stiffer than that of smooth muscle. The SEC length at maximum isometric tension for various types of smooth muscle varies somewhere from 7% to 20% of the optimum muscle length (l_o) (Herlihy and Murphy, 1974; Johansson, 1973; Lundholm and Mohme-Lundholm, 1966), while in skeletal muscle it is less than 1% (Sugi and Suzuki, 1980; Woledge et al, 1985). Also the thin/thick filament ratio for smooth muscle is much greater than that for skeletal muscle (Somlyo et al, 1984; Woledge et al, 1985). For example, the ratio is about 15:1 in rabbit portal vein compared to the ratio of 2:1 in frog sartorius. It is possible that a significant part of the series compliance in smooth muscle is of non-crossbridge origin, unlike that in skeletal muscle.

The theoretical relationship between the various sources of series compliance and the apparent muscle stiffness was well described by Ford et al (1981) for striated muscle. The description is probably valid for smooth muscle if one accepts that the sliding-filament, cycling-crossbridge mechanism is responsible for smooth muscle contraction. At $l < l_o$, the extensibility of the thin filament is critical in determining the behavior of the apparent muscle stiffness with respect to length. If we assume that the non-overlap portion of the thin filaments

contributes to the series compliance of the muscle, then as the muscle shortens, an apparent increase in muscle stiffness would be observed due to the diminution of the non-overlap portion. A shorter SEC will produce a smaller length response when it is subjected to a constant load step. In other words, the change in SEC length (ΔL) due to a constant load step is directly proportional to the SEC length itself (L). It follows that muscle stiffness must be inversely proportional to the SEC length. Our experiments (Fig. 20) showed that indeed stiffness and 1/[SEC length] are highly correlated ($r=0.945$). This suggests that in canine trachealis, the increase in SEC stiffness may be due to a decrease in SEC length itself, and the decrease in SEC length may be associated with the diminution of the non-overlap zones during contraction.

Additional evidence supporting the notion that the increase in muscle stiffness was due to the non-overlap portion of the thin filaments comes from the observation that the initial elastic modulus (E_o) increased as the muscle length decreased, or as the non-overlap portion diminished. Table 1 shows that E_o and 1/L values have a very high correlation coefficient ($r=0.9934$). Theoretically, spring stiffness (k) at different spring lengths (under a constant tension) can be expressed as $k(L_o/L)$, where L_o is a reference length at which the k value is obtained, and L is any given length. For example if $L=0.5\ L_o$, then the spring will appear to be twice as stiff as the spring with length

L_o. The muscle's SEC can be regarded as a spring with stiffness characteristics described by Eq. 7 ($k = E_o + A\sigma$). If we assume that the SEC length becomes shorter as muscle shortens, as it would in the case when the non-overlap portion of the thin filaments contribute to series compliance, then the SEC stiffness at different SEC lengths can be expressed as $(E_o + A\sigma)(L_o/L)$, where L_o is defined as the SEC length when the muscle length is l_o, and L is any given SEC length. From the above expression, the initial elastic modulus at short SEC length ($L < L_o$) is: $(E_o)(L_o/L)$. Therefore, if the above assumption regarding the source of the series compliance is true, the initial elastic modulus should be inversely proportional to the SEC length (L). Our experimental data (Table 5) show that E_o values obtained at different L's correlate very closely to the 1/L values, supporting the above assumption that the non-overlap portion of the thin filaments constitutes part of the muscle's SEC, and the SEC length decreases as muscle shortens. Previous results (Fig. 14) showed that if muscle length was held constant, the E_o value remained constant throughout contracton although the overall SEC stiffness changed with time during contraction.

Stiffness change during an isotonic contraction can be attributed to at least two variables: time and length. The time effect on stiffness while muscle length and stress were held constant, was examined in previous sections (Fig. 14; Table 3). Zero load (or near zero load) shortening velocity

of smooth muscle (an index of crossbridge cycling rate) has been shown to vary with time (Figs. 11 and 14). Dillon et al (1981) showed that in vascular smooth muscle, shortening velocity and myosin light chain (LC 20) phosphorylation varied in a similar manner during an isometric contraction. Kamm and Stull (1986) showed that stiffness also varied with myosin light chain phosphorylation during the initial phase of contraction in smooth muscle. This evidence suggests that the number of active crossbridges could vary during the time course of smooth muscle contraction, and give rise to the observed change in stiffness (Fig. 14). The difference between the stiffness vs. length curves shown in Fig. 20 and Fig. 21 is that the former was obtained when time variable was fixed, while the latter was obtained during an isotonic contraction in which both time and muscle length changed. The difference in values between the two curves can be attributed to the time variable, which could be associated with the variation of the number of attached crossbridges during contraction. Comparing the curves in Fig. 20 and Fig. 21, it can be seen that stiffness (at any given length) was greater early in contraction than that at the plateau of contraction (10 s). This is in agreement with the previous finding (Fig. 14; Table 3) that stiffness (at a specific stress and muscle length) increased rapidly during contraction, reached the peak within about 2 s after onset of contraction, and then gradually decreased as contraction proceeded. During relaxation there was a rapid decrease in

muscle stiffness shortly after the termination of stimulus, followed by a more gradual decrease in stiffness as the muscle lengthened (Fig. 21). Stiffness (at any length) at the plateau of contraction was greater than that during relaxation. This suggests that the number of attached crossbridges was less in a relaxing muscle.

Inactivation is another phenomenon that is associated with muscle shortening (Jewell and Blinks, 1968; Stephens et al, 1984; Taylor and Rudel,1970). Taylor and Rudel (1970) observed that myofibrils in the core of frog semitendinosus fibres became "wavy" at short muscle lengths during active shortening, and appeared not to contribute to the generation of active tension. Inactivation at short lengths was also observed in tracheal smooth muscle (Stephens et al, 1984). Inactivation is always associated with decrease in isometric tension, which has a positive correlation with stiffness. Therefore it is highly unlikely that the increase in stiffness at short muscle lengths observed in our experiments (Fig. 20 and Fig. 21) could be due to shortening inactivation.

The values of the SEC stiffness measured by the two methods, namely the force perturbation and load clamp methods, are comparable. The force perturbation method measures the stiffness at a single stress level while the load clamp method gives the whole stress-strain characteristics of the SEC. The force perturbation only provides a means of estimating the stiffness ($\Delta P/\Delta L$). By

definition stiffness is the limit of $\Delta P/\Delta L$ when ΔL is infinitesimally small. But, for purpose of this study, stiffness estimated by $\Delta P/\Delta L$ (with a finite ΔL) is accurate enough. In fact it showed no statistical difference when compared to the stiffness calculated from quick-release method under the same experimental conditions (time, stress) (Table 3).

For the load clamp method, data obtained by quick-release and those obtained by quick-stretch fall onto the same curve that characterizes the stress-strain relations of the SEC (Fig. 19). The continuity of the data suggest that the behavior of the SEC is independent of the direction of the force applied to it. However, it was observed in the experiments that if the afterload was too large when stretching, the muscle's stiffness would suddenly appear to decrease and the data would start to deviate from the curve. The "yield point" of the SEC occurred when the afterload was about twice as large as the load on muscle before the load clamp. In the experiments large afterloads were avoided when stretching the muscle, because large loads could potentially break the crossbridges and cause sliding of the thick and thin filaments in the direction opposite to contraction. Under such circumstance if the observed "elastic length transient" were taken as the length change of the SEC, the SEC compliance would be overestimated.

A viscoelastic multi-segment model similar to the one used by Sugi and Kobayashi (1984) is worth mentioning here.

Although the model was developed for skeletal muscle, it was never very popular in the field of skeletal muscle mechanics. This was due to the findings that the crossbridges were the major source of series compliance in skeletal muscle (Bressler and Clinch, 1975; Ford et al, 1981; Huxley and Simmons, 1971). Julian and Morgan (1981), however, found that by assuming a small filament compliance, a better fit between the experimental data and the theoretical calculations could be obtained. The usefulness of the model is that it relates the SEC to subcellular structures of the muscle. The model is basically a Voigt model, with a length dependent SEC. A Maxwell model can also be used. In using either model, one has to accept that stiffness of the SEC is non-linear (stress dependent) and, as this study indicated, the SEC was also length dependent for tracheal smooth muscle. The length dependency of the SEC in vascular smooth muscle was also found by Cox (1978).

The increase in muscle stiffness in shortened airway smooth muscle may have important physiological implications. It may stabilize the airways by preventing the narrowed airways from collapsing.

f) Conclusions

1) The maximum tension obtained from extrapolating the F-V curve [$P_o(t)$] is greater than the directly measured isometric tension [$P_o'(t)$] during contraction and is less during relaxation. $P_o(t)$ equals $P_o'(t)$ at the plateau of contraction where $dP/dt=0$. The difference between $P_o(t)$ and

$P_o'(t)$ is likely due to the internal movement of the CE during ascending and descending phases of isometric contraction.

2) The reduction in tension associated with the CE movement could be due to the velocity-dependent distribution of the number of attached (both possitively and negatively strained) crossbridges as predicted by Huxley' 1957 model. It could also be partly due to the muscle's intrinsic viscous element that is in parallel with the contractile element. Formation of the "latch" bridges is another possible cause that could account for the movement-associated tension loss.

3) The relations between tension loss and CE movement are further characterized by allowing the muscle to shorten against constant loads that are less than the isometric tension and hence obtaining the F-V curve. The change of F-V characteristics with time is probably caused by a progressive increase in "internal resistance" to shortening during contraction. Formation of the "latch" bridges during contraction could account for this resistance increase. A change, with respect to time, in the association and dissociation constants in the crossbridge cycle [$f(x)$ and $g(x)$ in Huxley' 1957 Model] could also cause the increase in the apparent internal resistance to shortening.

4) The length-dependent unloaded velocity can be described by a parabolic function with constants V_{max} and l_{min}. V_{max}, however, is not a constant with respect to time: Upon

stimulation there is a transient increase in V_{max}. l_{min} is time independent. V_{max} appears to be governed by the degree of myosin phosphorylation whereas l_{min} probably is determined by passive mechanical properties of the muscle.

5) The time-dependent behavior of the SEC is best seen when the effect of stress is held constant or eliminated. A phasic time behavior of the SEC stiffness is revealed by the change in the slope of the stiffness-stress curve (constant A) with time. If the stress is allowed to increase with time as it does during an isometric contraction, a monotonic increase in the SEC stiffness would be observed (as in dynamic stiffness measurements). The stiffness of the muscle in rigor state is much higher than that at resting state. The stiffness of normal muscle during contraction varies significantly with time but within the limits of the stiffness of muscle in rigor and that at resting state.

6) The SEC stiffness of tracheal smooth muscle increased as muscle length decreased. The increase in SEC stiffness correlated very closely to the decrease in the SEC length itself. This suggested that the diminution of the length of SEC is the cause of the apparent increase in the SEC stiffness, and also the source of the SEC could include the non-overlap portion of the thick- and thin-filaments.

TABLES

P_o and P_o' Values During Isometric Contraction

Exp.	1	2	3	4	5	6	mean±SE	t-test
0.6 sec								
P_o	---	16.0	25.5	---	12.9	---	18.1±3.8	
P_o'	---	22.4	50.0	---	24.0	---	32.1±8.9	P<0.025
1 sec								
P_o	26.1	42.9	58.3	25.1	37.8	66.6	42.8±6.9	
P_o'	27.3	51.2	85.0	40.5	66.1	89.6	60.0±10.1	P<0.01
2 sec								
P_o	65.2	107.2	126.5	81.6	101.1	142.2	104.0±11.5	
P_o'	80.4	128.0	165.0	108.1	135.1	162.4	129.8±13.2	P<0.005
4 sec								
P_o	80.4	160.9	172.1	169.2	154.9	179.4	152.8±14.9	
P_o'	91.3	172.8	215.0	196.0	177.2	195.9	174.7±17.8	P<0.005
7 sec								
P_o	113.0	202.7	203.2	214.0	188.8	199.6	186.9±15.1	
P_o'	120.4	215.5	220.0	217.8	195.2	218.4	197.9±15.9	P<0.005
10 sec								
P_o	140.3	222.3	215.0	216.4	200.5	212.5	201.2±12.5	
P_o'	140.3	223.6	215.0	216.2	201.7	212.8	201.6±12.6	N. S.
13 sec								
P_o	130.5	198.7	164.3	---	140.9	---	158.6±15.1	
P_o'	111.9	174.0	151.4	---	116.9	---	138.6±14.7	P<0.005
17 sec								
P_o	55.9	97.9	96.2	---	75.8	---	81.5±9.9	
P_o'	43.3	78.0	86.7	---	54.2	---	65.6±10.1	P<0.01

Table 1. Values of directly measured isometric tension (P_o') and maximum force extrapolated from F-V data (P_o) at various times after onset of stimulation. Each pair of data was tested by the Student's paired t-test for the null hypothesis. P_o and P_o' are measured in mN/mm^2.

F–V Parameters at 2 and 8 s in Contraction

	2 s	8 s	t Test
$a\pm$SE, mN/mm^2	23.07±1.84	47.32±4.04	$P < 0.005$
$b\pm$SE, l_o/s	0.0713±0.0061	0.0775±0.0024	NS
$P_o\pm$SE, mN/mm^2	108.4±8.5	146.9±11.4	$P < 0.005$
$V_o\pm$SE, l_o/s	0.356±0.0429	0.2488±0.0304	$P < 0.005$
$a/P_o\pm$SE	0.2170±0.0197	0.3387±0.0569	$P < 0.025$

Table 2. Force-velocity parameters at 2 and 8 s in contraction. Values are means±SE for 5 trials. Student's paired t-test was used to test the null hypothesis.

Values of Constants A, E_o and P_o'

Muscle Condition	Exp No.				Means ± SE
	1	2	3	4	
P_o', mN/mm²	224.7	205.7	236.7	221.0	222.0±6.4
Resting					
A	20.0	36.5	40.0	55.0	37.9±7.2
E_o	30.0	76.6	20.8	16.5	36.0±13.8
After stimulation, s					
0.5					
A	21.0	55.0	47.0	63.0	46.5±9.1
E_o	31.5	115.5	31.9	18.3	49.3±22.3
1.0					
A	29.0	67.0	66.0	73.0	58.8±10.1
E_o	43.5	140.7	44.9	21.2	62.6±26.6
2.0					
A	42.0	78.0	78.0	102.0	75.0±12.4
E_o	50.4	109.2	32.8	9.2	50.4±21.3
3.0					
A	38.0	70.0	77.0	86.0	67.8±11.0
E_o	60.8	168.0	38.5	13.76	70.3±34.0
5.0					
A	36.0	61.0	67.0	78.0	60.6±8.9
E_o	54.0	128.5	34.8	14.8	58.0±25.0
7.0					
A	35.0	56.0	56.0	78.0	56.3±8.8
E_o	52.5	145.6	31.36	7.8	59.3±30.2
10.0					
A	34.0	53.5	56.0	78.0	55.4±9.0
E_o	47.6	112.4	39.2	7.8	51.7±22.0
Rigor					
A	66.0	155.0	138.0	180.0	134.8±24.5
E_o	26.4	46.5	27.6	18.0	29.6±6.0

Table 3. Constants A, E_o, and P_o' from four experiments. l_o, optimum muscle length; P_o', isometric tension (in SEC). Constant A (slope) is measured in l_o^{-1}; constant E_o (initial elastic modulus) is measured in mN/(mm²·l_o).

V_{max} and l_{min} Values

Exp. No.	#1	#2	#3	#4	#5	#6	#7	#8	MEAN±SE
After stimulation,s				V_{max} (l_o/s)					
1	.357	.351	.259	.288	.303	.349	.440	.350	.337±.019
2	.527	.516	.466	.502	.422	.570	.600	.470	.509±.020
3	.519	.507	.457	.491	.416	.565	.590	.460	.500±.020
4	.453	.444	.374	.408	.369	.480	.530	.400	.432±.019
5	.438	.430	.358	.489	.359	.456	.510	.406	.431±.019
6	.423	.415	.338	.370	.349	.437	.500	.340	.396±.020
7	.408	.402	.321	.351	.339	.417	.490	.380	.388±.019
8	.393	.387	.302	.333	.328	.397	.470	.370	.373±.018
9	.372	.367	.278	.306	.312	.368	.450	.360	.352±.019
10	.364	.359	.261	.296	.309	.359	.450	.360	.345±.020
				l_{min} (%l_o)					
	.365	.240	.381	.343	.310	.200	.200	.330	.296±.026

Table 4. V_{max} and l_{min} values for 8 experiments. V_{max},
maximum shortening velocity at optimum muscle length (l_o);
l_{min}, minimum muscle length.

Stress-Strain Parameters at 4 Muscle Lengths

Exp. No.	1	2	3	4	5	mean±S.E.
P_o', mN/mm²	223	181	235	197	208	208±9.5
l, l_o	.54	.682	.67	.706	.709	.661±.031
L, l_o	.0093	.0103	.0044	.0143	..0103	.0097±.0016
A, l_o^{-1}	104	122	175	150	145	139.2±12.2
E_o, mN/mm²·l_o	707.2	439.2	1750	195.0	435.0	705±273.5
r^2	.9920	.9990	.9608	.9978	.9944	.9888±.0071
l, l_o	.747	.76	.847	.873	.875	.820±.028
L, l_o	.0191	.0150	.0282	.0291	.0188	.0220±.0028
A, l_o^{-1}	115	98	102	71.5	82.5	93.8±7.6
E_o, mN/mm²·l_o	161	264.6	71.4	100.1	231.0	165.6±36.9
r^2	.9988	.9916	.9676	.9988	.9984	.9910±.0060
l, l_o	.87	.92	.94	.94	.96	.926±.015
L, l_o	.0450	.0386	.0583	.0572	.0326	.0463±.0051
A, l_o^{-1}	70	65	75	53	59.5	64.5±3.86
E_o, mN/mm²·l_o	35	52	11.3	26.5	104.1	45.8±16.0
r^2	.9888	.9966	.9948	.9976	.9984	.9952±.0017
l, l_o	1.0	1.0	1.0	1.0	1.0	1.0±0.0
L, l_o	.0875	.0688	.0874	.0799	.0715	.0790±.004
A, l_o^{-1}	54	50	54.5	49	50	51.5±1.1
E_o, mN/mm²·l_o	5.4	15	5.5	9.8	15	10.1±2.1
r^2	.9996	.9988	.9896	.9928	.9982	.9958±.0020
r (E_o, $1/L$)	.9786	.9984	.9979	.9932	.9989	.9934±.0040

Table 5. Stress-strain relations of SEC obtained by quick releasing and quick stretching muscle at four different muscle lengths. P_o', isometric tension (in SEC); l_o, optimum muscle length; l, muscle length measured in l_o; L, series elastic component (SEC) length measured in l_o; A and E_o, constants from fitting stress-strain curve of SEC (Eq. 8), measured in l_o^{-1} and mN.mm⁻².l_o^{-1}, respectively; r^2, coefficient of determination for fitting SEC stress-strain curve (for obtaining A, E_o values); r (E_o, $1/L$), correlation coefficient of E_o and $1/L$ values.
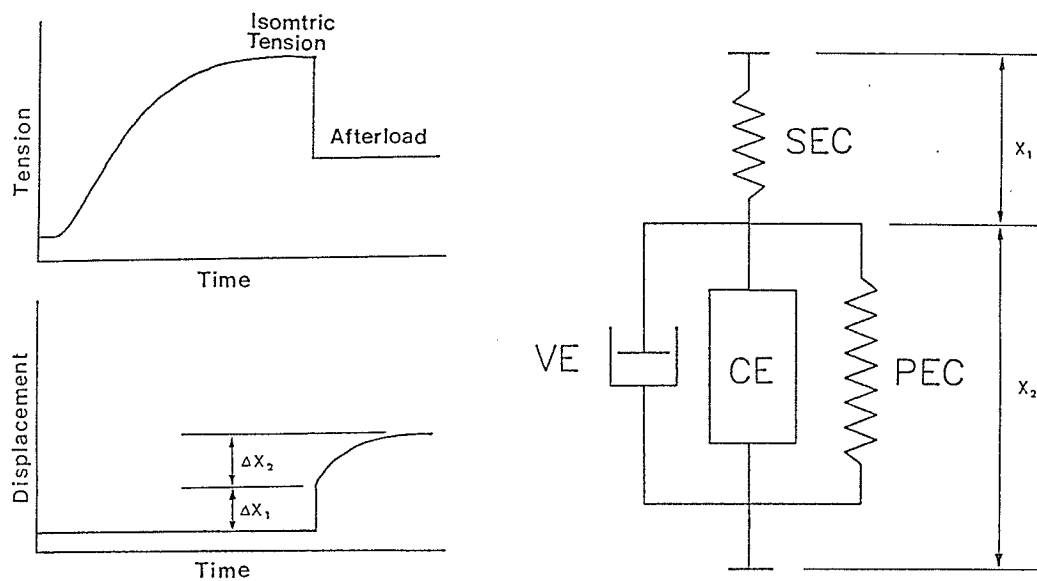
FIGURES

Figure 1. A: Idealized tension and displacement records of a quick-release experiment. B: Conceptual model of muscle. ΔX_1 and ΔX_2 represent displacements (after quick-release) of X_1 and X_2 respectively. For detailed description, see text.
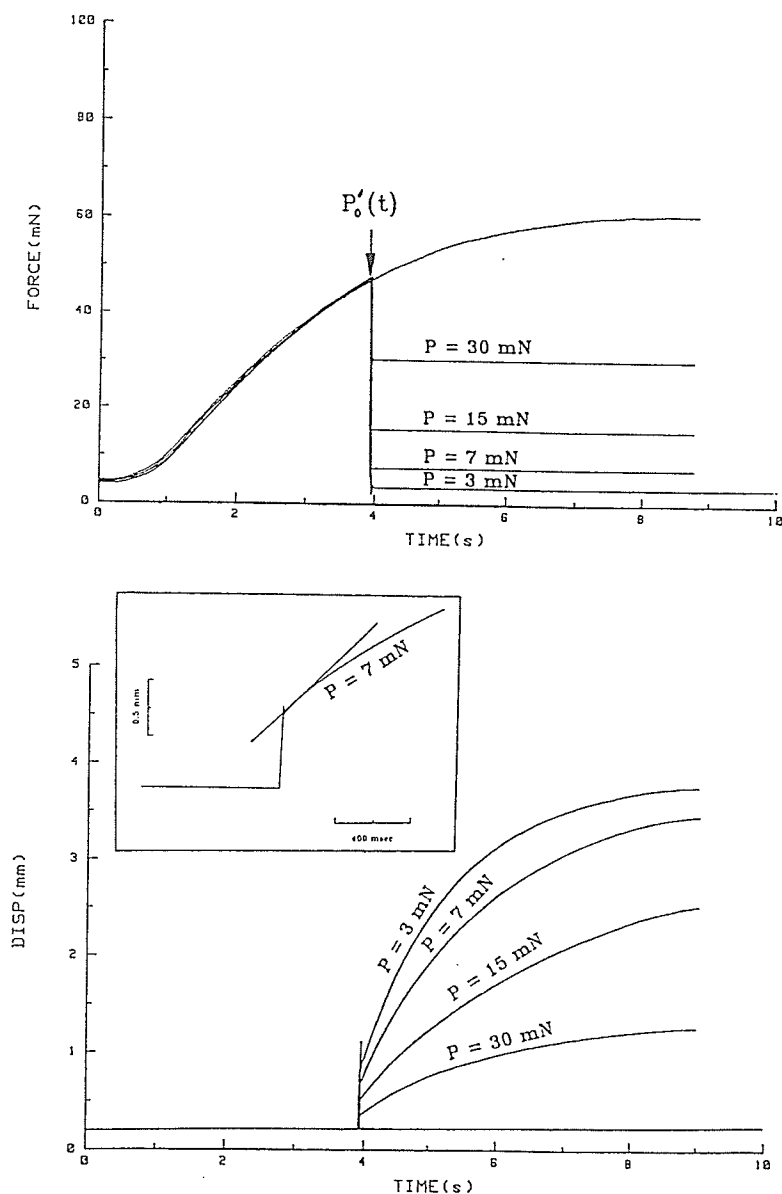
Figure 2. Actual experimental records of force and displacement (DISP) traces (superimposed). Signals from force and displacement transducers were recorded simultaneously. Four quick releases are shown in the figure. The constant loads (P) after quick-release are labelled on the traces. Small inset is a magnified displacement-time curve and shortening velocity after quick-release was obtained by measuring slope of curve as shown. $P_o'(t)$, isometric tension measured at time t.

$$V=b(Po-P)/(P+a)$$

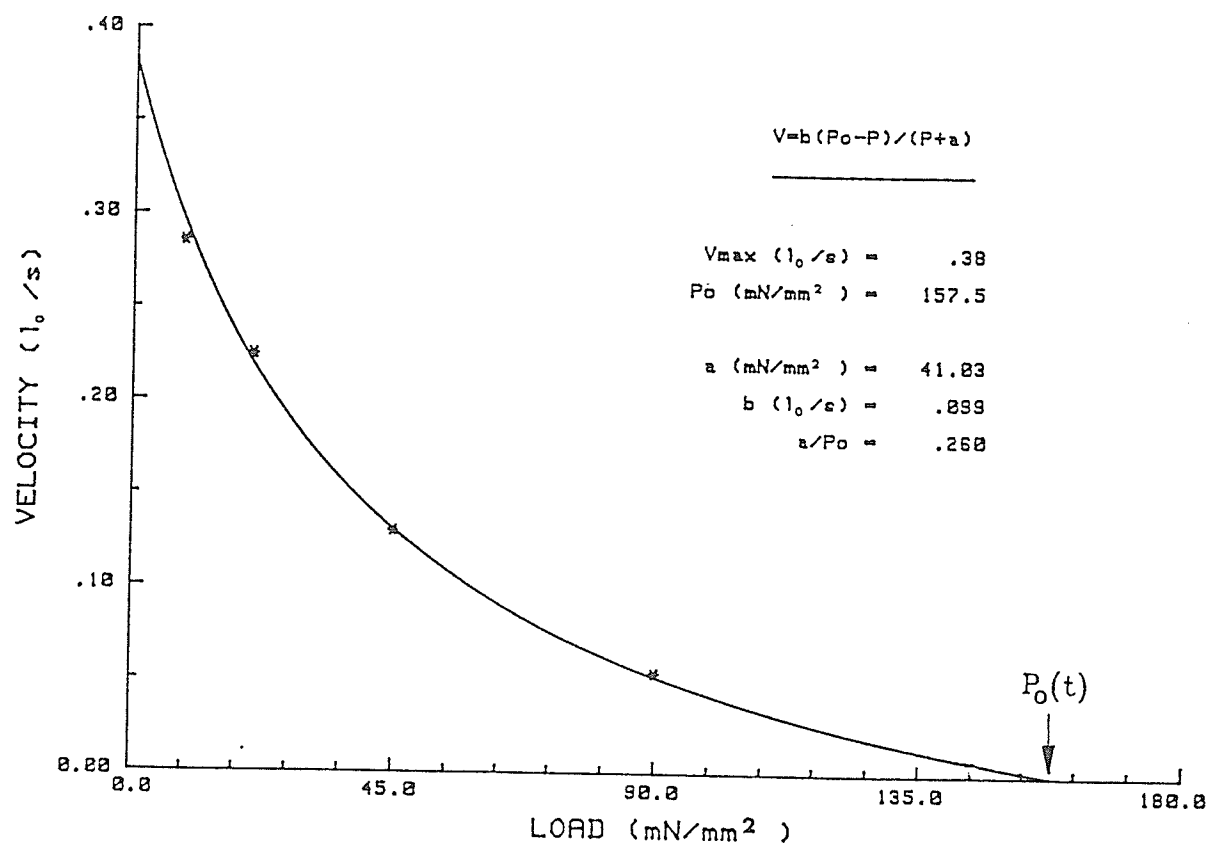|		
Vmax (l_o/s) =	.38	
Po (mN/mm^2) =	157.5	
a (mN/mm^2) =	41.83	
b (l_o/s) =	.099	
a/Po =	.260	

Figure 3. Force-velocity curve obtained from quick-release experiment such as the one shown in Fig. 2. Hill's hyperbolic equation was used to fit the data. $P_o(t)$, maximum isometric tension extrapolated from F-V curve obtained at time t.
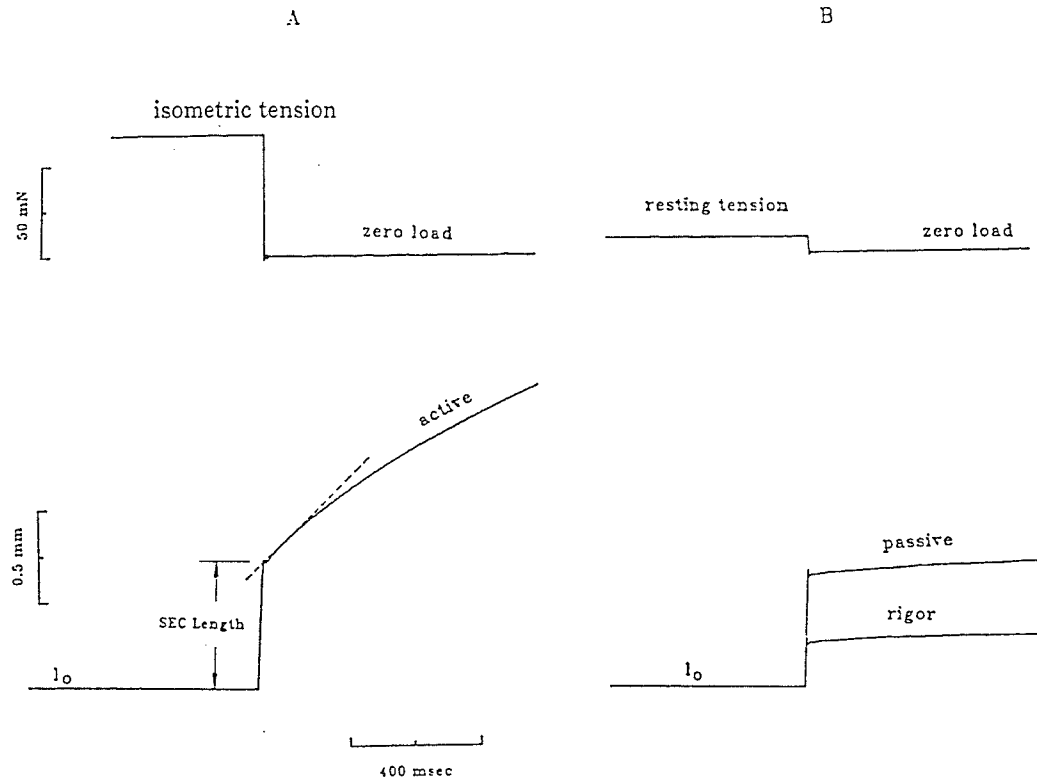
A   B

Figure 4. A: Simultaneous records of tension and displacement of muscle contraction. Muscle was quick-released from isometric tension to various afterloads. This procedure was repeated at different points in time in contraction (not shown). Series elastic component (SEC) length and velocity was measured as illustrated. B: Similar records as in A, but releases were from resting tension and muscle was not stimulated. Some slow shortening was observed after releasing muscle (after quick transient), although shortening velocity was much less than that of active shortening. Slow phase shortening probably was result of returning of the parallel elastic component to equilibrium position countered by internal viscous resistance. l_o, optimum muscle length.

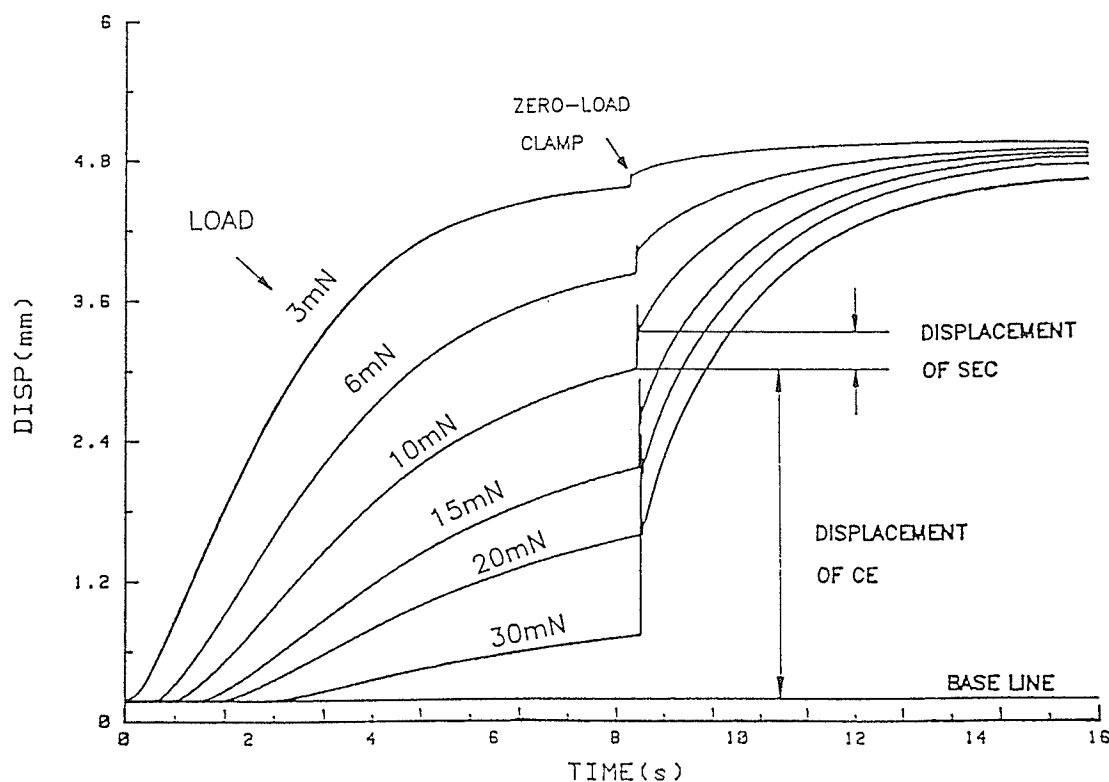Figure 5. Experimental records (superimposed) for obtaining zero-loading velocity-length curve. Muscle length was obtained by subtracting displacement (DISP) of muscle immediately after load clamp from optimum length (e.g., 10-mN curve). Velocity was obtained by measuring slope of displacement curve 100 ms after zero-load clamp., as shown in the inset. Optimum muscle length was 8.5 mm and weight was 2 mg.
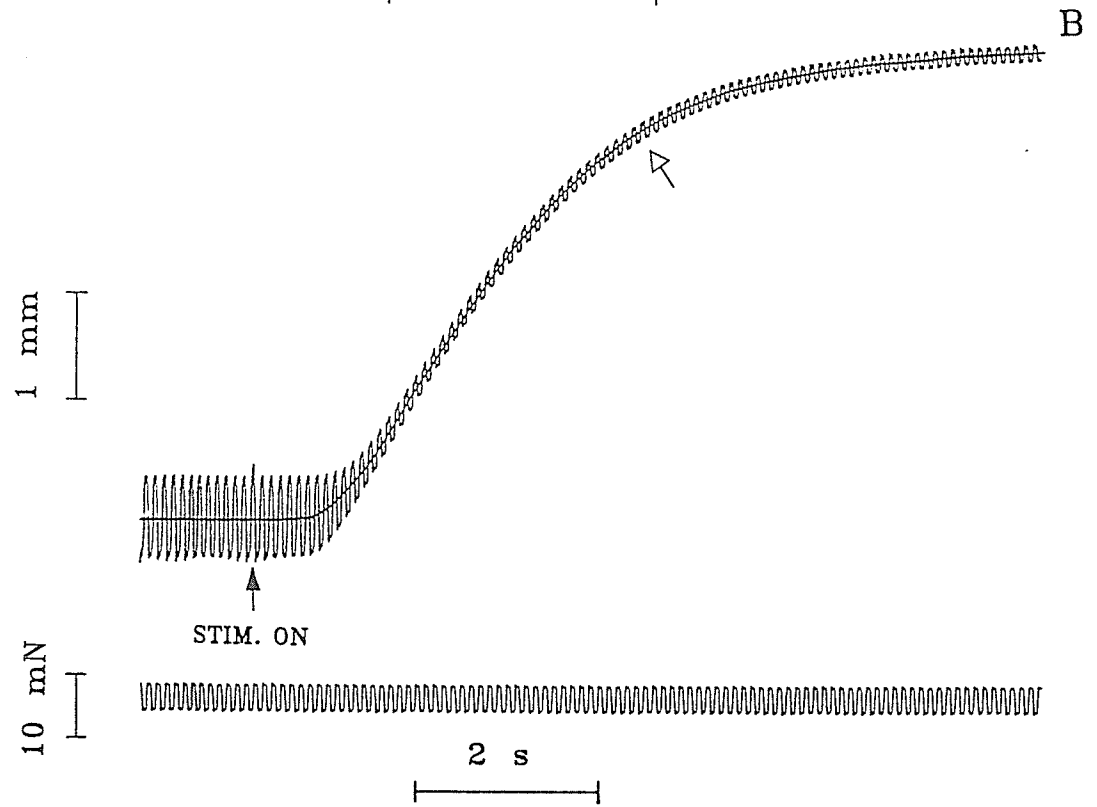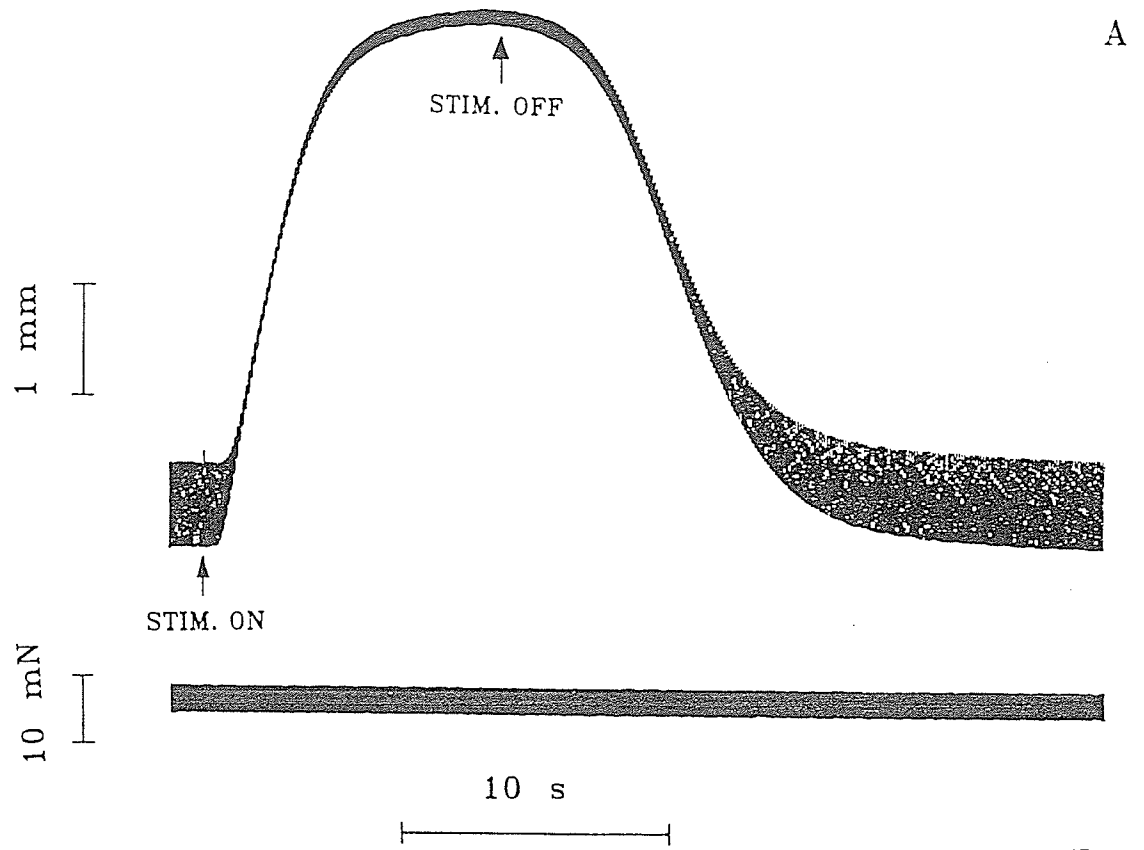
C
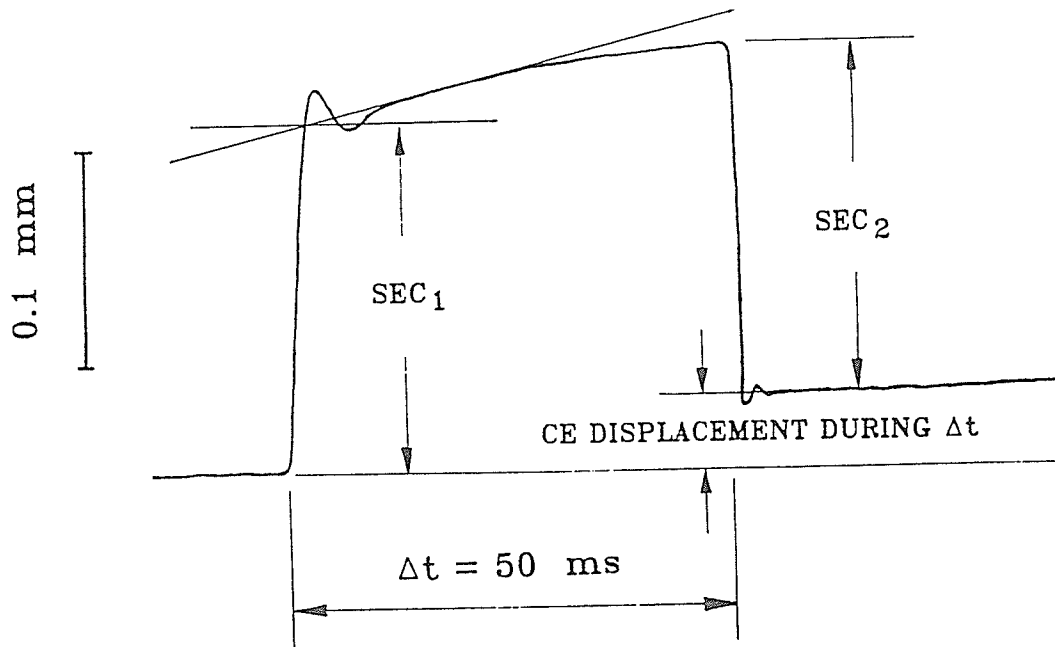
Figure 6. A: Records of input force perturbations (lower trace) and resulting length perturbation (upper trace) during active shortening and relaxation. Force perturbations were produced by rapidly (10 cycles/s) changing force level in lever from 0 to 4 mN repetitively (rectangular force wave). Amplitude of force wave was about 10% of P_o. Onset and termination of electrical stimulation are indicated on traces. Shortening is indicated in upward direction. B: Portions of traces in A are here diplayed at different time scale. Rectangular shape of force wave is visible here. Line through middle of upper trace was displacement curve of the muscle under a preload of 2 mN (mean value of force levels of rectangular force wave). C: Magnification of a small portion of length perturbation trace around area indicated by the arrow in B. SEC length was obtained by averaging lengths of SEC_1 and SEC_2 and subtracting compliance of thread and lever from averaged value. Data were recorded with a sampling frequency of 4000 Hz to show details of trace. See text for definitions.
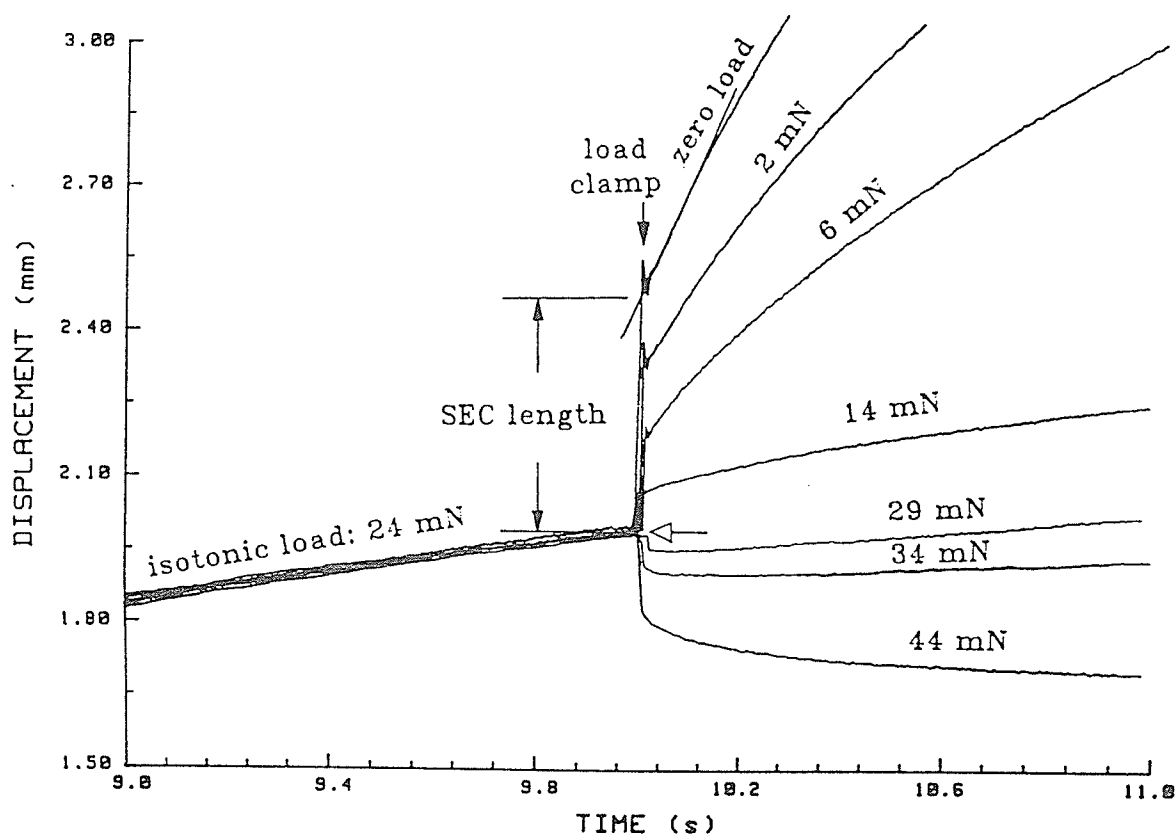
figure 7. Experimental records from which the SEC length of muscle under various afterloads were obtained. Apparent SEC length revealed by quick releasing muscle from isotonic load (24 mN) to zero load was labelled on the curve as an example. Compliance of the measuring system (thread and lever) was subtracted from the apparent SEC length to give the true SEC length of muscle. Muscle length just before onset of load clamping (10 s) was controlled by isotonic load. See text for more details and definitions.
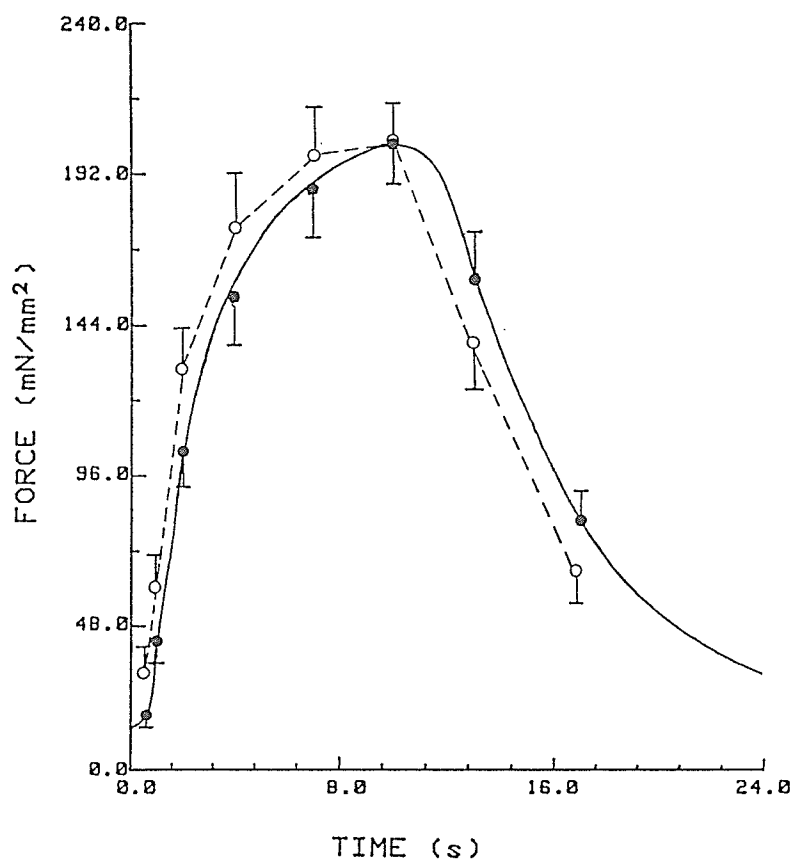
Figure 8. Functions of directly measured isometric tension (P_o') and maximum force extrapolated from F-V data (P_o) with respect to time. The filled circles represent the mean values of P_o' from 6 experiments. The solid line was hand drawn to fit the data. The open circle represent the mean values of P_o. They are connected by dashed line. Standard error bars are shown on the curves.
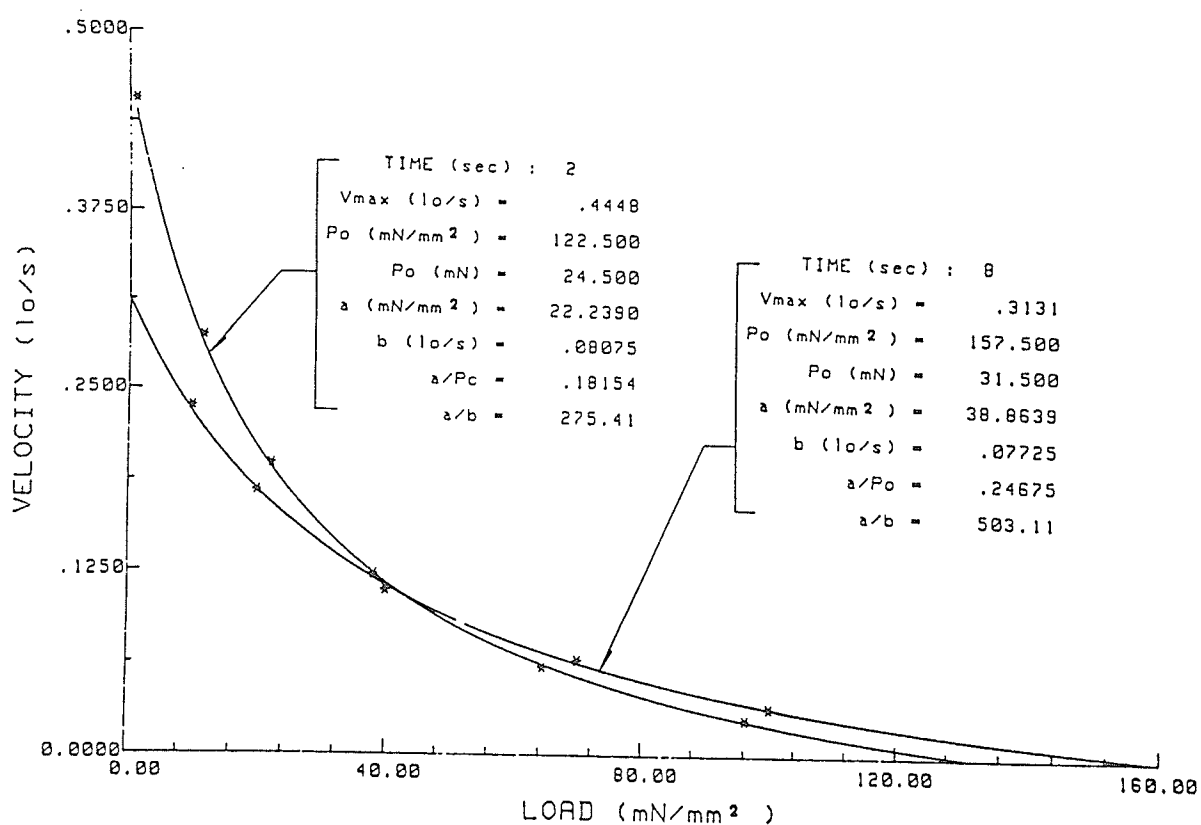
Figure 9. Typical force-velocity curves obtained by quick-release technique at 2 and 8 s in course of an isometric contraction. See text for definitions.
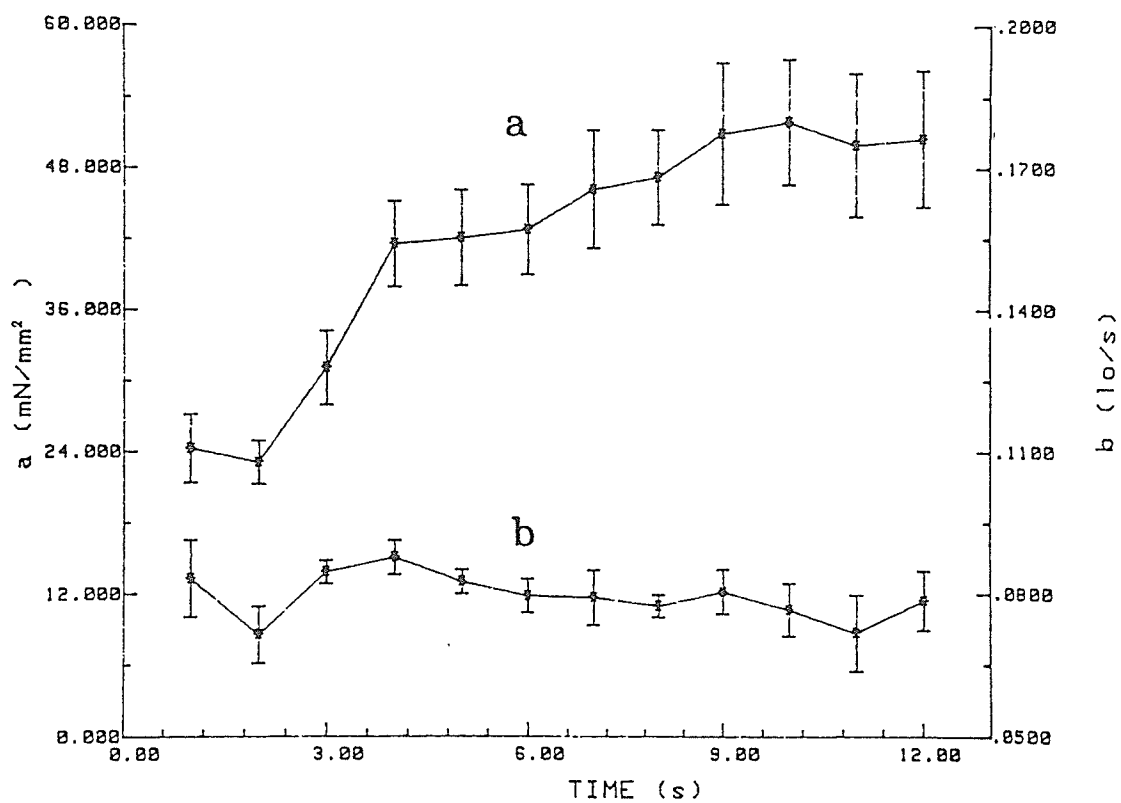
Figure 10. Hill's constants a and b as functions of time.
Mean±SE are shown. n=5.
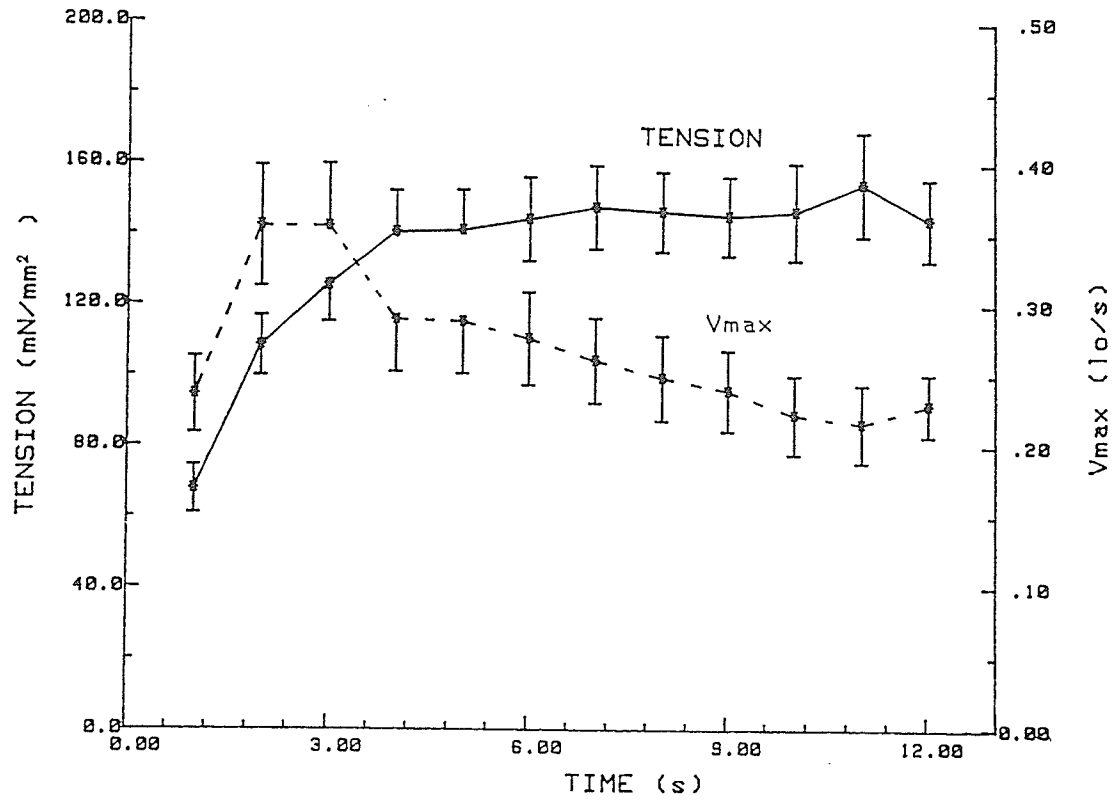
Figure 11. Isometric tension (P_o) (solid line) and zero-load velocity (broken line) as functions of time. Mean±SE are shown. n=5.
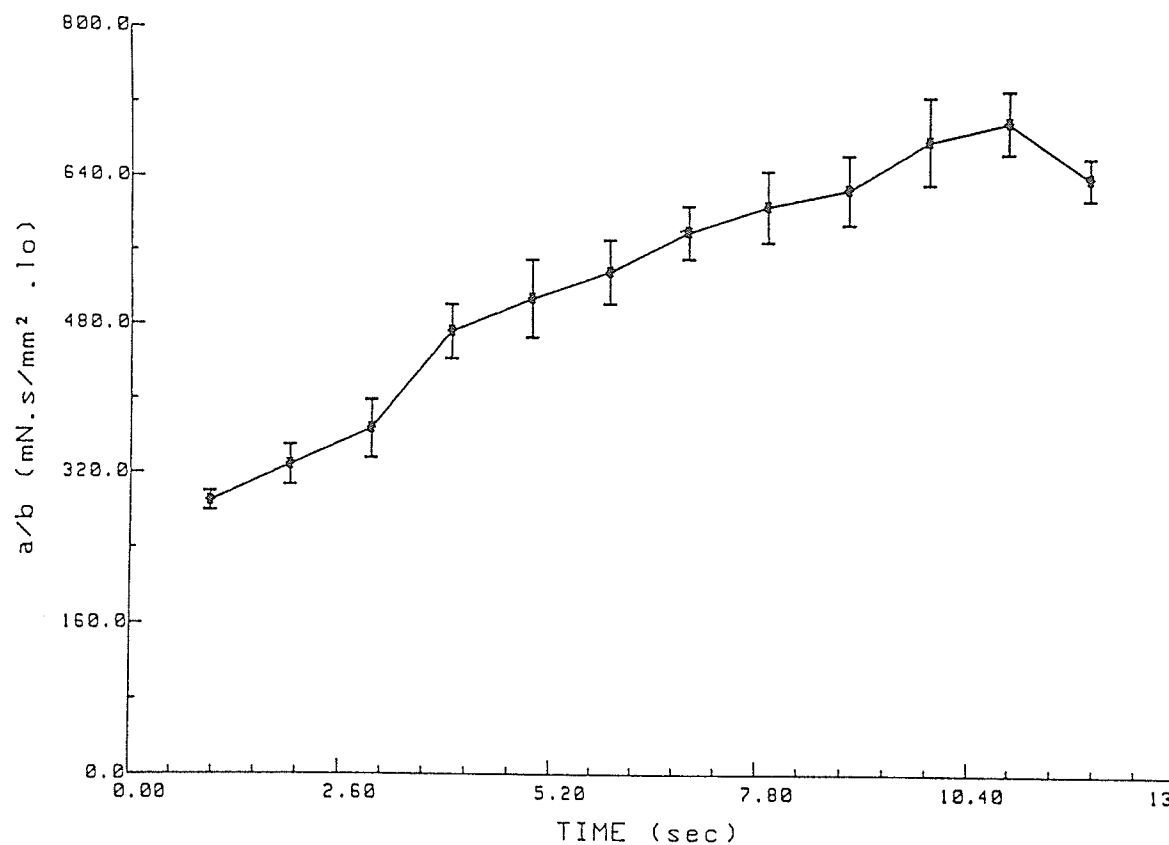
Figure 12. "Internal resistance" to shortening under zero load (a/b) as a function of time. Mean±SE are shown. n=5.
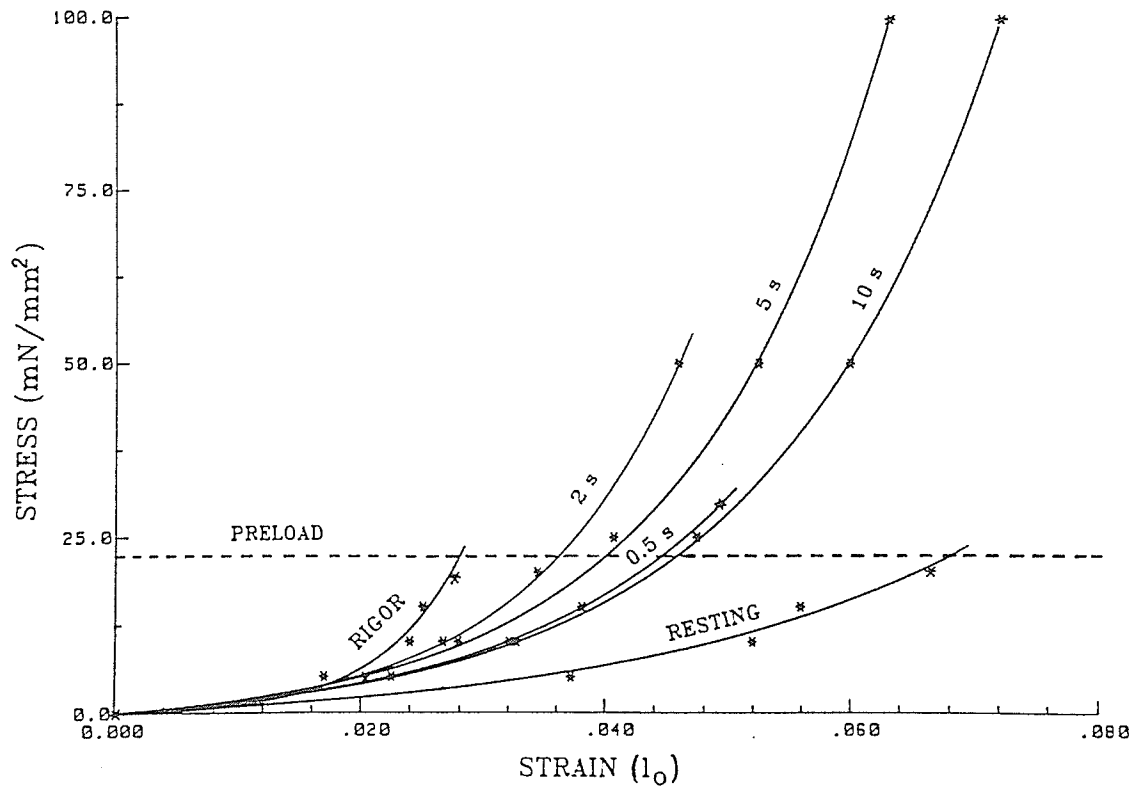
Figure 13. Stress-strain curve of the SEC from a single experiment. Eq. 8 was used to fit the data. Labels on the curves indicate state of muscle under which the curves were obtained. Time (in s) labelled on the curve indicates time when muscle was released. Stimulation started at time 0. Dashed line indicates stress level (preload, in this case) at which stiffnesses of SEC were compared. Constant-stress stiffnesses were obtained by measuring slopes of stress-strain curves at intersections of the dashed line and the curves. See text for definitions.
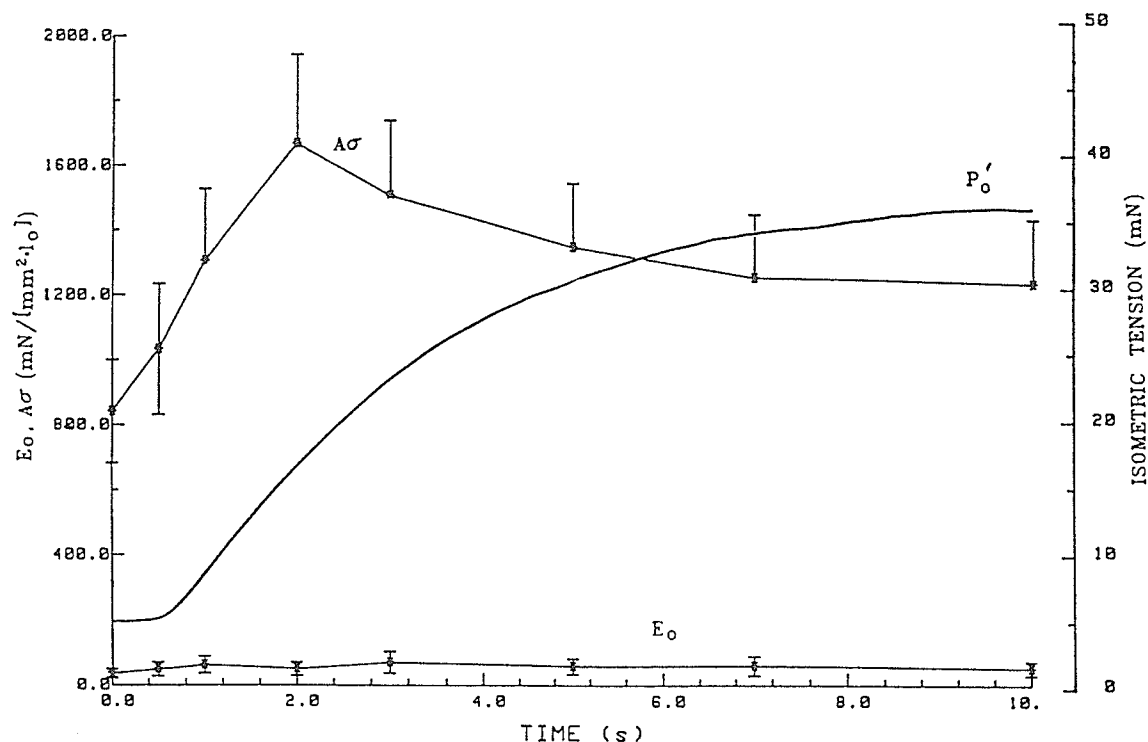
Figure 14. SEC stiffness is broken into 2 components: E_o (initial elastic modulus, stress independent) and $A\sigma$ (stress dependent, where A is slope and σ is stress) and are both plotted against time (n=4, SE bars shown). Isometric tension curve (P_o') (solid line with no error bar) is plotted to illustrate time relationship of stages in contraction. See text for details and definitions.
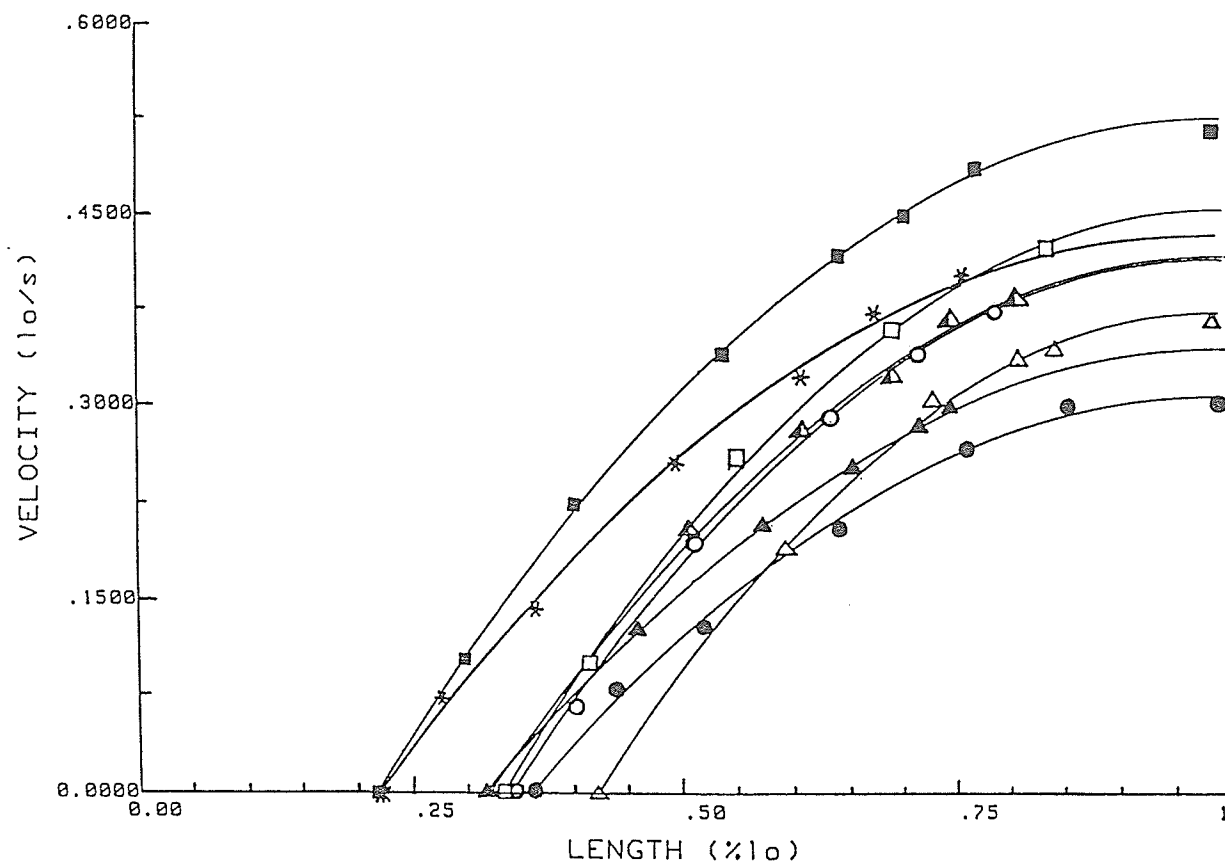
Figure 15. Zero load velocity-length curves for 8 preparations from 8 dogs. Curves were all obtained at 5 s after stimulation. Data were fitted with parabolic equation described in text. Each symbol represents a different muscle preparation.
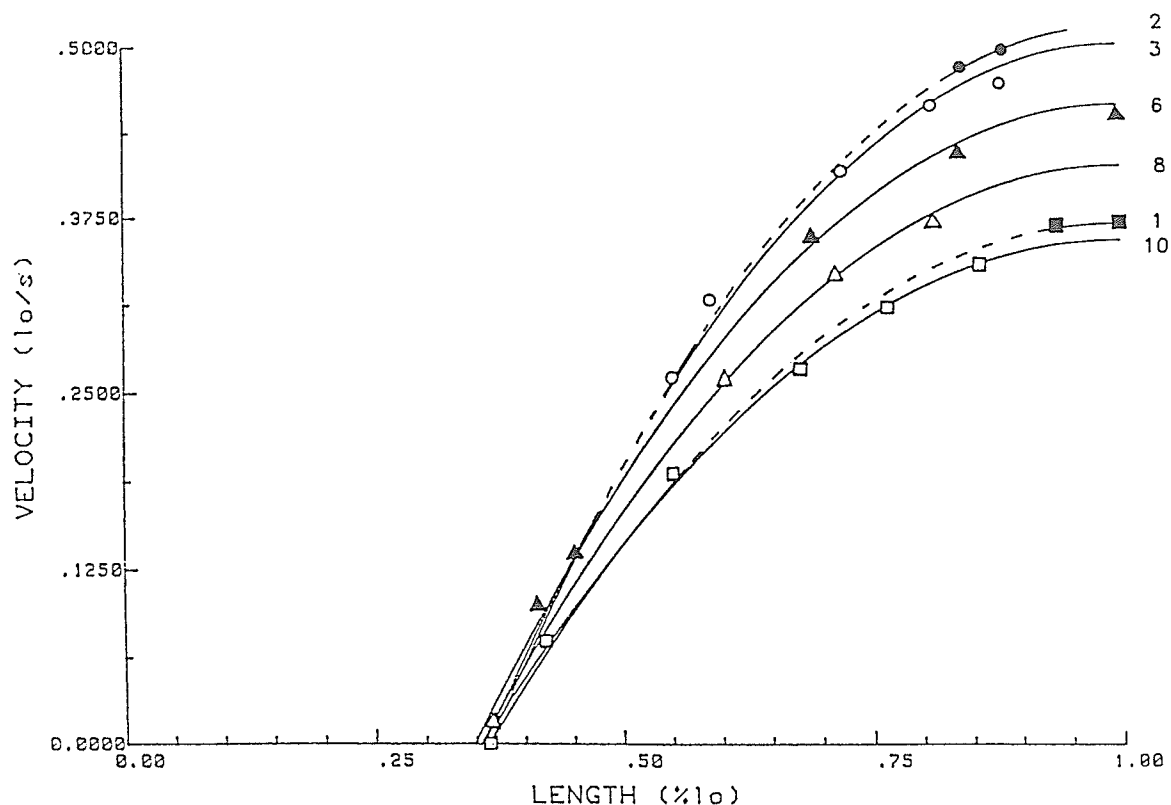
Figure 16. Family of zero-loading velocity-length (V_o-l) curves obtained from single preparation. Number that labels each curve indicates time (in s) after onset of stimulation when zero-load clamps were applied and V_o-l data were measured. Note that early in contraction there was not enough time for muscle to produce an adequate amount of shortening and therefore V_o data at short muscle length could not be obtained. ---, portion of curve that was technically impossible to measure.
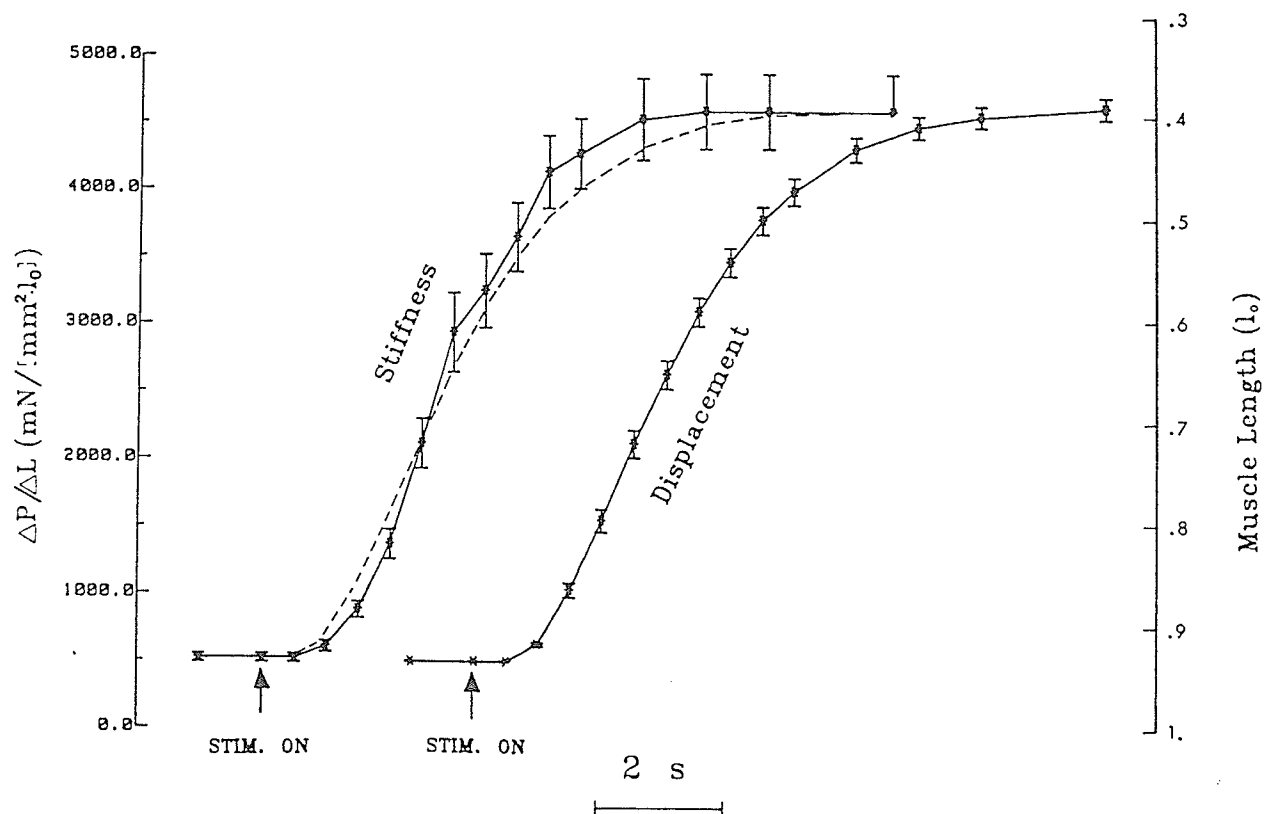
Figure 17. SEC stiffness and displacement (shortening) of
muscle as functions of time. Standard error bars are shown
on curves (n=5). If displacement curve was shifted so that
time of onset of stimulation superimposes that of stiffness
curve, displacement curve would occupy position indicated by
dashed line. $\Delta P/\Delta L$, stiffness estimated by force
perturbation method. Shortening is indicated by the upward
direction.
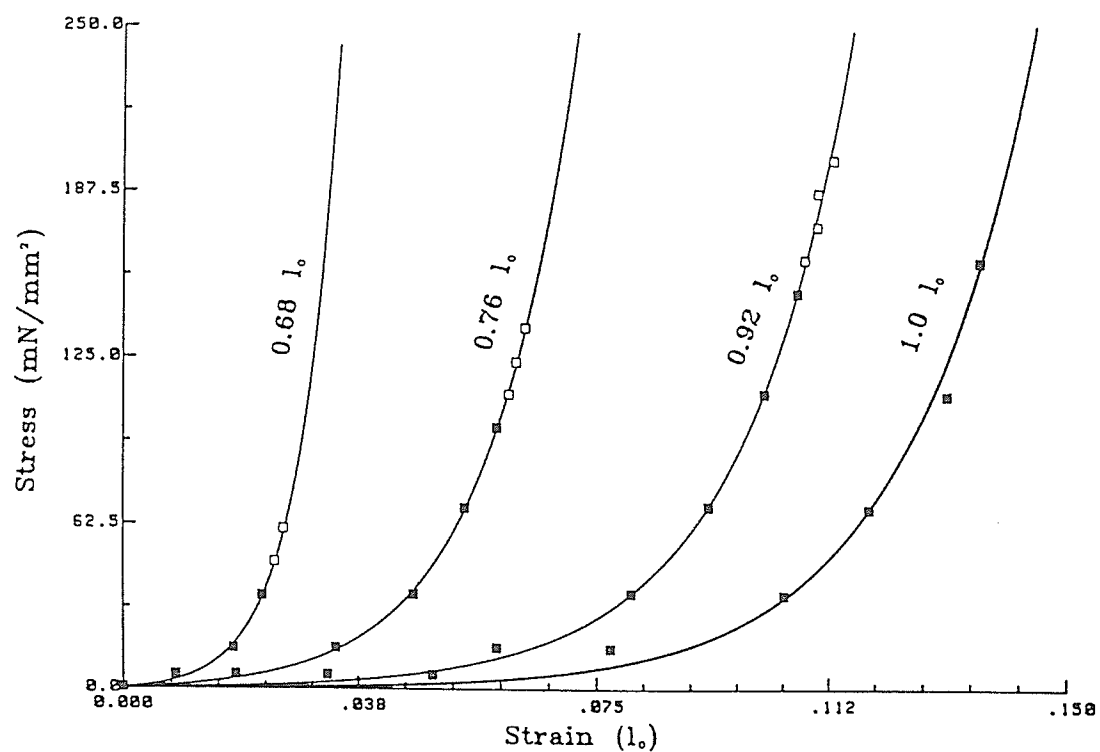
Figure 18. SEC stiffness and displacement during relaxation (lengthening) of muscle, as functions of time. Termination of stimulation for both curves occurs at time 0. Standard error bars are shown (n=5).
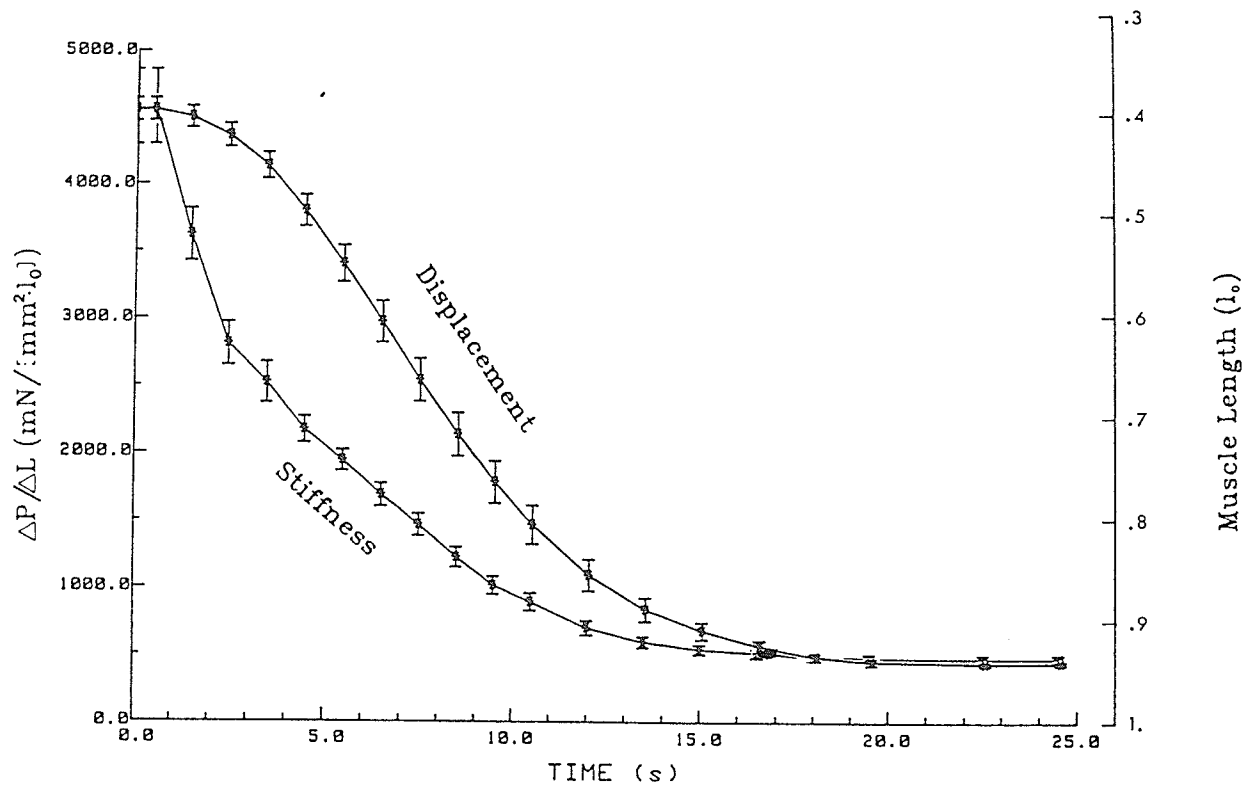
Figure 19. Stress-strain curves from a single experiment (Expt. 2 in Table 5). Muscle lengths at which curves were obtained are labelled on the curves. ▨, data obtained from quick-releases. ▢, data obtained from quick-stretches. Data were fitted by Eq. 8. l_o, optimum muscle length.
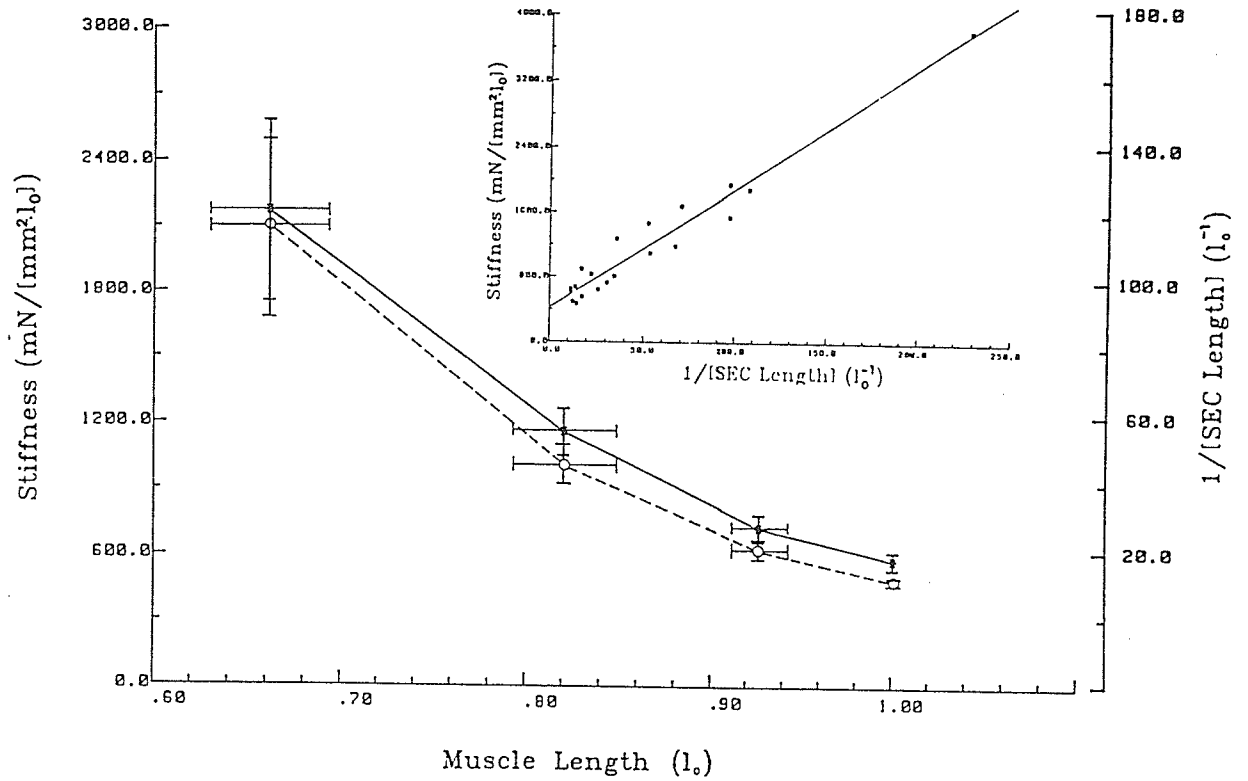
Figure 20. Constant-stress stiffness (solid line) and 1/L (or 1/[SEC length]) (dashed line) as functions of muscle length obtained 10 s after onset of stimulation. Correlation of stiffness and reciprocal of SEC length is shown in the inset. Correlation coefficient (r) is 0.945. Standard error bars are shown (n=5). See text for definitions.
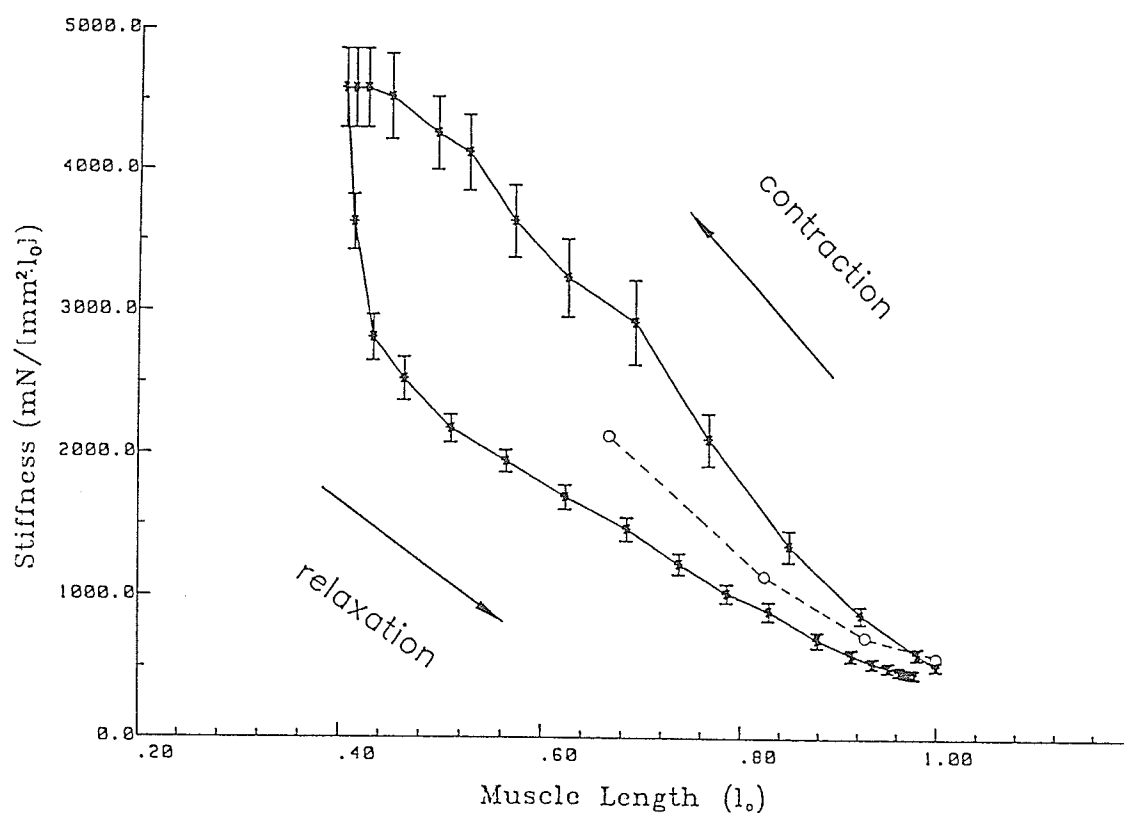
Figure 21. Stiffness change during isotonic contraction and relaxation as a function of muscle length (solid line). The upper curve was obtained during contraction, and the lower curve was obtained during relaxation. Standard error bars are shown (n=5). Dashed line is stiffness vs. muscle length curve redrawn from Fig. 20 for purpose of comparison. Note that dashed line was obtained with time variable held constant.
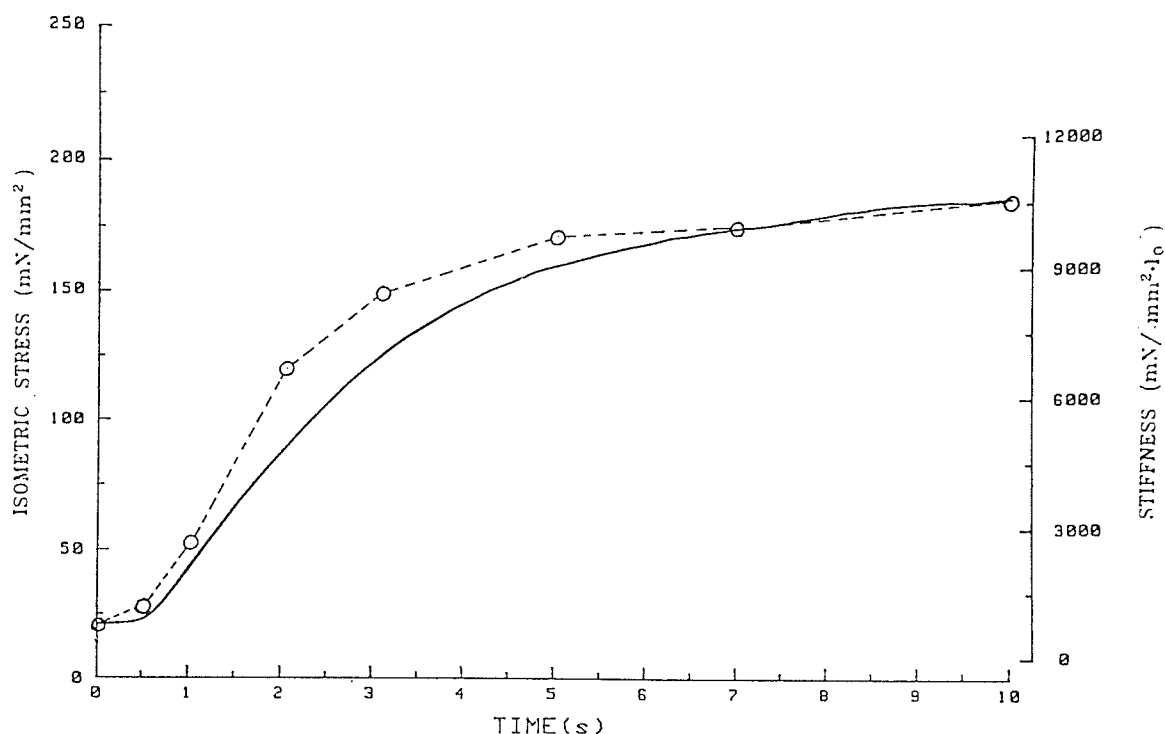
Figure 22. Typical isometric stress curve (solid line) and associated continuous (or dynamic) stiffness curve (dashed line). Circles are stiffnesses at various times calculated from Eq. 7. Values of E_o (initial elastic modulus) and A (slope) for different times are obtained from Table 3. The stress (σ) at corresponding times are obtained from isometric stress curve shown in figure. Note that, unlike stiffness curves shown in Fig. 14, stiffness here is obtained at different stress levels. l_o, optimum muscle length.
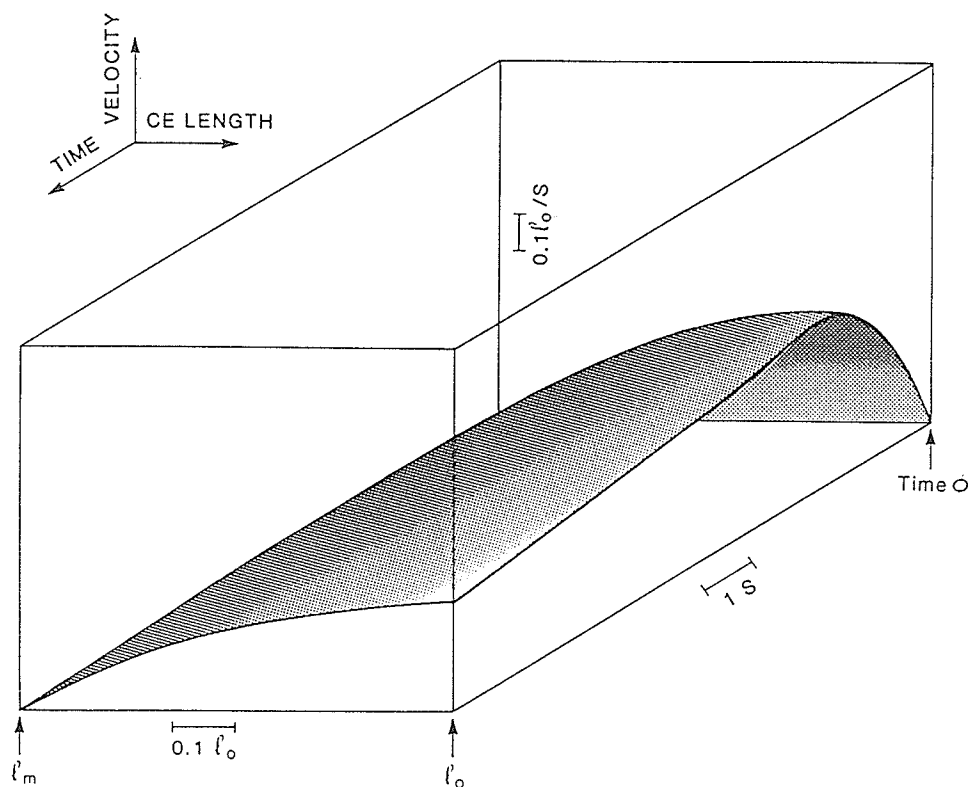
Figure 23. Three-dimensional plot of velocity-length-time surface. l_o, optimum muscle length; l_m, muscle length at which unloaded shortening velocity is zero, or the minimum muscle length (contracted) under zero load. The velocity-time profile at l_o was modified from V_o curve in Fig. 11; l_m value was taken from the mean l_{min} values in Table 4. The velocity-length profile was assumed parabolic in shape. Therefore the surface was constructed from infinte number of parabolic curves possessing constants l_m and $V_{max}(t)$. The equation describing the velocity-length relationship is $V_o(l) = V_{max}\{1 - [(1-l)/(1-l_{min})]^2\}$. See text for definitions.

REFERENCES

Antonissen, L. A., R. W. Mitchell, E. A. Kroeger, W. Kepron, K. S. Tse, and N. L. Stephens. (1979). Mechanical alterations in airway smooth muscle in canine asthmatic model. J. Appl. Physiol. 46: 681-687.

Bose, D. (1984). Mechanical changes during smooth muscle rigor. In: Smooth Muscle Contraction, edited by N. L. Stephens. New York: Dekker, p. 199-217.

Brenner, B., M. Schoenberg, J. M. Chalovich, L. E. Greene, and E. Eisenberg. (1982). Evidence for cross-bridge attachment in relaxed muscle at low ionic strength. Proc. Natl. Acad. Sci.(USA) 79:7288-7291.

Bressler, B. H., and N. F. Clinch. (1975). Crossbridges as the major source of compliance in contracting skeletal muscle. Nature Lond. 250: 221-222.

Brutsaert, D. L., and V. A. Claes. (1974). Onset of mechanical activation of mammalian heart muscle in calcium and strontium containing solution. Circ. Res. 35: 345-347.

Brutsaert, D. L., V. A. Claes, and E. H. Sonnenblick. (1971). Effect of abrupt load alterations on force-velocity-length and time relation during isotonic contractions of heart muscle: load clamping. J. Physiol. Lond. 216: 319-330.

Buchthal, F., and P. Rosenfalck. (1957). Elastic properties of striated muscle. In: Tissue Elasticity, edited by J. W. Remington. Washington, DC: Am. Physiol. Soc.

p. 73-97.

Cecchi, G., P. J. Griffiths, and S. Taylor. (1982). Muscular contracton: Kinetics of crossbridge attachment studied by high frequecy stiffness measurements. Science Wash. DC 217: 70-72.

Chiu, Y., E. W. Ballou, and L. E. Ford. (1982). Velocity transients and viscoelastic resistance to active shortening in cat papillary muscle. Biophys. J. 40: 121-128.

Close, R. I. (1972). The relations between sarcomere length and characteristics of isometric twitch contractions of frog sartorius muscle. J. Physiol. (Lond). 220: 745 -761.

Cooke, P. H., G. Kargacin, R. Craig, K. Fogarty, and F. S. Fay. (1987). Molecular structure and organization of filaments in single, skinned smooth muscle cells. In: Regulation and Contraction of Smooth Muscle, edited by M. J. Siegman, A. P. Somlyo and N. L. Stephens. New York: Alan Liss Inc., p. 1-25.

Cox, R. H. (1987). Influence of muscle length on series elasticity in arterial smooth muscle. Am. J. Physiol. 234(5): C146-C154.

Dabrowska, R., J. M. F. Sherry, D. Aromatorio, and D. J. Hartshorne. (1978). Modulator protein as a component of the myosin light chain kinase. Biochemistry 17: 253-261.

Dillon, P. F., M. O. Aksoy, S. P. Driska, and R. A.

Murphy. (1981). Myosin phosphorylation and the crossbridge cycle in arterial smooth muscle. Science Wash. DC 211: 495-497.

Edman, K. A. P.(1966). The relation between sarcomere length and active tension in isolated semitendinosus fibres of the frog. J. Physiol. (Lond). 183: 407-417.

Edman, E. A. P. (1979). The velocity of unloaded shortening and its relation to sarcomere length and isometric force in vertebrate muscle fibers. J. Physiol. Lond. 291: 143-159.

Eisenberg, E., and L. E. Greene. (1980). The relation of muscle biochemistry to muscle physiology. Annu. Rev. Physiol. 42: 293-309.

Eisenberg, E., and T. L. Hill. (1985). Muscle contraction and free energy transduction in biological systems. Science Wash. DC 227: 999-1006.

Fenn, W. O. (1924). The relation between the work performed and the energy liberated in muscular contraction. J. Physiol. 85: 277-297.

Ford, L. E., A. F. Huxley, and R. M. Simmons.(1986). Tension transients during the rise of tetanic tension in frog muscle fibre. J. Physiol. 372: 595-609.

Ford, L. E., A. F. Huxley, and R. M. Simmons.(1981). The relation between stiffness and filament overlap in stimulated frog muscle fibres. J. Physiol. 311: 219-249.

Goldman, Y. E., M. G. Hibberd, J. A. McCray, and D. R.

Trentham. (1982). Relaxation of muscle fibers by photolysis of caged ATP. Nature 300: 701-705.

Gordon, A. M., A. F. Huxley, and F. J. Julian. (1966) The variation in isometric tension with sarcomere length in vertebrate muscle fibers. J. Physiol. 184: 170-192.

Groschel-Stewart, U., J. H. Chamley, J. D. McConnell, and G. Buenstock. (1975). Comparison of the reaction of cultured smooth and cardiac muscle cells and fibro-blasts to specific antibodies to myosin. Histochem. 43: 215.

Gunst, S. J. (1986). Effect of length history on contractile behavior of canine tracheal smooth muscle. Am J. Physiol. 250(Cell Physiol. 19): C134-C154.

Hai, C. M., and R. A. Murphy. (1988). Cross-bridge phosphorylation and regulation of latch state in smooth muscle. Am. J. Physiol. 254(Cell Physiol. 23): C99-C106.

Hellstrand, P., and B. Johansson. (1979). Analysis and the length response to a force step in smooth muscle from rabbit urinary bladder. Acta. Physiol. Scand. 106: 219-249.

Herlihy, J. T., and R. A. Murphy. (1974). Force-velocity and series elastic characteristics of smooth muscle from the hog carotid artery. Circ. Res. 34: 461-466.

Hill, A. V. (1922). The maximum work and mechanical efficiency of human muscle, and their most economical

speed. J. Physiol. 56: 19-41.

Huxley, A. F. (1957). Muscle structure and theories of
contraction. Prog. Biophys. biophys. Chem. 7: 255-318.

Huxley, A. F. (1973). A note suggesting that the cross-
bridge attachment during muscle contraction may take
place in two stages. Proc. Roy. Soc. B. 183: 83-86.

Huxley, A. F., and F. J. Julian. (1964). Speed of unloaded
shortening in frog striated muscle fibers. J. Physiol.
177: 60P-61P.

Huxley, A. F., and R. A. Simmons. (1971a). Proposed
mechanism of force generation in striated muscle.
Nature 233: 533-538.

Huxley, A. F., and R. A. Simmons. (1971b). Mechanical
properties of the crossbridges of frog striated muscle.
J. Physiol. 218: 59-60P.

Huxley, H. E. (1979). Time resolved X-ray diffraction
studies on muscle. In: Cross-bridge Mechanism in
Muscle Contraction, edited by H. Sugi and G. H.
Pollack. Tokyo: Univ. of Tokyo Press. p. 391-405.

Huxley, H. E., and J. Hanson. (1954). Changes in the cross-
striations of muscle during contraction and stretch
and their structural interpretation. Nature 173:
973-976.

Jewell, B. R., and J. R. Blinks. (1968). Drugs and the
mechanical properties of heart muscle. Annu. Rev.
Pharmacol. 8: 113-130.

Johansson, B. (1973). Active state in the smooth muscle of

the rat portal vein in relation to electrical activity
and isometric force. Circ. Res. 32: 246-257.

Julian, F. J., and D. L. Morgan. (1981). Tension, stiffness,
unloaded shortening speed and potentiation of frog
muscle fibres at sarcomere lengths below optimum. J.
Physiol. 319: 205-217.

Julian, F. J., and M. R. Sollins.(1975). Variation of muscle
stiffness with force at increasing speeds of shorten-
ing. J. Gen. Physiol. 66: 287-302.

Kamm, E. K., and J. T. Stull. (1986). Activation of smooth
muscle contracton: Relation between myosin phosphory-
lation and stiffness. Science Wash. DC 232: 80-82,

Kennedy, J. B., and A. M. Neville. (1976). Basic Statisti-
cal Methods for Engineers and Scientists. New York:
Harper & Row. p. 177-181.

Kepron, W., J. M. James, B. Kirk, A. H. Sehon, and K. S.
Tse. (1977). A canine model for reaginic hyper-
sensitivity and allergic bronchoconstriction. J.
Allergy Clin. Immunol. 59: 64-69.

Kroeger, E. A., and N. L. Stephens. (1975). Effect of
tetraethylammonium on tonic airway smooth muscle:
initiation of phasic electrical activity. Am J.
Physiol. 228(2): 633-636.

Lundholm, L., and E. Mohme-Lundholm. (1966). Length at
inactivated contractile elements, length-tension
diagram, active state and tone of vascular smooth
muscle. Acta. Physiol. Scand. 68: 347-359.

Marston, S. B., C. D. Rodger, and R. T. Tregear. (1976). Changes in muscle crossbridges when β, -imido-ATP binds to myosin. J. Mol. Biol. 104: 263-276.

Meiss, R. A.(1978). Dynamic stiffness of rabbit mesotubarium smooth muscle: Effect of isometric length. Am. J. Physiol. 234(1): C14-C26.

Meiss, R. A. (1982). Transient response and continuous behavior of active smooth muscle during controlled stretches. Am J. Physiol. 242(11): C146-C158.

Mulvany, M. J., and D. M. Warshaw. (1981).The anatomical location of the series elastic component in rat vascular smooth muscle. J. Physiol. 314: 321-330.

Packer, C. S., and N. L. Stephens. (1985). Force-velocity relationships in hypertensive arterial smooth muscle. Can. J. PHysiol. Pharmacol. 63: 669-674.

Ramsey, R. W., and S. F. Street. (1940). The isometric length-tension diagram of isolated skeletal fibres of the frog. J. Cell Comp. Physiol. 15: 11-34.

Rasmussen, H., Y. Takuwa, and S. Park. (1987). Protein kinase C in the regulation of smooth muscle contraction. FASEB J. 1: 177-185.

Seow, C. Y. (1989) Mechanical properties of airway smooth muscle. In: Airway Smooth Muscle: Modulation of Receptors and Responses, edited by D. K. Agrawal and R. G. Townley, New York, CRC Press.

Seow, C. Y., and N. L. Stephens. (1986). Force-velocity curves for smooth muscle: analysis of internal factors

reducing velocity. Am. J. Physiol. 251(Cell Physiol. 20): C362-C368.

Seow, C. Y., and N. L. Stephens. (1987). Time dependence of series elasticity in tracheal smooth muscle. J. Appl. Physiol. 62(4): 1556-1561.

Seow, C. Y., and N. L. Stephens. (1988). Velocity-length-time relations in canine tracheal smooth muscle. J. Appl. Physiol. 64(5): 2053-2057.

Seow, C. Y., and N. L. Stephens. (1989). Changes of tracheal smooth muscle stiffness during an isotonic contraction. Am. J. Physiol. 256(Cell Physiol. 25):

Siegman, M. J., T. M. Butler, S. U. Moore, and R. E. Davies. (1976). Crossbridges: attachment, resistance to stretch and viscoelasticity in resting mammalian smooth muscle. Science Wash. DC 191: 383-385.

Sobieszek, A., and J. V. Small. (1977). Regulation of the actin-myosin interaction in vertebrate smooth muscle: Activation via a myosin light chain kinase and the effect of tropomyosin. J. Mol. Biol. 112: 559-576.

Somlyo, A. P., C. E. Devine, A. V. Somlyo, and R. V. Rice. (1973). Filament organization in vertebrate smooth muscle. Phil. Trans. R. Soc. Lond. B. 265: 223-229.

Somlyo, A. V., M. Bond, P. F. Berner, F. T. Ashton, H. Holtzer, and A. P. Somlyo. (1984). The contractile apparatus of smooth muscle: An update. In: Smooth Muscle Contraction, edited by N. L. Stephens. New York: Dekker, p. 1-20.

Somlyo, A. V., Y. Goldman, T. Fujimori, M. Bond, D. Trentham and A. P. Somlyo. (1987). Crossbridge transients initiated by photolysis of caged nucleotides and crossbridge structure, in smooth muscle. In: Regulation and Contraction of Smooth Muscle, edited by M. J. Siegman, A. P. Somlyo and N. L. Stephens. New York: Alan Liss Inc. p. 27-41.

Squire, J. (1981).Structural evidence on the contractile event. In: The Structural Basis of Muscular Contraction, edited by J. Squire. New York: Plenum, p. 523-615.

Stephens, N. L. (1970) The mechanics of isolated airway smooth muscle. In: Airway Dynamics: Physiology and Pharmacology, edited by A. Bouhuys. Springfield, IL: Thomas, p. 191-208.

Stephens, N. L., U. Kromer. (1971). Series elastic component of tracheal smooth muscle. Am. J. Physiol. 220: 1890-1895.

Stephens, N. L., E. A. Kroeger, and U. Kromer. (1975). Induction of a myogenic response in tonic airway smooth muscle by tetraethylammonium. Am J. Physiol. 228(2): 628-632.

Stephens, N. L., E. A. Kroeger, and J. A. Mehta. (1969). Force-velocity characterization of respiratory airway smooth muscle. J. Appl. Physiol. 26: 685-692.

Stephens, N. L., R. W. Mitchell and D. L. Brutsaert. (1984). Shortening inactivation, maximum force potential,

relaxation, contractility. In: Smooth Muscle Contrac-
tion, edited by N. L. Stephens. New York: Dekker,
p. 91-112.

Stephens, N. L., and C. M. Skoog. (1974). Tracheal smooth
muscle and rate of oxygen uptake. Am. J. Physiol.
226: 1462-1467.

Sugi, H., and S. Suzuki. (1980). Extensibility of the
myofilaments in vertebrate skeletal muscle as studied
by stretching rigor muscle fibres. Proc. Jap. Acad.
B56: 290-293.

Sugi, H., and T. Kobayashi. (1984). Sarcomere length and
force changes in single tetanized frog muscle fibres
following quick changes in fibre length. In: Contractile
Mechanisms in Muscle, edited by G. H. Pollack and H.
Sugi. New york: Plemum Press, p. 623-635.

Taylor, S. R., and R. Rudel. (1970). Striated muscle
fibres: Inactivation of contraction induced by
shortening. Science Wash. DC 167: 882-884.

Uvelius, B. (1979). Shortening velocity, active force and
homogeneity of contraction during electrically
evoked twitches in smooth muscle from rabbit urinary
bladder (Abstract). Acta Physiol. Scand. 106: 481.

Wang, K., and R. Ramirez-Mitchell. (1983). A network of
transverse and longitudinal intermediate filaments is
associated with sarcomeres of adult vertebrate skeletal
muscle. J. Cell Biol. 96: 562-570.

Warshaw, D. M., and F. S. Fay.(1983). Crossbridge elasticity

in single smooth muscle cells. J. Gen. Physiol. 82: 157-199.

Warshaw, D. M., W. J. McBride, and S. S. Work. (1987). Corksrew-like shortening in single smooth muscle cells. Science Wash. DC 236: 1457-1459.

Wilkie, D. R. (1954). Facts and theories about muscle. Prog. Biophysics 4: 288-324.

Woledge, R. C., N. A. Curtin, and E. Homsher. (1985). Energetic Aspects of Muscle Contraction. London: Academic Press, p. 1-26.

APPENDICES

Original Publications

Force-velocity curves for smooth muscle: analysis of internal factors reducing velocity

C. Y. SEOW AND N. L. STEPHENS
*Department of Physiology, Faculty of Medicine, University of Manitoba,
Winnipeg, Manitoba R3E OW3, Canada*

SEOW, C. Y., AND N. L. STEPHENS. *Force-velocity curves for smooth muscle: analysis of internal factors reducing velocity.* Am. J. Physiol. 251 (Cell Physiol. 20): C362–C368, 1986.—In tracheal smooth muscle, we obtained quantitatively different force-velocity (F-V) curves at early (2 s) and late (8 s) stages of an isometric tetanus whose contraction time was 12 s. These were essentially two samples from a continuum of F-V curves operating between 0 and 12 s. The cross-bridge cycling velocity at 8 s was slower and less sensitive to external load change compared with that at 2 s. This is possibly due to the presence of two types of cross bridges with different F-V characteristics; at 2 s most of the bridges resemble a cycling type, whereas at 8 s there is a population of what Dillon et al. (6) have called slowly cycling or latch type interactions. Another possibility is that, due to some intrinsic factors, the whole population of cross bridges gradually change their F-V characteristics. Functions $a(t)$ and $b(t)$ were obtained by applying load clamps at 1-s intervals throughout a tetanus (a and b are asymptote values derived from the F-V hyperbolic curves): a increased with time, b remained constant. Analysis suggested that a/b was a valid index of internal factors that affect shortening velocity of unloaded muscle, and it is progressively increased in value during contraction.

trachea; zero-load velocity; normally cycling bridges; slowly cycling bridges; internal factors reducing velocity

IN SMOOTH MUSCLE CONTRACTION, initially relatively rapid shortening velocity is observed. This velocity is very sensitive to load. That is, a slight increase in load will cause a drastic decrease in velocity. This force velocity (F-V) characteristic is quickly (within 2 s of a 12-s contraction) changed to one that is less sensitive to load but has relatively slow velocity. This phenomenon has been recognized in the laboratories of Murphy (6), Siegman (8), Uvelius (12), and Stephens (9), and it is believed that the progressive, sequential recruitment of two types of cross bridges is responsible. Initially the normally (rapidly) cycling bridges are predominant. These are soon replaced by slowly cycling, or noncycling latch bridges. This replacement is not a discontinuous process, rather the transition is a gradual one.

The classic Hill equation used to describe the F-V relations in tetanized, isolated skeletal muscle is often used to describe the same relations in smooth muscle. But the validity of its use in smooth muscle is questionable, since in skeletal muscle it appears that fundamentally only one type of force, or shortening-generating mechanism (the crossbridge), is active throughout the entire time course of a contraction (i.e., the F-V relationship is time independent), although in smooth muscle, as mentioned earlier, the F-V characteristics change with time. Therefore, the velocity predicted by the Hill equation should not be a function of load alone, but also of time. Therefore a more generalized Hill equation (at least for smooth muscle) should more correctly be

$$V(P,t) = b(t) \cdot [P_o(t) - P]/[P + a(t)]$$

where $a(t)$, $b(t)$ are functions of time, and $P_o(t)$ is maximum isometric tension at *time t.*

From the mechanical data alone it is impossible to distinguish the following two mechanisms that could be responsible for the slowing down in shortening velocity later in contraction: the latch mechanism in which the latch bridges impede the cycling rate of normally cycling bridges; and the gradual decrease in cycling velocity of all cross bridges due to some unknown change in internal properties of the cross bridges. In this paper, without distinguishing the two mechanisms, we attempt *1*) to determine the F-V curves of the early (2 s) and late (8 s) cross bridges; *2*) to separate the time-dependent F-V characteristics [$a(t)$ and $b(t)$] associated with these two types of cross bridges; and *3*) to examine how these characteristics varied with time in the course of contraction. The study also focused on deriving information relating to internal factors that affect shortening velocity from the functions $a(t)$ and $b(t)$.

METHODS

Preparation of muscle strip. The control dog was anesthetized by an intravenous injection of 30 mg/kg body wt of pentobarbital sodium. This was followed by rapid removal of the cervical trachea via a midline incision, followed by an intracardiac injection of saturated potassium chloride solution to kill the animal. The trachea was placed immediately in a beaker of ice-cold, aerated Krebs-Henseleit solution of the following composition (millimolar): NaCl, 115; NaHCO$_3$, 25; NaH$_2$PO$_4$, 1.38; KCl, 2.51; MgSO$_4$·7H$_2$O, 2.46; CaCl$_2$, 1.91; dextrose, 5.56. A strip of muscle (with the connective tissues carefully dissected away under a binocular microscope) was cut from the trachea. Details for preparing strips of canine tracheal smooth muscle have been previously reported by us (11). The strips used in the experiments possessed

an average length of 6 mm, an average weight of 1.5 mg, with an average width of 0.5 mm. One end of the strip was connected to the lever by a highly noncompliant surgical thread (7-0 silk) 5 cm long. The other end of the strip was fixed in the muscle bath by a clamp. The bath containing Krebs-Henseleit solution was aerated with a 95% O_2-5% CO_2 mixture that maintained a P_{O_2} of 600 Torr, a P_{CO_2} of 40 Torr and pH of 7.40 at a temperature of 37°C. The strip was equilibrated in the bath for 2 h. During this time it was stimulated electrically by 15 V, 60 Hz alternating voltage applied to mass platinum plate electrodes that were positioned on either side of the muscle (~4 mm apart). The current density was 200 mA/cm^2 and the stimulation duration was 12 s. An equilibrium state was achieved when the muscle developed a steady maximum tetanic tension during stimulation.

The optimum length of the muscle (l_o) was obtained by varying the preload (and hence the length of the muscle strip), and measuring the isometric tetanic tension. The length that was associated with the development of P_o was identified as l_o. All experiments to be described were always conducted at this predetermined l_o.

Data acquisition and curve fitting. The instantaneous force and displacement produced by the muscle were recorded with the use of an electromagnetic lever system which incorporated force and displacement transducers. The apparatus was originally developed by Brutsaert et al. (2, 3). The voltage signal was converted to digital signal by an analogue-to-digital converter, and the signal was input to a HP9836 computer that analyzed and plotted out the data in graphic form.

By applying critically damped, abrupt load clamps, we were able to measure the velocity of muscle contraction under a given load at a given time (see Ref. 2 for a discussion of optimal load clamping). Applying a series of such load clamps ranging from zero to $P_o(t)$, the *F-V* relationship was obtained (for *time t* after stimulation), and the data were fitted with the hyperbolic Hill equation with constants *a* and *b* (see Figs. 1 and 2). The Hill equation was linearized so that the least-squares best-fit method could be employed.

Data were obtained at random with respect to time and load. Load clamps were applied at 1-s intervals from 1 to 12 s. Some experiments started from 1 to 12 s, others from 12 to 1 s. No significant difference was found in data obtained by the two procedures. With respect to load, some experiments ranged from heavy to light, others from light to heavy.

In fitting the data to the equation, the isometric tension developed at the time when the muscle was released, $P_o(t)$, had to be specified. The $P_o(t)$ curve obtained from isometric contraction varied slightly but significantly from one contraction to another, due to the intrinsic instability of the muscle. Application of load clamps (especially zero load clamp) increased this instability. Therefore, during the course of the experiment, P_o could vary as much as 12%. Due to the nature of the hyperbolic equation, the goodness of fit of the experimental data to the calculated equation was very sensitive to the value of $P_o(t)$ chosen. Thus a trial and error process was carried

out (within the 12% range) to obtain a value of $P_o(t)$ that gave the best fit. By varying $P_o(t)$, different curves were obtained. The one that fitted the data best was chosen and the constants *a* and *b* associated with that curve were selected.

Validity of methods for obtaining F-V curves. The load-clamp method was employed in this study. The velocity measurements were made a fifth of a second after the release of the isometrically contracting muscle to various afterloads (see Fig. 1). The one-fifth second was allowed for the oscillation (caused by abrupt change in load) of the muscle to settle down such that the measured velocity was truly the velocity of the contractile element (CE). The oscillation was critically damped to minimize the effect on velocity caused by load clamping (under- or over-damping will decrease the velocity). The assumption made here is that there is not enough time during the abrupt change in load (load clamping) for the CE to change length significantly. The interactions of the cross bridge in the CE make it much more difficult for the latter to change length, than for the series elastic component (SEC). The abrupt change in the muscle length presumably comes entirely from the SEC. Because all the measurements were made a fifth of a second after the onset of load clamp, the time variable was held constant. The length of the CE, the state of activation of the muscle, and the condition under which the muscle is stimulated up to the moment of release were the same for all the data points in an *F-V* curve.

In this study, the muscle in a single experiment was usually subjected to 60–80 stimulations (12 s in duration, at 4-min intervals). The stability of the muscle during the course of experiment becomes very important for obtaining consistent, valid results. The isometric tension of the muscle was used as an indicator of the stability and was checked every half an hour during the experiments. If P_o changed >12% from the beginning to the end of experiment, the experimental results were discarded.

Measurement of the internal factor reducing shortening velocity in muscle. From Fig. 1 it is clear that the larger the force step, $[P_o(t)\text{-}P]$, the greater the shortering velocity. In other words, the force step is proportional (but not necessarily directly proportional) to shortening velocity, or $[P_o(t)\text{-}P] \propto V$. We can equate the two by putting in a constant of proportionality α

$$[P_o(t)\text{-}P] = \alpha V \qquad (1)$$

Equation 1 is true only when the velocity is constant with respect to time. If $dV/dt \neq 0$, then the inertial force, I, of the muscle caused by the force step has to be considered. And *equation 1* becomes

$$[P_o(t)\text{-}P] = \alpha V + I \qquad (2)$$

Buchthal and Rosenfalck (1) have shown that the magnitude of I of an isolated muscle in contraction is negligible. Our calculations based on the experimental data revealed that the value of I ranged from 0 to 1×10^{-5} mN/mm^2 (a typical value of P_o for tracheal smooth muscle ws 250 mN/mm^2). Therefore I could be neglected without introducing a significant error in studying *F-V*
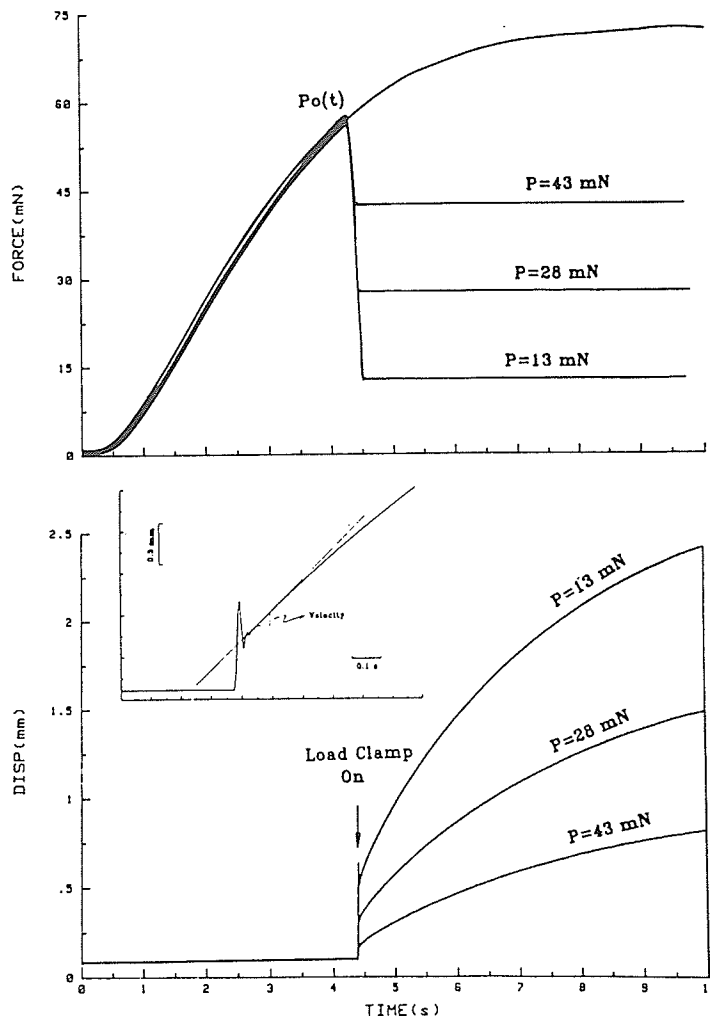
FIG. 1. Quick-release of muscle to various loads at *time t* from onset of isometric contractions. Small insert is a magnified displacement-time curve and shortening velocity after quick-release was obtained by measuring slope of curve as shown. P was the constant after-load after quick-release.

relations of isolated muscle, and *equation 1* was used to describe the *F-V* relations. The coefficient was determined experimentally according to the relations given by *equation 1*: $\alpha = [P_o(t)\text{-}P]/V$. The correlating factor of force step and velocity is, then, α. It possesses the same unit as the coefficient of viscosity, and in muscle contraction, resembles an internal resistance to shortening.

If shortening velocities are measured under certain conditions such that the change in velocity is entirely due to the change of load on muscle, then a hyperbolic *F-V* curve is usually obtained, and α is found to be a linear function of load (P). If we arbitrarily define the linear function as $\alpha = (P + a)/b$, where a and b are constants, then *equation 1* becomes Hill's equation. So, in a hyperbolic *F-V* relation, the internal factor that reduces shortening velocity can be represented by (P + a)/b. If the muscle is shortening under zero load (P = 0), the internal factor is a/b.

Therefore, α is a lump-sum manifestation of all factors that reduce shortening velocity of muscle. A force step (load clamp) applied at 2 s (after stimulation) in muscle contraction results in a much greater velocity than if the

same force step were applied at 8 s (after stimulation). This means that the *F-V* property of the muscle changes from 2 to 8 s. This change is reflected by the increase in α value. In this case, α helps us to quantitate the change in muscle property.

RESULTS

By applying load clamps at 2 and 8 s after stimulation, two distinct *F-V* curves were obtained. A typical set of curves is shown in Fig. 2. On comparing the 8-s with the 2-s curve, a significant increase in the value of a (+75%) was found, although the change in b was small (−4.3%). The maximum zero load velocity (V_o) dropped by 30% from 2 to 8 s. The $P_o(t)$ values obtained from the curves (24.5 and 32.5 mN) corresponded quite well with the isometric tension measured at 2 and 8 s (23 and 33 mN, respectively). Statistical analysis of the two groups ($n = 5$) of data obtained at 2 and 8 s showed that there was a highly significant difference ($P < 0.005$) between the values of a at 2 and 8 s, whereas there was no significant difference for values of b (see Table 1). For values of
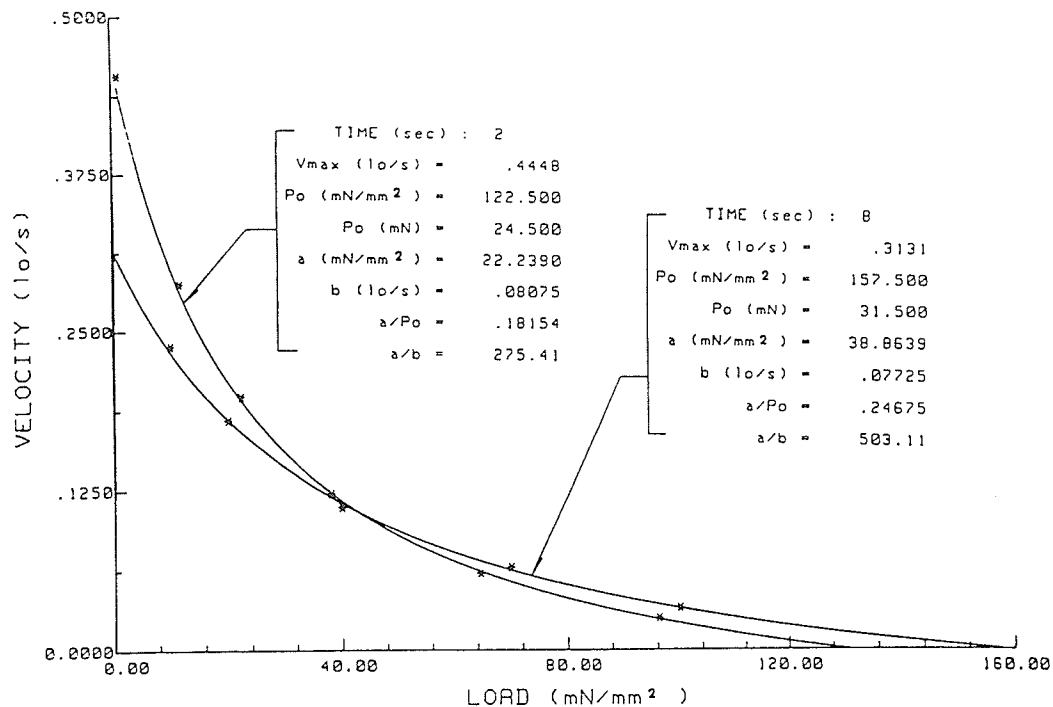
FIG. 2. Typical force-velocity curves measured by load clamp (quick release) technique at the 2- and 8-s points in course of an isometric contraction.

TABLE 1. *Force-velocity parameters at 2 and 8 s in contraction*

	2 s	8 s	t Test
$a\pm$SE, mN/mm^2	23.07±1.84	47.32±4.04	$P < 0.005$
$b\pm$SE, l_o/s	0.0713±0.0061	0.0775±0.0024	NS
$P_o\pm$SE, mN/mm^2	108.4±8.5	146.9±11.4	$P < 0.005$
$V_o\pm$SE, l_o/s	0.356±0.0429	0.2488±0.0304	$P < 0.005$
$a/P_o\pm$SE	0.2170±0.0197	0.3387±0.0569	$P < 0.025$

Values are means ± SE for 5 trials.

$P_o(t)$, $V_o(t)$, and a/P_o, see Table 1.

To gain insights into how a and b varied with time, we applied load clamps at 1-s intervals in the course of a 12-s contraction. The mean values of a and b obtained from five experiments (± SE) are shown in Fig. 3. The value of a remained relatively low during the first 2 s of contraction, then increased rapidly for the next couple of seconds. The rate of increase then decreased, and the curve reached a maximum at ~10 s. In contrast, b remained relatively constant with time at a value of ~0.081 l_o/s.

A mean plot ($n = 5$, mean ± SE) of V_o and isometric tension vs. time is shown in Fig. 4. Maximum shortening velocity occurred ~2 s after stimulation.

A mean plot ($n = 5$, mean ± SE) of the values of a/b is shown in Fig. 5. It reveals a progressive increase with time.

DISCUSSION

The earliest and the most important theory in the field showing that two types of cross bridges are activated in sequence during a contraction, is that of Dillon et al. (6). They postulate that calcium-calmodulin-dependent myosin light chain phosphorylation is responsible for the development of early, normally cycling bridges, whereas dephosphorylation and calcium binding to an unspecified site on the myosin molecule is responsible for the late, slow cycling, latch bridges. This is not meant to exclude the possibility that other sites of calcium binding may also be involved.

Although the exact contractile protein biochemistry of smooth muscle contraction is not yet clear, the two types of cross bridges (reflected by the shortening velocities) have been observed (6, 8, 9, 12). The "latch" bridge theory of Dillon et al. (6) offers an explanation of the decrease in velocity in the sustained phase of contraction. Other explanations, for instance, fatigue of muscle, cannot be excluded. However, there is no evidence to suggest that fatigue occurs in smooth muscle during 2-12 s in contraction, since during that period the isometric tension is rising (see Fig. 4). Another factor that causes the drop in shortening velocity could be the length effect (at $l <$ l_o, deactivation of muscle could occur, and isometric tension of the muscle usually decrease at short CE length). Stephens and Kromer (10) have shown that the length of the SEC is ~7.5% of l_o when tracheal smooth muscle is at the plateau of its isometric contraction (P_o). Therefore, under P_o, the CE length is only 0.925 l_o (according to the Voigt model). Experimental results (our own unpublished observations) showed that in smooth muscle the reduction in V_o due to the change in CE length from l_o to 0.925 l_o is ~1% of V_o. Therefore the
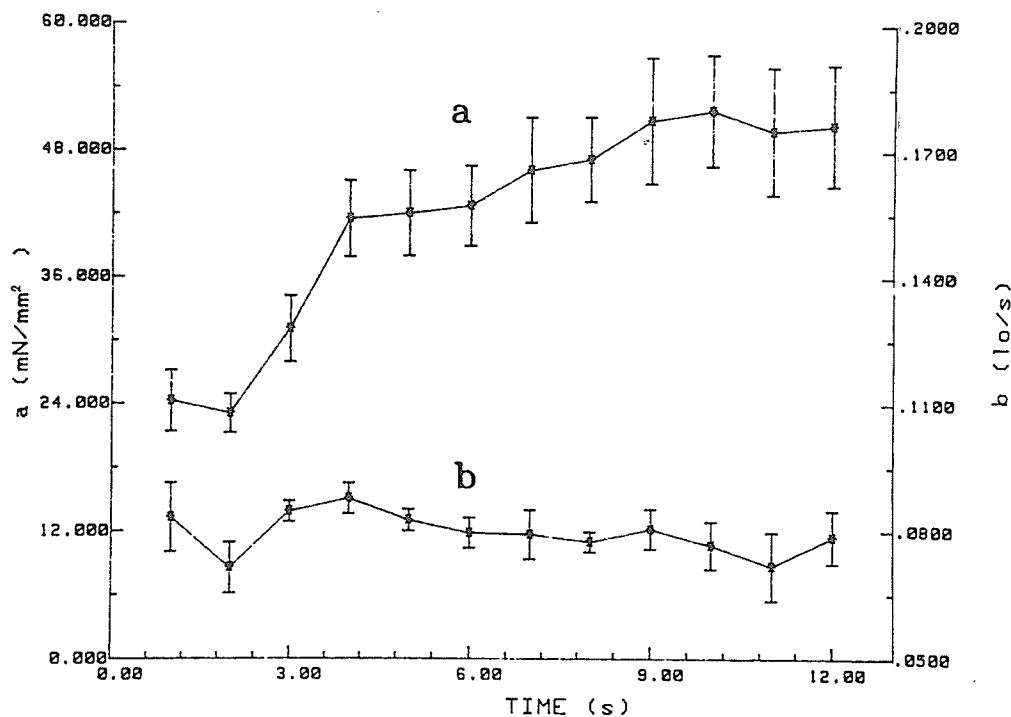
FIG. 3. Hill's constants a and b as functions of time. Means ± SE are shown. $N = 5$.
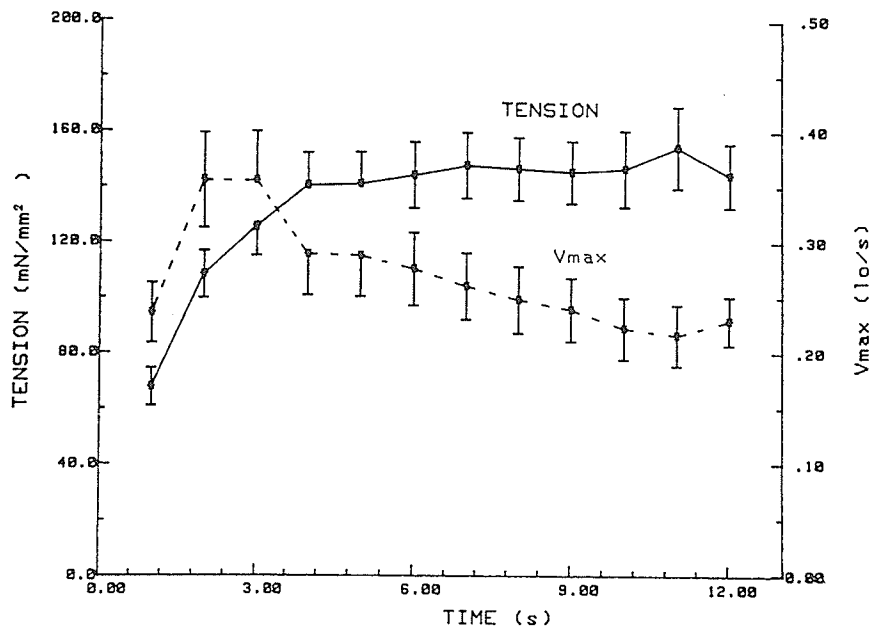
FIG. 4. Isometric tension (*solid line*) and zero-load velocity (*broken line*) as functions of time. Means ± SE are shown. $N = 5$.

30% drop in V_o from 2 to 8 s (Fig. 4) cannot be accounted for by the length effect. As mentioned earlier, the decrease in shortening velocity could also be the result of some unknown gradual alterations in intrinsic properties of the whole population of cross bridges.

No evidence (such as an abrupt change in F-V prop-

erties) was found in this study to support the idea that all normally cycling bridges abruptly change to slowly cycling bridges. Conversely the relatively smooth functions $a(t)$, $b(t)$, $P_o(t)$, and $V_o(t)$ found in this study suggest that the transition from normally cycling to slowly cycling stage is gradual. If the latch mechanism is
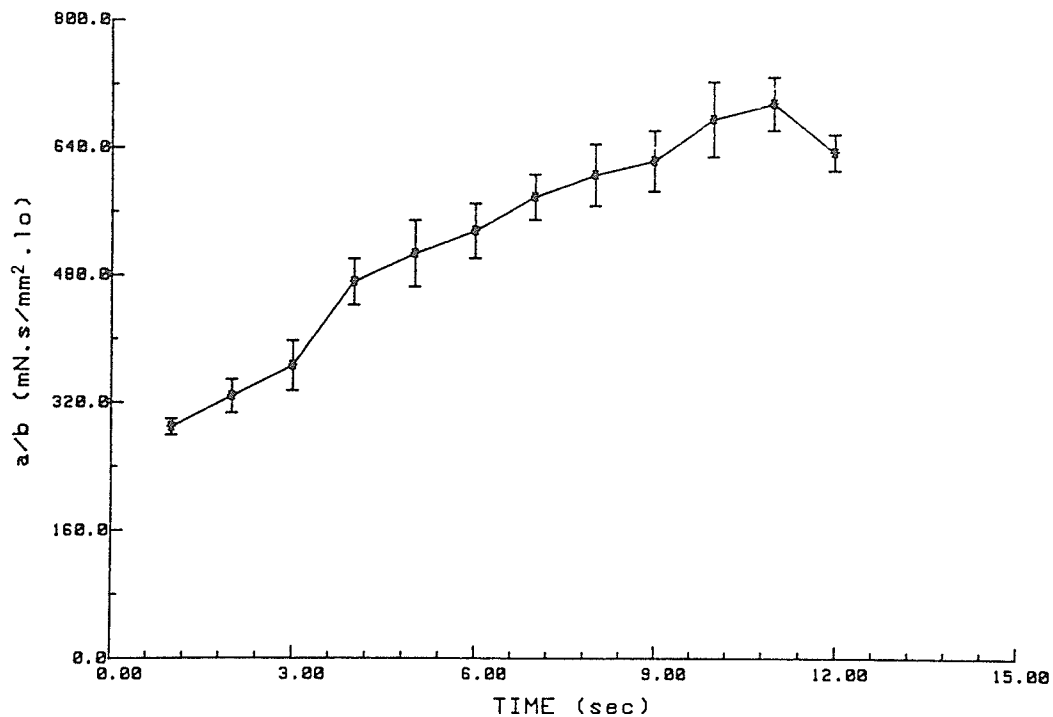
FIG. 5. Internal resistance to shortening under zero load (a/b) as a function of time. Means $\pm$ SE are shown. $N = 5$.

operating, the increase in size of the latch bridge population should be gradual.

There is little change in F-V characteristics after 8 s. Normally cycling bridges could be characterized by high V_o, and a low value of the a/b factor. On the other hand, slowly cycling bridges could be characterized by low V_o, and high a/b. As mentioned earlier, a/b is the internal factor that reduces shortening velocity when muscle is shortening under zero load, at or near l_o. In general, α is both load and time dependent. Hill's equation is generally regarded as empirical and used only to fit the experimental data. In this internal factor analysis we use Hill's constants (a and b) to approximate the value of α. So the equation $\alpha = (P + a)/b$ is purely empirical. There is, a priori, no reason to determine Hill's constants to find α. A more straight forward way to determine α is through equation 1. However the usefulness in relating α to a and b is apparent. Since A. V. Hill, many investigators have characterized mechanical properties of muscle in terms of a and b. Now these data (from different types of muscles) can be used to assess the internal factors that reduce shortening velocity of muscle from the relationship: $\alpha = (P + a)/b$. If the latch mechanism is operating, the increase in value of a/b with time directly reflects the internal resistance to shortening caused by the presence of latch bridges.

Mechanically speaking the force step, $[P_o(t)$-$P]$, is the single most important factor that determines the shortening velocity of muscle. The correlating factor between force step and velocity (α) could be defined as the internal resistance of muscle. This is analogous to

electrical resistance correlating voltage drop and current, or flow resistance correlating pressure drop and flow velocity of fluid through a pipe. There are many factors that could contribute to the internal resistance of muscle, for instance the presence of latch bridges. The parallel viscoelastic elements described by Chiu et al. (5) could contribute to the internal resistance also. However the fact that the resistance is load dependent [$\alpha = (P + a)/b$] suggest that the resistance is largely cross-bridge related. According to Eisenberg's model (7) constraints (from internal or/and external load) will reduce the cross-bridge cycling velocity as well as the rate of energy utilization. Increase in external load has double effects on shortening velocity in that it reduces the force step $[P_o(t) - P]$ and at the same time increases the internal resistance $[(P + a)/b]$. The coefficient α therefore lumps all the above factors together. To gain insights into the internal resistance, and hence the mechanism of muscle contraction, it is useful to break down this lump-sum effect (α) into more specific components relating to the corresponding causes. (This is analogous to characterizing flow resistance as a function of fluid viscosity, pipe diameter, and length, etc.)

The evidence for time-dependent F-V properties in smooth muscle, speculatively, should have an impact on pharmacological studies on smooth muscle tissue. In dose-response studies of smooth muscle, measurements are usually made at the plateau phase of contraction. This obviously will provide inadequate data. Stephens (9) has shown that in hypoxic canine tracheal smooth muscle, zero load velocity in the plateau phase (8 s) is

not significantly different from that of a control. But there is a highly significant difference in V_o between the two types of muscles in the early phase (3 s) of contraction. By conventional methods this early phase property difference would not be detected. The amount of shortening of smooth msucle has a decisive effect on its regulatory function and also is the cause of diseases such as hypertension and asthma. The contractility of the muscle in the shortening phase determines the amount of shortening. Therefore studies of smooth muscle properties should place emphasis more on the dynamic shortening phase rather than the plateau phase in contraction.

REFERENCES

1. BUCHTHAL, F., AND P. ROSENFALCK. Elastic properties of striated muscle. In: *Tissue Elasticity*, edited by J. W. Remington. Washington, DC: Am. Physiol. Soc. p. 73–97.
2. BRUTSAERT, D. L., V. A. CLAES, AND E. H. SONNENBLICK. Effects of abrupt load alterations on force-velocity-length and time relations during isotonic contractions of heart muscle: load clamping. *J. Physiol. Lond.* 216: 319–330, 1971.
3. BRUTSAERT, D. L., AND V. A. CLAES. Onset of mechanical activation of mammalian heart muscle in calcium and ssrontium containing solution. *Circ. Res.* 35: 345–347, 1974.
4. BRUTSAERT, D. L., AND E. H. SONNENBLICK. Force-velocity-length-time relations of the contractile element. *Circ. Res.* 24: 137–149, 1969.
5. CHIU, Y., E. W. BALLOU, AND L. E. FORD. Velocity transients and viscoelastic resistance to active shortening in cat papillary muscle. *Biophys. J.* 40: 121–128, 1982.
6. DILLON, P. F., M. O. AKSOY, S. P. DRISKA, AND R. A. MURPHY. Myosin phosphorylation and the crossbridge cycle in arterial smooth muscle. *Science Wash. DC.* 211: 495–497, 1981.
7. EISENBERG, E., AND T. L. HILL. Muscle contraction and free energy transduction in biological systems. *Science Wash. DC.* 227: 999–1006, 1985.
8. SIEGMAN, M. J., T. M. BUTLER, S. U. MOOER, AND R. E. DAVIES. Crossbridges: attachment, resistance to stretch and viscoelasticity in resting mammalian smooth muscle. *Science Wash. DC* 191: 383–385, 1976.
9. STEPHEN, J. L. Smooth muscle contractility: effects of hypoxia. In: *Pulmonary Vascular Reactivity*, edited by E. K. Weir, I. McMurtry, and J. H. Reeves. In Press.
10. STEPHENS, N. L., AND U. KROMER. Series eleastic component of tracheal smooth muscle. *Am. J. Physiol.* 220: 1890–1895, 1971.
11. STEPHENS, N. L., E. A. KROEGER, AND J. A. MEHTA. Force-velocity characterization of respiratory airway smooth muscle. *J. Appl. Physiol.* 26: 685–692, 1969.
12. UVELIUS, B. Shortening velocity, active force and homogeneity of contraction during electrically evoked twitches in smooth muscle from rabbit urinary bladder (Abstract). *Acta Physiol. Scand.* 106: 481, 1979.

Time dependence of series elasticity in tracheal smooth muscle

C. Y. SEOW AND N. L. STEPHENS
Faculty of Medicine, Department of Physiology, University of Manitoba,
Winnipeg, Manitoba R3E 0W3, Canada

SEOW, C. Y., AND N. L. STEPHENS. *Time dependence of series elasticity in tracheal smooth muscle.* J. Appl. Physiol. 62(4): 1556–1561, 1987.—The stress-strain curve for the series elastic component (SEC) of tracheal smooth muscle was obtained by quick releasing the muscle from isometric tension to various afterloads and measuring the elastic recoils (SEC lengths) at a specific time after stimulation. A family of such curves was obtained by releasing the muscle at different points in time during contraction. Stiffnesses of the SEC (slopes of the stress-strain curves) at a specific stress level calculated from these curves (constant-stress stiffness) showed significant difference from one another. The same difference can also be characterized by the slope of the linear stiffness-stress curve, the constant A. The constant A during a 10-s isometric contraction was maximal at 2 s. It then decreased with time. This stiffness behavior is only seen when the effect of stress is held constant or eliminated. If stress is allowed to increase with time as it does during a tetanus then stiffness appears to increase monotonically. The SEC stiffness during active contraction was found to vary within the boundaries of the stiffness of muscle in rigor (upper limit) and that at resting state (lower limit).

series elastic component; stress-strain curve; rigor state; resting state; cross-bridge attachment

IT IS GENERALLY AGREED that stiffness of the series elastic component (SEC) of muscle is related to the number of attached cross bridges. As to the source of the series elastic behavior of the muscle, most investigators believe that in smooth muscle some of the SEC is intracellular (1, 11, 18, 28), and the activities (attachment and detachment) of the cross bridges could affect the stiffness of the SEC. In striated muscle, electron microscopy of insect flight muscle by Reedy (19) suggests that muscle in rigor have more cross-bridge attachment than that in resting muscle. X-ray diffraction studies of frog skeletal muscle confirm that in rigor state, the thin filaments are heavily labeled (attached) with myosin cross bridges (13, 14). The same situation is conceivable in smooth muscle because both smooth and striated muscle are believed to have the same mechanism of contraction. Mechanical studies on both smooth and striated muscles reveal that a rigor state is associated with high SEC stiffness (1, 20, 22). It seems, therefore, that stiffness has a positive correlation with the number of attached cross bridges. In the present study the SEC stiffness of the tracheal smooth muscle at resting and in rigor states, as well as the stiffness at a specific stress level at different points in time in an isometric contraction, were examined.

METHODS

Preparation of muscle strip and data acquisition. The control dog was anesthetized by an intravenous injection of 30 mg/kg body wt of pentobarbital sodium. This was followed by rapid removal of the cervical trachea via a midline incision and an intracardiac injection of saturated KCl solution to kill the animal. The trachea was placed immediately in a beaker of ice-cold aerated Krebs-Henseleit solution of the following composition (in mM): NaCl, 115; NaHCO$_3$, 25; NaH$_2$PO$_4$, 1.38; KCl, 2.51; MgSO$_4$-7H$_2$O, 2.46; CaCl$_2$, 1.91; dextrose, 5.56. With the connective tissues carefully dissected away under a binocular microscope, a strip of muscle was cut from the trachea [details for preparing strips of canine tracheal smooth muscle have been previously reported by us (24)]. The strips used in experiments possessed an average length of 8 mm, an average weight of 2 mg, and a width of 0.5 mm. One end of the strip was connected to the lever by a highly noncompliant surgical thread (7-0 silk) 10-cm long. The other end of the strip was fixed in the muscle bath by a clamp. The bath containing Krebs-Henseleit solution was aerated with a 95% O$_2$-5% CO$_2$ mixture that maintained Po$_2$ of 600 Torr, a Pco$_2$ of 40 Torr, and pH of 7.40 at a temperature of 37°C. The strip was equilibrated in the bath for 2 h. During this time it was stimulated every 4 min electrically by 17-V, 60-Hz alternating voltage applied to platinum electrodes positioned on either side of the muscle (~4 mm apart). The duration of stimulation was 10 s, which also was the contraction time for the muscle. An equilibrium state was achieved when muscle developed a steady tetanic tension under stimulation. The optimum length of the muscle (l_o) was obtained by varying the preload (and hence the length) of the muscle strip and measuring the isometric tetanic tension. The length that was associated with the development of maximum isometric tension (P$_o$) was identified as l_o. All experiments to be described were always conducted at this predetermined l_o. The preload associated with l_o was ~10% of P$_o$.

The instantaneous force and displacement produced by the muscle were recorded with the use of an electromagnetic lever system incorporated with force and displacement transducers. The apparatus was originally developed by Brutsaert and Claes (3) and Brutsaert et

al. (4) and adapted for use with the slower smooth muscle. The voltage signal was converted to digital signal by an analog-to-digital converter, and the signal was fed to a HP9836 computer that analyzed and plotted out data in graphic and numeric forms.

The total compliance of the lever system is 0.2 μm/mN, and the total equivalent moving mass is 225 mg. The thread connecting the muscle strip to the lever had a nonlinear force-length relationship. Therefore, after each experiment the force-length curve for the connecting thread was obtained by applying force to the thread and measuring the corresponding elongation. The curve was later used to correct the experimental data. The average compliance of the thread was ~4 μm/mN. The time resolution of the lever system is 2 ms, and the maximum sampling frequency of the recording system is 1,000 Hz.

Experimental procedure and data analysis. Both Voigt and Maxwell models can be used in analyzing the results of this study. Since only quick release was performed in the experiments, the muscle was never stretched beyond l_o. The range of the muscle length within which the experimental data were recorded was ~0.9 to 1.0 l_o. Therefore, the parallel elastic component (PEC) of the muscle had little effect on the experimental results. Under these circumstances, the Voigt model is a more convenient and straightforward one to use in the analysis.

The tension-extension (TE) curve of the SEC (Voigt model) was obtained by releasing muscle during isometric contraction to various isotonic afterloads and measuring the elastic recoils (SEC lengths). A typical experimental record is shown in Fig. 1. The degree of damping was adjusted so that the zero-load clamp was critically

damped. Usually critical damping could be obtained also in other load steps using the same degree of damping. Sometimes slight adjustment of the damping degree was needed. The damping was provided electronically by differentiating and inverting the displacement signal and adding this negative velocity signal to the original displacement signal through an adjustable resistor that controlled the degree of damping [see Brutsaert et al. (4) for a discussion of optimal load clamping]. The amount of rapid elastic recoil after quick release was taken as the change in length of the SEC caused by the force step (from isometric tension to afterload). The SEC length was measured by drawing a tangent line over the displacement curve 100 ms after the onset of release (as shown in Fig. 1A). The SEC length under zero load was arbitrarily defined as zero. The extension of the SEC under a given afterload was determined by subtracting the length of the elastic recoil under the afterload from that obtained with zero afterload. The same method was used by Herlihy and Murphy (12).

Since the main objective of this study was to determine the SEC characteristics at different times during the course of an isometric contraction, the quick releases were performed at various times after stimulation of muscle. The load clamp was controlled by a digital timer that triggered the release of the muscle at a preset time. The timer also controlled the onset and duration of stimulation of muscle. At given moments in the contraction the same procedure (of releasing the muscle from isometric tension to various afterloads) was performed, and a TE curve for various moments was obtained. A muscle usually underwent 60–80 contractions throughout the course of experiment (7 h). The maximum isometric tension P_o was used to detect deterioration of the muscle. If P_o changed by >10% from beginning to end of experiment, the experimental results were discarded. Data were obtained in random fashion with respect to time and load. Load clamps were applied at several points in time in an isometric contraction. The sequence in which the load clamps were applied were randomized. The afterloads also were randomized.

The TE curve of the SEC of resting muscle was obtained by releasing the muscle from its l_o or resting tension (~5 mN) to various afterloads without stimulating the muscle. The passive response of the muscle to a force step (release) was qualitatively similar to the active response (Fig. 1) and consisted of a rapid elastic recoil and a slow shortening phase. The TE curve for the SEC of muscle in rigor was obtained in the same way as in resting muscle except the muscle was incubated in the bath containing zero-glucose Krebs-Henseleit solution bubbled with 95% N_2-5% CO_2 gas mixture for 1 h. Electrical stimulation was applied every 4 min during incubation. The duration of stimulation was 10 s. A slight rise in resting tension and diminished isometric tension response (to near zero) on stimulation indicated a rigor or near-rigor state. The muscle could recover to a near normal state when incubated again in normal Krebs-Henseleit solution aerated with 95% O_2-5% CO_2 gas mixture. Again, the passive response of the muscle in rigor to a force step was qualitatively similar to the

FIG. 1. *A:* simultaneous records of tension and displacement of muscle contraction. Muscle was quick released from isometric tension to various afterloads. This procedure was repeated at different points in time in contraction (not shown). Series elastic component (SEC) length and velocity was measured as illustrated. *B:* similar records as in *A,* but releases were from resting tension and muscle was not stimulated. Some slow shortening was observed after releasing muscle (after quick transient), although shortening velocity was much less than that of active shortening. Slow phase shortening probably was result of returning of the parallel elastic component to equilibrium position countered by internal viscous resistance. $P_o(t)$, instantaneous isometric tension; l_o, optimum length of muscle.

response of active normal muscle and consisted of a rapid elastic recoil and a slow phase (Fig. 1). The shortening velocity in the slow phase of resting muscle and rigor muscle was much less (40 times less) than that of an active muscle. The production of rigor in tracheal smooth muscle and the associated ATP concentration is described in detail by Bose (1).

The present study and others (2, 12, 25, 28) show that stiffness of SEC is a function of load on the muscle. In fact, it can be shown that the stiffness is linearly related to the load. A formula widely used to describe the relation is of the form

$$d\sigma/d\epsilon = E_o + A\sigma \tag{1}$$

where σ is the stress in muscle, ϵ is the strain of the SEC (normalized to l_o), $d\sigma/d\epsilon$ is the stiffness, E_o is the initial elastic modulus, and A is the slope of the linear stiffness-stress curve.

By arbitrarily defining that $\epsilon = 0$ when $\sigma = 0$, $Eq. 1$ can be integrated to give

$$\sigma = (E_o/A)\ (e^{A\epsilon} - 1) \tag{2}$$

Equation 2 describes the stress-strain relationship of the SEC, and it was used in this study to fit the experimental data. The computer was used to perform the two-dimensional (A, E_o) search for the minimum deviation of the experimental data from the curve described by *Eq. 2*.

RESULTS

Typical stress-strain curves of the SEC from a single experiment are shown in Fig. 2. *Equation 2* was used to fit the experimental data. The constants A and E_o associated with the best-fitting curve were obtained for each SEC. We also tried to fit the experimental data to linear and parabolic functions. The coefficients of determination were 0.854 ± 0.022 (SE), 0.949 ± 0.016, and 0.995 ± 0.004 for linear, parabolic, and exponential functions,
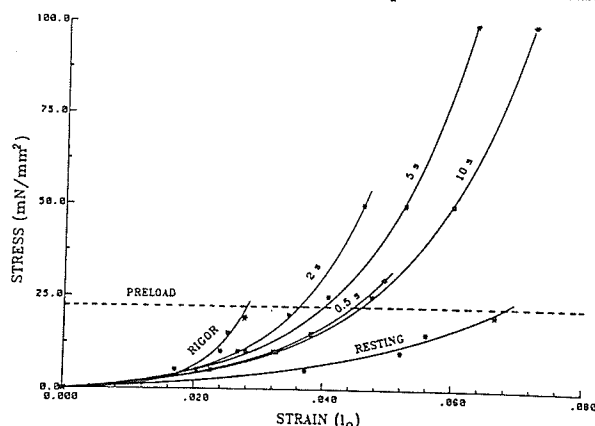

FIG. 2. Stress-strain curves of the series elastic component from a single experiment. The equation $\sigma = (E_o/A)\ (e^{A\epsilon} - 1)$ was used to fit experimental data. Labels on *curves* indicate state of muscle under which *curves* were obtained. Time (in s) labeled on *curves* indicates time when muscle was released. Stimulation started at *time 0*. *Dashed line* indicates stress level (preload) at which stiffnesses of series elastic components were compared. Constant-stress stiffnesses were obtained by measuring slopes of stress-strain curves at intersections of *dashed line* (preload) and *curves*. l_o, optimum length of muscle.

respectively. The exponential function (*Eq. 2*) was therefore chosen in this study to characterize the SEC stress-strain curve. It was found that the SEC stress-strain curves were different at different times after stimulation, although each of them can be fitted by an exponential curve. The SEC of the muscle in rigor was the stiffest; the resting muscle was the most compliant. At 0.5 s after stimulation, before the isometric tension was detected, the stiffness of the SEC increased significantly (Fig. 3).

Stiffness of the SEC is broken down into two components according to *Eq. 1*: one is the initial elastic modulus E_o which is stress independent; the other is $A\sigma$, which depends on stress (σ) linearly. (Both components were plotted in Fig. 3.) To compare the stiffness of the SEC's, the magnitude of the stress in the SEC has to be specified. However, because the stress independent stiffness (E_o) is relatively small and remains quite constant throughout contraction (Fig. 3), the only parameter that determines the stiffness at any stress level is the constant A. Constant A therefore is an index of the stiffness that excludes the effect of stress in the SEC. The constant A as a function of time is shown in Fig. 3; it represents the time variation of the SEC stiffness. Here the value of A is multiplied by a constant stress value of 22.2 mN/mm^2 (10% of P_o) so that the relative values of E_o and $A\sigma$ can be compared. It should be realized that, if different stress levels were used, the shape of the $A\sigma$ curve would be the same but the magnitude would be different. A typical isometric tension-time curve is also shown in Fig. 3 to indicate the time course of contraction.

The constants E_o and A and P_o of the four muscle strips (from four dogs) used in the experiments are shown in Table 1.

DISCUSSION

Continuous measurement of the SEC stiffness in an isometric contraction using small sinusoidal length perturbations and measures the amplitude and phase of the resulting tension perturbations (5, 16) is not applicable to the present study because load on the SEC is not held constant during the measurement. (The load on the SEC
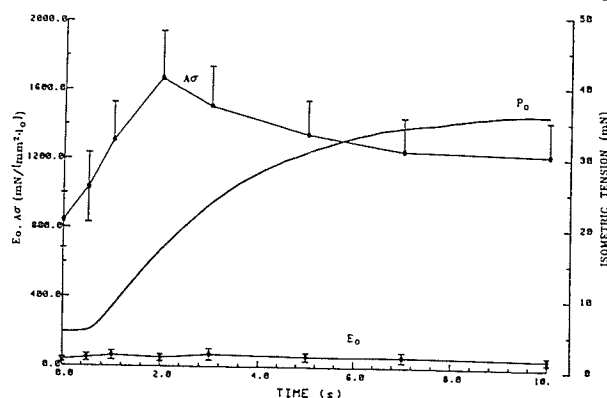
FIG. 3. Series elastic component stiffness is broken down into 2 components: E_o (initial elastic modulus, stress independent) and $A\sigma$ (stress dependent, where A is slope and σ is stress) and are both plotted against time ($n = 4$, SE *bars* shown). Isometric tension curve (*solid line* with no error *bar*) is plotted to illustrate time relationship of stages in contraction (see text). l_o, optimum length of muscle.

TABLE 1. *Constants A, E_o, and P_o from four experiments*

Muscle Condition	Exp No.				Means ± SE
	1	*2*	*3*	*4*	
P_o, mN/mm²	224.7	205.7	236.7	221.0	222.0±6.4
Resting					
A	20.0	36.5	40.0	55.0	37.9±7.2
E_o	30.0	76.6	20.8	16.5	36.0±13.8
After stimulation, s					
0.5					
A	21.0	55.0	47.0	63.0	46.5±9.1
E_o	31.5	115.5	31.9	18.3	49.3±22.3
1.0					
A	29.0	67.0	66.0	73.0	58.8±10.1
E_o	43.5	140.7	44.9	21.2	62.6±26.6
2.0					
A	42.0	78.0	78.0	102.0	75.0±12.4
E_o	50.4	109.2	32.8	9.2	50.4±21.3
3.0					
A	38.0	70.0	77.0	86.0	67.8±11.0
E_o	60.8	168.0	38.5	13.76	70.3±34.0
5.0					
A	36.0	61.0	67.0	78.0	60.6±8.9
E_o	54.0	128.5	34.8	14.8	58.0±25.0
7.0					
A	35.0	56.0	56.0	78.0	56.3±8.8
E_o	52.5	145.6	31.36	7.8	59.3±30.2
10.0					
A	34.0	53.5	56.0	78.0	55.4±9.0
E_o	47.6	112.4	39.2	7.8	51.7±22.0
Rigor					
A	66.0	155.0	138.0	180.0	134.8±24.5
E_o	26.4	46.5	27.6	18.0	29.6±6.0

l_o, optimum length of muscle; P_o, maximum isometric tension. Constant A (slope) is measured in l_o^{-1}; constant E_o (initial elastic modulus) is measured in mN/mm²·l_o.

in an isometric contraction is the isometric tension developed by the contractile element.) With the use of such measurements it is found that the stiffness at P_o is higher than that early in contraction. If we were to conclude on this basis that more cross bridges were attached at the plateau phase than they were early in contraction, it would be erroneous. Because the stiffnesses were obtained at different portions of the nonlinear stress-strain (or tension-extention) curve, they cannot be compared. To compare the SEC stiffness, either stress or strain of the SEC has to be specified. It is clear from Fig. 3 that the magnitude of E_o is relatively small and remains quite constant throughout contraction. This makes possible another way of comparing the SEC stiffness, which is to compare the slope of the stiffness-stress curves (the constant A in *Eq. 1*).

In tracheal smooth muscle, constant A is not a constant with respect to time, however (Fig. 3), nor is isometric tension constant throughout the time course of contraction. The continuous measurement of the SEC stiffness using high-frequency perturbations therefore involves a changing value of A with time and a changing P_o with time, and it can be described by the modified *Eq. 1*: $d\sigma/d\epsilon = E_o + A(t) \cdot P_o(t)$, where $A(t)$ is a function of time. The instantaneous isometric tension $P_o(t)$ is the load on the SEC when the muscle is contracting isometrically. By plotting the dynamic stiffness [$E_o + A(t) \cdot P_o(t)$] and the isometric tension [$P_o(t)$] vs. time (Fig. 4), we find that there is a shift to the left of the stiffness
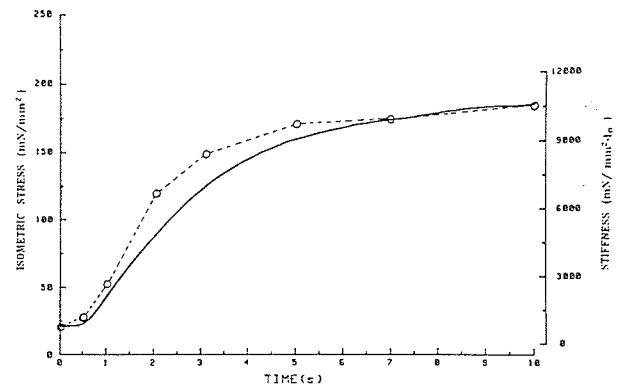

FIG. 4. Typical isometric stress curve (*solid line*) and associated continuous (or dynamic) stiffness curve (*dashed line*). Circles are stiffnesses at various times calculated from *Eq. 1*. Values of E_o (initial elastic modulus) and A (slope) for different times are obtained from Table 1. The stress (σ) at corresponding times are obtained from isometric stress curve shown in figure. Note that, unlike stiffness curves shown in Fig. 3, stiffness here is obtained at different stress levels. l_o, optimum length of muscle.

curve compared with the isometric tension curve. This seems to suggest that the development of stiffness precedes the development of isometric tension. Similar results have been found in skeletal muscle (5, 10) and smooth muscle (8, 16). Their interpretation is that a long-lived state exists between cross-bridge attachment and force generation. Our experiment seems to confirm the existence of such a state in our preparation, because at 0.5 s after the onset of stimulation, while no development of isometric tension can be observed, there is a significant increase in the SEC stiffness estimated by the values of $E_o + A\sigma$ ($P < 0.05$). However, it seems that the shift to the left of the stiffness curve cannot be totally explained by the existence of the long-lived cross-bridge state. Mathematically speaking, it is the time dependence of constant A that prevents the superimposition of the stiffness and isometric tension curves. If we assume that A is constant with respect to time, then the continuous (or dynamic) stiffness [$E_o + A \cdot P_o(t)$; note that the function $A(t)$ here is assumed to be a constant with respect to time; that is, A] is proportional to the isometric tension [$P_o(t)$], and by plotting the two curves and selecting the proper units, the two curves can be made to superimpose. Therefore, it is the behavior of the function $A(t)$ that determines how the stiffness curve is going to differ from the isometric tension curve. In our experiment it is the fact that $A(t)$ is greater early in contraction compared with the $A(t)$ at the plateau of contraction that results in the shift to the left of the stiffness curve. What does the function $A(t)$ represent physiologically then?

As mentioned earlier, since the value of E_o is relatively small and time independent, constant A directly reflects the SEC stiffness (at any stress level), which could be directly related to the number of attached cross bridges. Therefore the shift to the left of the stiffness curve could partly be due to the fact that the number of attached cross bridges is greater early in contraction than that at plateau.

It is interesting to note that the zero-load velocity of

electrically stimulated canine tracheal smooth muscle (21) and the constant A vary in a very similar manner with time. The peak velocity and peak stiffness both occur at 2 s after stimulation. Dillon et al. (7) found that both shortening velocity and phosphorylation of myosin light chain (LC 20) varied in a similar manner with time. Kamm and Stull (15) also obtained similar results in bovine tracheal smooth muscle. These findings together with our observation that stiffness (constant A) and zero-load velocity varied in a very similar way with time suggest that myosin phosphorylation, maximal shortening velocity, and stiffness of muscle are intimately related. The stiffness of the SEC during contraction falls within the limits of the stiffness of resting muscle and that of muscle in rigor (Fig. 2, Table 1). This is in agreement with the X-ray diffraction studies of striated muscle in which it is found that "the changes in structure that occur when a relaxed muscle is activated are in the direction of those changes that occur when a relaxed muscle goes into rigor" (23). Studies on the rate of O_2 uptake in tracheal smooth muscle (26) indicate that early in contraction the O_2 uptake rate is more than three times higher than that in plateau phase. This seems to support the notion that the number of active cross bridges is higher early in contraction. Of course the high O_2 uptake rate could also stem from the high cross-bridge cycling rate early in contraction [according to Eisenberg and Hill (9)].

If we insist that the SEC stiffness is directly proportional to the number of attached cross bridges [which seems to be supported by X-ray, electron microscopy, and mechanical studies (1, 13, 14, 19, 20, 28)], there still remains the question of how the attachment of cross bridges affects the stiffness. To understand the mechanism it is necessary to know where in the muscle the series elasticity resides. Unfortunately this is an unsettled question. Sugi and Suzuki's electron microscopy studies (27) on striated muscle reveal that the elastic element is at the nonoverlap zones in sarcomeres. This conclusion is based on the observation that the thick filaments are extensible only at the H zones, whereas the thin filaments are extensible everywhere except for the zone of overlap in rigor muscle. This finding in striated muscle is not totally inapplicable to smooth muscle, because in smooth muscle it is believed that contraction is brought about by the interaction of actin and myosin filaments just as that in striated muscle, and hence there must exist overlap and nonoverlap zones. Therefore the intracellular SEC does not necessarily associate with the cross bridges, specifically the myosin S-2 linkage. In an isometric contraction the extracellular and intracellular SEC's are inevitably stretched. If the stress-strain relationship of the combined SEC is not linear, then the degree of stretch would affect the stiffness measured and an increase in stiffness due to a more stretched SEC cannot be simplistically interpreted as due to an increase in attachment of cross bridges.

If stress in the SEC is held constant, then the SEC stiffness stemming from the cross bridges could be proportional to the number of attached cross bridges per cross section of the muscle. Because each cross bridge can be visualized as a spring, if the number of cross bridges (per cross section) increases, the number of parallel springs increases and the stiffness increases. On the other hand, each nonoverlap zone can also be visualized as a spring (27). The nonoverlap zones could include the unattached zones within the overlap zones (not all the cross bridges are attached even in an active muscle). If the number (or the total length) of the unattached zones increases, the number of series springs increases, and the stiffness decreases.

In conclusion, the time-dependent behavior of the SEC is best seen when the effect of stress is held constant or eliminated. A phasic time behavior of the SEC stiffness is revealed by the change in the slope of the stiffness-stress curve (constant A) with time. If the stress is allowed to increase with time as it does during an isometric contraction, a monotonic increase in the SEC stiffness would be observed (as in the high-frequency dynamic stiffness measurements). The stiffness of the muscle in rigor state is much higher than that at resting state. The stiffness of normal muscle during contraction varies significantly with time but within the limits of the stiffness of muscle in rigor and that at resting state.

REFERENCES

1. BOSE, D. Mechanical changes in smooth muscle during rigor. In: *Smooth Muscle Contraction*, edited by N. L. Stephens. New York: Dekker, 1984, p. 199–217.
2. BRESLER, B. H., AND N. F. CLINCH. Crossbridges as the major source of compliance in contracting skeletal muscle. *Nature Lond.* 256: 221–222, 1975.
3. BRUTSAERT, D. L., AND V. A. CLAES. Onset of mechanical activation of mammalian heart muscle in calcium and strontium containing solution. *Circ. Res.* 35: 345–347, 1974.
4. BRUTSAERT, D. L., V. A. CLAES, AND E. H. SONNENBLICK. Effects of abrupt load alterations on force-velocity-length and time relations during isotonic contraction of heart muscle: load clamping. *J. Physiol. Lond.* 216: 319–330, 1971.
5. CECCHI, G., P. J. GRIFFITHS, AND S. TAYLOR. Muscular contraction: kinetics of crossbridge attachment studied by high-frequency stiffness measurements. *Science Wash. DC* 217: 70–72, 1982.
6. COX, R. H. Influence of muscle length on series elasticity in arterial smooth muscle. *Am. J. Physiol.* 234 (*Cell Physiol.* 3): C146–C154, 1978.
7. DILLON, P. F., M. O. AKSOY, S. P. DRISKA, AND R. A. MURPHY. Myosin phosphorylation and the cross-bridge cycle in arterial smooth muscle. *Science Wash. DC* 211: 495–497, 1981.
8. DILLON, P. F., AND R. A. MURPHY. Tonic force maintenance with reduced shortening velocity in arterial smooth muscle. *Am. J. Physiol.* 242 (*Cell Physiol.* 11): C102–C108, 1982.
9. EISENBERG, E., AND T. L. HILL. Muscle contraction and free energy transduction in biological systems. *Science Wash. DC* 227: 999–1006, 1985.
10. FORD, L. E., A. F. HUXLEY, AND R. M. SIMMONS. Tension transients during the rise of tetanic tension in frog muscle fibres. *J. Physiol. Lond.* 372: 595–609, 1986.
11. HELLSTRAND, P., AND B. JOHANSSON. Analysis of the length response to a force step in smooth muscle from rabbit urinary bladder. *Acta Physiol. Scand.* 106: 221–238, 1979.
12. HERLIHY, J. T., AND R. A. MURPHY. Force-velocity and series elastic characteristics of smooth muscle from the hog carotid artery. *Circ. Res.* 34: 461–466, 1974.

13. HUXLEY, H. E. Structural difference between resting and rigor muscle; evidence from intensity changes in the low-angle equitorial x-ray diagram. *J. Mol. Biol.* 37: 507–520, 1968.

14. HUXLEY, H. E., AND W. BROWN. The low-angle x-ray diagram of vertebrate striated muscle and its behavior during contraction and rigor. *J. Mol. Biol.* 30: 383–434, 1967.

15. KAMM, K. E., AND J. T. STULL. Myosin phosphorylation, force, and maximal shortening velocity in neurally stimulated tracheal smooth muscle. *Am. J. Physiol.* 249 (*Cell Physiol.* 18): C238–C247, 1985.

16. KAMM, E. K., AND J. T. STULL. Activation of smooth muscle contraction: relation between myosin phosphorylation and stiffness. *Science Wash. DC* 232: 80–82, 1986.

17. MEISS, R. A. Dynamic stiffness of rabbit mesotubarium smooth muscle: effect of isometric length. *Am. J. Physiol.* 234 (*Cell Physiol.* 3): C14–C26, 1978.

18. MULVANY, M. J., AND D. M. WARSHAW. The anatomical location of the series elastic component in rat vascular smooth muscle. *J. Physiol. Lond.* 314: 321–330, 1981.

19. REEDY, M. K. Ultrastructure of insect flight muscle. I. Screw sense and structural grouping in the rigor crossbridge lattice. *J. Mol. Biol.* 31: 155–176, 1968.

20. SANDOW, A., AND C. A. SCHNEYER. Mechanics of iodoacetate rigor of muscle. *J. Cell. Comp. Physiol.* 45: 131–156, 1955.

21. SEOW, C. Y., AND N. L. STEPHENS. Force-velocity curves for smooth muscle: analysis of internal factors reducing velocity. *Am. J. Physiol.* 251 (*Cell Physiol.* 20): C362–C368, 1986.

22. SIEGMAN, M. J., T. M. BUTLER, S. U. MOOERS, AND R. E. DAVIES. Crossbridge attachment, resistance to stretch, and viscoelasticity in resting mammalian smooth muscle. *Science Wash. DC* 191: 383–385, 1976.

23. SQUIRE, J. Structural evidence on the contractile event. In: *The Structural Basis of Muscular Contraction*, edited by J. Squire. New York: Plenum, 1981, p. 523–615.

24. STEPHENS, N. L., E. A. KROEGER, AND J. A. MEHTA. Force-velocity characterization of respiratory airway smooth muscle. *J. Appl. Physiol.* 26: 685–692, 1969.

25. STEPHENS, N. L., AND U. KROMER. Series elastic component of tracheal smooth muscle. *Am. J. Physiol.* 220: 1890–1895, 1971.

26. STEPHENS, N. L., AND C. M. SKOOG. Tracheal smooth muscle and rate of oxygen uptake. *Am. J. Physiol.* 226: 1462–1467, 1974.

27. SUGI, H., AND S. SUZUKI. Extensibility of the myofilaments in vertebrate skeletal muscle as studied by stretching rigor muscle fibres. *Proc. Jpn. Acad. Ser. B* 56: 290–293, 1980.

28. WARSHAW, D. M., AND F. S. FAY. Cross-bridge elasticity in single smooth muscle cells. *J. Gen. Physiol.* 82: 157–199, 1983.

Velocity-length-time relations in canine tracheal smooth muscle

C. Y. SEOW AND N. L. STEPHENS
Department of Physiology, Faculty of Medicine, University of Manitoba,
Winnipeg, Manitoba R3E 0W3, Canada

SEOW, C. Y., AND N. L. STEPHENS. *Velocity-length-time relations in canine tracheal smooth muscle.* J. Appl. Physiol. 64(5): 2053–2057, 1988.—Zero-load velocity (V_0) as a function of the length of canine tracheal smooth muscle was obtained by applying zero-load clamps to isotonically contracting muscle under various loads. The load clamps were applied at a specific time after onset of contraction. The magnitude of the isotonic load therefore determines the length of the muscle at the moment of release or at the moment the unloaded shortening velocity was measured. A family of such V_0-muscle length (L) curves was obtained at 1-s intervals in the time course of contraction. The V_0-L curve was fitted by a parabolic function with satisfactory goodness of fit. The maximum shortening velocity at optimum muscle length varied with time, but the minimum length at which V_0 diminished to zero was time independent.

zero-load velocity; shortening inactivation; internal load

IN MUSCLE CONTRACTION, shortening per se results in reduction of the muscle's shortening velocity (3, 4, 6, 7). In skeletal muscle it was found that at sarcomere length <1.65 μm (~75% of the sarcomere length) the velocity of shortening decreased linearly with length (6). In cardiac muscle the zero-load velocity (V_0) was reduced if the length was less than ~87% of optimum muscle length (L_{max}) (3). In smooth muscle our previous studies showed that V_0 obtained by applying zero-load clamp to an isotonically contracting muscle (14) was slower than that obtained by applying zero-load clamp to an isometrically contracting muscle (12), especially in the late phase of contraction where substantial shortening of the muscle has occurred. This indicated the presence of the depressive effect of reduced length on shortening velocity similar to that observed in striated muscle. However, smooth muscle is unique in that its shortening velocity is time dependent (5, 13, 19). Characterization of the V_0-L relations in smooth muscle therefore would not be complete without considering the time variable. In this study, quantitative relations among velocity, length, and time were examined in canine tracheal smooth muscle (TSM).

METHODS

Preparation of muscle strips and data acquisition. The control dog was anesthetized with pentobarbital sodium (30 mg/kg body wt iv). This was followed by rapid removal of the cervical trachea via a midline incision and an intracardiac injection of saturated KCl solution to kill the animal. The trachea was immediately placed in a beaker of ice-cold, aerated Krebs-Henseleit solution of the following composition (in mM): 115 NaCl, 25 NaHCO$_3$, 1.3 NaH$_2$PO$_4$, 2.5 KCl, 2.46 MgSO$_4\cdot$7H$_2$O, 1.92 CaCl$_2$, 5.6 dextrose. With the connective tissues carefully dissected away under a dissecting microscope, a strip of muscle was cut from the trachea. Details for preparing canine TSM have been previously reported (15). The strips used in the experiments were on average 6 mm long and 0.5 mm wide and weighed 1.5 mg. One end of the strip was connected to the lever by a highly noncompliant surgical thread (7-O silk) ~7 cm long. The other end of the strip was fixed in the muscle bath by a clamp. The bath containing Krebs-Henseleit solution was aerated with 95% O$_2$-5% CO$_2$ that maintained a Po$_2$ of 600 Torr, a Pco$_2$ of 40 Torr, and pH of 7.4 at 37°C. The strip was equilibrated in the bath for 1–2 h. During this time it was electrically stimulated every 4 min by a 17-V, 60-Hz alternating current applied through the platinum electrodes that were positioned on either side of the muscle. The duration of stimulation was 10 s, which was also the contraction time of the muscle. The isometric tetanic force was usually low initially but rose to a higher steady-tension level (30% higher) after the equilibrating period. The steady state usually lasted for several hours. The L_{max} was obtained by varying the preload (and hence the length of the muscle strip and measuring the isometric tetanic tension. The length that was associated with the development of maximum tension (P$_o$) was identified as L_{max}. The preload associated with L_{max} was ~10% of P$_o$.

The instantaneous force and displacement produced by the muscle were recorded with the help of an electromagnetic lever system. The lever is fashioned from Mg and is attached by epoxy cement to a coil suspended in a strong magnetic field provided by a permanent magnet. This system has a total compliance of 0.2 μm/g and a total equivalent moving mass of 225 mg. The equivalent moving mass of the lever is 40 mg. The time resolution of the lever system was 2 ms. The apparatus was originally developed by Brutsaert and Claes (2) for cardiac muscle and was adapted for use with slower smooth muscle. The signals from the lever system were digitized by an analog-to-digital converter, and the digital signals were fed to an HP-9836 computer that analyzed and plotted data in both graphical and numerical forms. The

maximum sampling frequency of the recording system was 1,000 Hz.

The compliance of the thread connecting the muscle strip to the lever was measured after each experiment. The muscle was removed, and the thread was fixed to the clamp in the bath. Load steps were applied to the thread, and the subsequent displacements were recorded. These measurements would later be used to correct the experimental data. The average compliance of the thread was 0.004 mm/mN.

Experimental procedure and data analysis. Because smooth muscle shortening velocity is time dependent (5, 13, 19), the time variable must be held constant when studying the V_0-L relations of the muscle. Also because of the time dependency, a single V_0-L curve is not adequate to characterize the relationship between velocity and length of the muscle; instead, a family of V_0-L curves obtained at various points in the time course of contraction must be used. The V_0-L curve was obtained from raw data similar to those shown in Fig. 1. The V_0 was obtained by measuring the slope of the displacement curve 100 ms after the quick release (zero-load clamp). The load clamp was critically damped. The damping was provided electronically by differentiating and inverting the displacement signal and feeding it back to the original displacement signal through an adjustable resistor that controlled the degree of damping. The "zero-load" to which the muscle was released was in fact a finite load of ~0.2 mN (~ 0.4% of P_o), which was partially counterbalanced by the weight of the thread that connected the muscle to the level. The muscle length at the moment the muscle was released was controlled indirectly by the load on the muscle. The afterloads used in the experi-

ments varied from ~5 to 100% P_o, which corresponded to ~50–100% L_{max} (before load clamp). The muscle length (L) used in the V_0-L plot referred to the length immediately after the load clamp, at which the velocity was measured. V_0 here referred to zero-load velocity, regardless of the length at which the velocity was measured. So V_0 did not represent maximum shortening velocity of the muscle if $L < L_{max}$.

RESULTS

The velocity-length data shown in Figs. 2 and 3 were fitted with a parabolic function of the form

$$V_0(L) = V_{max}\{1 - [(1 - L)/(1 - L_{min})]^2\}$$

where V_{max} was the maximum shortening velocity or zero-load velocity at L_{max} [i.e., $V_{max} = V_0(L_{max})$] and L_{min} was the length of the maximally contracted muscle under zero load or the minimum muscle length. L was expressed as percent of L_{max}, and therefore L_{max} was unity. The coefficients of determination (r^2) for the curves in Figs. 2 and 3 were all >0.94. Because of the close fit, for any given values of L_{max} and L_{min}, the parabolic equation was sufficient to define the V_0-L curve. For this reason the parameters V_{max} and L_{min} are emphasized in this study. The values for each of the eight experiments are listed in Table 1. Note that V_{max} varied with time, whereas L_{min} was time independent, as shown in Fig. 3. The maximum value of the parabolic function V_{max} varied from second to second, but the x-axis intercept of the function remained the same.

DISCUSSION

In skeletal muscle (single fiber) there seems to be a length range over which the shortening velocity is rela-

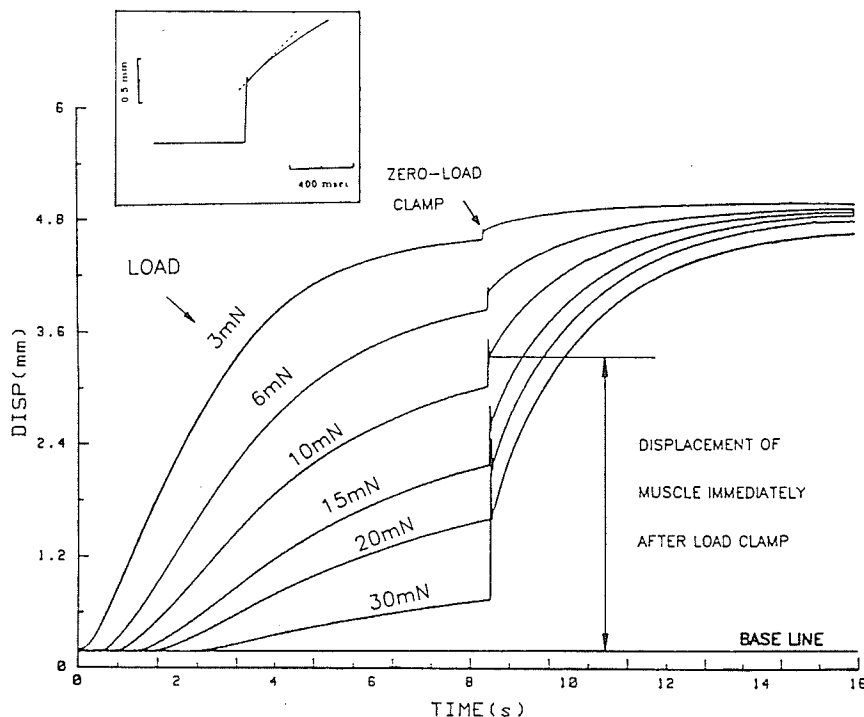FIG. 1. Experimental records (superimposed) for obtaining zero-loading velocity-length curve. Muscle length was obtained by subtracting displacement (DISP) of muscle immediately after load clamp from optimum length (e.g., 10-mN curve). Velocity was obtained by measuring slope of displacement curve 100 ms after zero-load clamp, as shown in *inset.* Optimum length of muscle was 8.5 mm and weight was 2 mg.
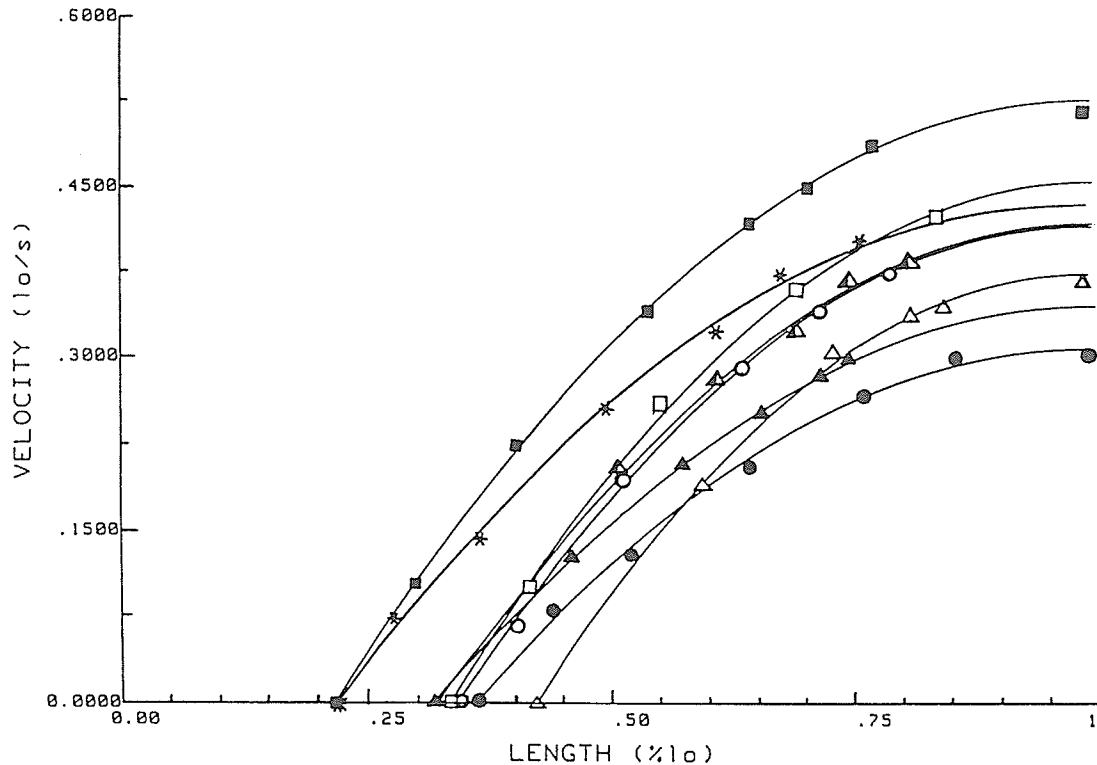
FIG. 2. Zero-loading velocity-length curves for 8 preparations from 8 dogs. Curves were all obtained at 5 s after stimulation. Data were fitted with parabolic equation described in text. Each symbol represents different muscle preparation. L_o, optimum length.

tively constant. Edman (6) reported that this range was from 1.65 to 2.7 μm of the sarcomere length. In cardiac muscle this range is somewhat smaller (3). Under normal physiological conditions, skeletal and cardiac muscles are probably operating in or near the constant velocity-length range. In smooth muscle, a physiological working length range is hard to define. In airway and vascular smooth muscle, from a pathological point of view, it is the behavior of the muscle near L_{min} that seems to be important. [Asthma and essential hypertension in animal models seem to be associated with an increased ability of the smooth muscles to shorten (1, 10, 11, 17).] Our present study focuses on the velocity behavior that was length dependent, at short muscle length. However, the relatively length-independent shortening velocity near L_{max} could be seen in both Figs. 2 and 3.

Although the parabolic equation $V_0(L) = V_{max}\{1 - [(1 - L)/(1 - L_{min})]^2\}$ is purely empirical, it helps in simplifying the data analysis and in constructing V_0-L curves out of the V_{max} and L_{min} data. The fact that the V_0-L curve was smooth and continuous and not like that reported by Edman (6), which consisted of a linear ascending limb and a flat plateau, probably was partly because our muscle preparation was multicellular. The asynchronous contraction of the individual cells and the effect of the nonmuscle components in the preparation, such as connective tissues, could smooth out the V_0-L curve. However, that does not exclude the possibility that the lack of length-independent velocity region in

smooth muscle is due to a more fundamental difference in the structure of the contractile apparatus. The recent finding that smooth muscle shortens in a corkscrew-like fashion (20) suggests that the contractile apparatus is helically oriented within the cell. The effect of this helical arrangement on the velocity-length relations needs further investigation. The behavior of the curve beyond L_{max} was not determined; therefore a plateau for the curve at $L > L_{max}$ is not excluded.

The fact that a parabolic curve fits the V_0-L curve implies that the change in V_0 due to the change in L (dV_0/dL) is linearly related to the deviation of the muscle length from its optimum ($L_{max} - L$). That is, $dV_0/dL \propto (L_{max} - L)$. By putting in a constant of proportionality and integrating the differential equation (providing that $V = 0$ when $L = L_{min}$ and expressing all the lengths as fractions of L_{max}), a parabolic function of the same form as the one we used to fit the V_0-L data, can be obtained.

The factors that cause the drop in shortening velocity at $L < L_{max}$ could be many. One well-observed phenomenon is shortening inactivation. This has been described in skeletal (18), cardiac (3, 9), and smooth muscles (16). This inactivation can be alleviated by increasing the extracellular calcium concentration. A reduced tension due to shortening inactivation could affect the shortening velocity. This may sound contradictory to Huxley's 1957 model (8). However, if the muscle shortens to such an extent that it compresses its internal structure, which in
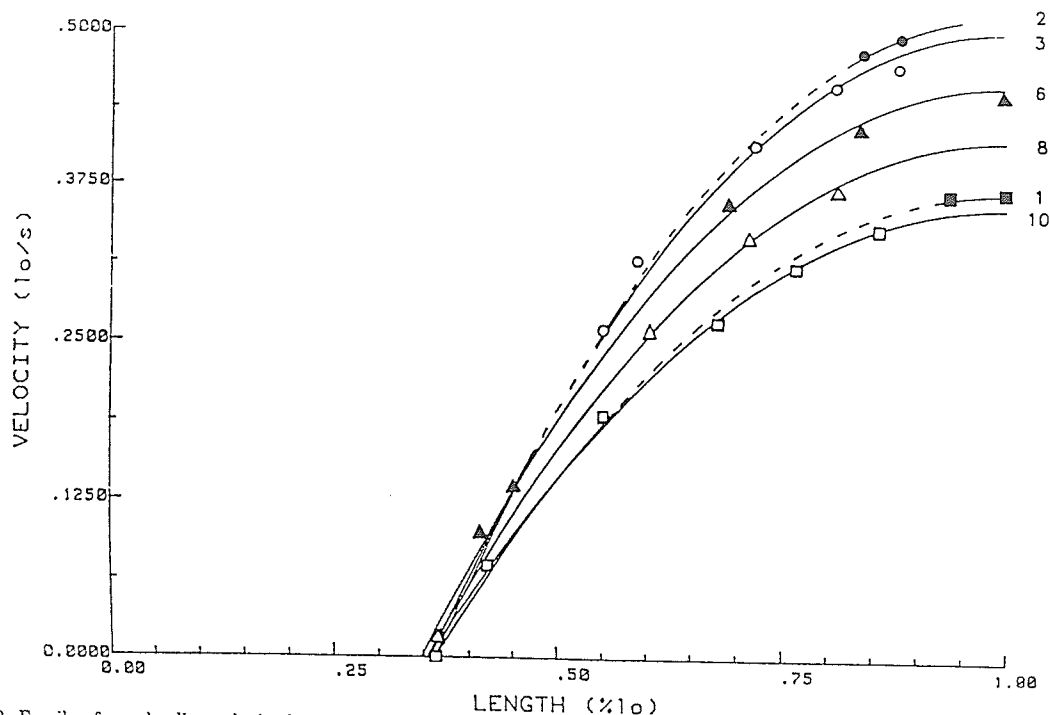
FIG. 3. Family of zero-loading velocity-length (V_0-L) curves obtained from single preparation. Number that labels each curve indicates time (in s) after onset of stimulation when zero-load clamps were applied and V_0-L data were measured. Note that early in contraction there was not enough time for muscle to produce large amount of shortening, and therefore V_0 data at short muscle length could not be measured. – – –, Portion of curve that was technically impossible to measure. L_o, optimum length.

TABLE 1. V_{max} and L_{min} values for 8 experiments

Time After Stimulation, s	Experiment No.								Mean ± SE
	1	2	3	4	5	6	7	8	
	V_{max}, L_{max}/s								
1	0.357	0.351	0.259	0.288	0.303	0.349	0.440	0.350	0.337±0.019
2	0.527	0.516	0.466	0.502	0.422	0.570	0.600	0.470	0.509±0.020
3	0.519	0.507	0.457	0.491	0.416	0.565	0.590	0.460	0.500±0.020
4	0.453	0.444	0.374	0.408	0.369	0.480	0.530	0.400	0.432±0.019
5	0.438	0.430	0.358	0.489	0.359	0.456	0.510	0.406	0.431±0.019
6	0.423	0.415	0.338	0.370	0.349	0.437	0.500	0.340	0.396±0.020
7	0.408	0.402	0.321	0.351	0.339	0.417	0.490	0.380	0.388±0.019
8	0.393	0.387	0.302	0.333	0.328	0.397	0.470	0.370	0.373±0.018
9	0.372	0.367	0.278	0.306	0.312	0.368	0.450	0.370	0.352±0.019
10	0.364	0.359	0.261	0.296	0.309	0.359	0.450	0.360	0.345±0.020
	L_{min}, $\%L_{max}$								
	0.365	0.240	0.381	0.343	0.310	0.200	0.200	0.330	0.296±0.026

V_{max}, maximum shortening velocity at optimum muscle length (L_{max}); L_{min}, minimum muscle length.

turn creates an internal load on the contractile apparatus, then the zero load will no longer be so, although the external load is zero. Under such circumstance, a reduced tension will result in a reduced shortening velocity. An internal viscoelastic load in actively shortening cat papillary muscle was well described by Chiu et al. (4). A reduced tension at short muscle length because the muscle is operating on the ascending limb of the muscle's length-tension curve could also reduce the shortening velocity if there is an internal load. A recent study by Gunst (7) on the effect of length history on contractile

behavior of TSM showed that the initial muscle length and the shortening process per se affected the rate and the magnitude of force redevelopment. This suggests that different V_0-length-time surfaces would be obtained if contraction started at different initial lengths. In this study, contraction always started at L_{max}.

In contrast to V_{max}, L_{min} is relatively time independent. This probably indicates that the maximum amount of shortening produced by a muscle is largely determined by the physical properties of passive components of the muscle, for instance, the stiffness of the parallel elastic

component, but not the degree of activation of the contractile element. However, the interaction of actin with myosin may be relatively inhibited because of the deformation of the cytoskeletal protein network and the packing of the filaments at short muscle lengths. In this case, however, the real factor that determines L_{min} would still be the noncontractile component of the muscle. Changes in L_{min} associated with pathological changes in smooth muscle function such as those found in the canine asthmatic and rat essential hypertension models (1, 10, 11, 17) therefore probably involve alterations in noncontractile components of the muscle, such as cytoskeletal proteins.

The time dependence of smooth muscle shortening velocity has been well documented (5, 13, 19). Although controversies still exist as to the cause of this time dependency, one explanation proposed by Dillon et al. (5) is that calcium-calmodulin-dependent myosin light-chain phosphorylation is responsible for the development of the "normally" cycling bridges early in contraction, and dephosphorylation is for the slow cycling "latch" bridges late in contraction.

Unloaded shortening velocity of muscle is generally regarded as an index of the maximum intrinsic crossbridge cycling rate. However, many nonmechanical factors such as pharmacological or biochemical ones, can affect this cycling rate. To study their effect, one should make allowances for the dependency of shortening velocity on length and time, especially when isotonic contractions are involved.

REFERENCES

1. ANTONISSEN, L. A., R. W. MICHELL, E. A. KROEGER, W. KEPRON, K. S. TSE, AND N. L. STEPHENS. Mechanical alterations in airway smooth muscle in canine asthmatic model. *J. Appl. Physiol.* 46: 681–687, 1979.
2. BRUTSAERT, D. L., AND V. A. CLAES. Onset of mechanical activation of mammalian heart muscle in calcium and strontium containing solution. *Circ. Res.* 35: 345–347, 1974.
3. BRUTSAERT, D. L., V. A. CLAES, AND E. H. SONNENBLICK. Effect of abrupt load alterations on force-velocity-length and time relation during isotonic contractions of heart muscle: load clamping. *J. Physiol. Lond.* 216: 319–330, 1971.
4. CHIU, Y., E. W. BALLOW, AND L. E. FORD. Velocity transients and visoelastic resistance to active shortening in cat papillary muscle. *Biophys. J.* 40: 121–128, 1982.
5. DILLON, P. F., M. O. AKSOY, S. P. DRISKA, AND R. A. MURPHY. Myosin phosphorylation and the crossbridge cycle in arterial smooth muscle. *Science Wash. DC* 211: 495–497, 1981.
6. EDMAN, E. A. P. The velocity of unloaded shortening and its relation to sarcomere length and isometric force in vertebrate muscle fibers. *J. Physiol. Lond.* 291: 143–159, 1979.
7. GUNST, S. J. Effect of length history on contractile behavior of canine tracheal smooth muscle. *Am. J. Physiol.* 250 (*Cell Physiol.* 19): C134–C154, 1986.
8. HUXLEY, A. F. Muscle structure and theories of contraction. *Prog. Biophys. Biophys. Chem.* 7: 255–318, 1957.
9. JEWELL, B. R., AND J. R. BLINKS. Drugs and the mechanical properties of heart muscle. *Annu. Rev. Pharmacol.* 8: 113–130, 1968.
10. KEPRON, W., J. M. JAMES, B. KIRK, A. H. SEHON, AND K. S. TSE. A canine model for reaginic hypersensitivity and allergic bronchoconstriction. *J. Allergy Clin. Immunol.* 59: 64–69, 1977.
11. PACKER, C. S., AND N. L. STEPHENS. Force-velocity relationships in hypertensive arterial smooth muscle. *Can. J. Physiol. Pharmacol.* 63: 669–674, 1985.
12. SEOW, C. Y., AND N. L. STEPHENS. Force-velocity curves for smooth muscle: analysis of internal factors reducing velocity. *Am. J. Physiol.* 251 (*Cell Physiol.* 20): C362–C368, 1986.
13. SIEGMAN, M. J., T. M. BUTLER, S. U. MOORE, AND R. E. DAVIES. Crossbridges: attachment, resistance to stretch and viscoelasticity in resting mammalian smooth muscle. *Science Wash. DC* 191: 383–385, 1976.
14. STEPHENS, N. L., M. L. KAGAN, AND C. S. PACKER. Time dependence of shortening velocity in tracheal smooth muscle. *Am. J. Physiol.* 251 (*Cell Physiol.* 20): C435–C442, 1986.
15. STEPHENS, N. L., E. A. KROEGER, AND J. A. MEHTA. Force-velocity characterization of respiratory airway smooth muscle. *J. Appl. Physiol.* 26: 685–692, 1969.
16. STEPHENS, N. L., R. W. MITCHELL, AND D. L. BRUTSAERT. Shortening inactivation, maximum force potential, relaxation, contractility. In: *Smooth Muscle Contraction*, edited by N. L. Stephens. New York: Dekker, 1984, p. 91–112.
17. STEPHENS, N. L., G. MORGAN, W. KEPRON, AND C. Y. SEOW. Changes in cross-bridge properties of sensitized airway smooth muscle. *J. Appl. Physiol.* 61: 1492–1498, 1986.
18. TAYLOR, S. R., AND R. RUDEL. Striated muscle fibers: inactivation of contraction induced by shortening. *Science Wash. DC* 167: 882–884, 1970.
19. UVELIUS, B. Shortening velocity, active force and homogeneity of contraction during electrically evoked twitches in smooth muscle from rabbit urinary bladder (Abstract). *Acta Physiol. Scand.* 106: 481, 1979.
20. WARSHAW, D. M., W. J. McBRIDE, AND S. S. WORK. Corkscrew-like shortening in single smooth muscle cells. *Science Wash. DC* 236: 1457–1459, 1987.

Changes of tracheal smooth muscle stiffness during an isotonic contraction

C. Y. SEOW AND N. L. STEPHENS
*Department of Physiology, Faculty of Medicine, University of Manitoba,
Winnipeg, Manitoba R3E 0W3, Canada*

SEOW, C. Y., AND N. L. STEPHENS. *Changes of tracheal
smooth muscle stiffness during an isotonic contraction.* Am. J.
Physiol. 256 (Cell Physiol. 25): C341–C350, 1989.—Stiffness of
the series elastic component (SEC) of canine tracheal smooth
muscle in isotonic contraction and relaxation was measured by
applying small force perturbations to the muscle and measuring
the resulting length perturbations. The quick, elastic length
transient was taken as the change in length of the SEC (ΔL).
The force perturbation was a train of 10-Hz rectangular force
waves varying from 0 to 10% maximum isometric tension (P_o)
in magnitude ($\Delta P = 10\%\ P_o$). Stiffness of the SEC was esti-
mated by the ratio $\Delta P/\Delta L$. The change in SEC stiffness with
respect to the change in muscle length was further studied by
obtaining the stress-strain curves of the SEC at different mus-
cle lengths using the load-clamping method. The clamps were
applied at a fixed time (10 s after stimulation). Length of the
muscle 10 s after contraction was controlled by the magnitude
of the isotonic afterload. It was found that the apparent SEC
stiffness increased as muscle length decreased. This stiffness
increase is not likely due to an increase in the number of
attached cross bridges, but it is probably due to the gradual
diminution of the SEC length itself during muscle shortening.

*force perturbation; length perturbation; stress-strain curve;
series elastic component*

STIFFNESS OF the series elastic component (SEC) of
muscle is thought to be directly proportional to the
number of attached cross bridges (1, 3, 8, 9, 12, 16, 17,
19). To correctly use the SEC stiffness as an index of
the number of attached cross bridges, however, all other
variables that influence the stiffness have to be identi-
fied, and their relations with the stiffness have to be
characterized. Sinusoidal length perturbation techniques
are widely used in measuring muscle stiffness during
isometric contraction (1, 3, 16, 17, 19). The increase in
the apparent SEC stiffness with time in isometric con-
traction is thought to be due to the increase in the
number of attached cross bridges and also due to the
increase in stress in the SEC that possesses a nonlinear
tension-extension characteristic. Measurement of stiff-
ness change during an isometric contraction character-
izes stiffness as a function of time (after stimulation)
and stress. Measurement of stiffness change during an
isotonic contraction, on the other hand, characterizes
the stiffness as a function of time and muscle length. In
this study, small force perturbation with a constant
amplitude (ΔP) was applied to an isotonically contract-
ing muscle, and the quick, elastic transient of the length
response was measured and taken as the change in the
SEC length (ΔL). The SEC stiffness was estimated by
the ratio $\Delta P/\Delta L$.

Our previous study (23) has shown that SEC stiffness
of canine trachealis is time dependent. Therefore, to
study the effect of muscle length on the stiffness, the
"time" variable has to be held constant. The second part
of the present study examined the effect of muscle length
on the SEC stiffness by applying load clamps to the
muscle at a fixed time (10 s after onset of electrical
stimulation). Changes in the shape of the SECs stress-
strain curves obtained from the load-clamping experi-
ments at different muscle lengths were used to indicate
the influence of muscle length on the SEC stiffness.

METHODS

Preparation of muscle strip and data acquisition. The
control dog was anesthetized by intravenous injection of
30 mg/kg body weight of pentobarbital. This was fol-
lowed by rapid removal of the cervical trachea via a
midline incision and an intracardiac injection of satu-
rated KCl solution to kill the animal. The trachea was
placed immediately in a beaker of ice-cold, aerated
Krebs-Henseleit solution of the following composition
(in mM): 115 NaCl, 25 NaHCO$_3$, 1.38 NaH$_2$PO$_4$, 2.51
KCl, 2.46 MgSO$_4$-7H$_2$O, 1.91 CaCl$_2$, 5.56 dextrose. With
the connective tissue carefully removed under a dissect-
ing microscope, a strip of muscle was cut from the trachea
[details for preparing strips of canine tracheal smooth
muscle have been previously reported by us (25)]. The
strips used in the experiments possessed an average
length of 8 mm, an average weight of 2 mg, and a width
of 0.5 mm. One end of the strip was connected to the
lever by a highly noncompliant surgical thread (7-0 silk).
The other end of the strip was fixed in the muscle bath
by a clamp. The bath containing Krebs-Henseleit solu-
tion was aerated with a 95% O$_2$-5% CO$_2$ mixture which
maintained Po$_2$ of 600 Torr, a Pco$_2$ of 40 Torr, and a
pH of 7.4 at a temperature of 37°C. The strip was
equilibrated in the bath for 2 h. During this time, it was
stimulated every 4 min electrically by 17 V, 60-Hz alter-
nating current applied to platinum electrodes that were
positioned on either sides of the muscle. Tension re-
sponse produced by the supramaximal electrical stimu-
lation was ~80% of that produced by high-potassium
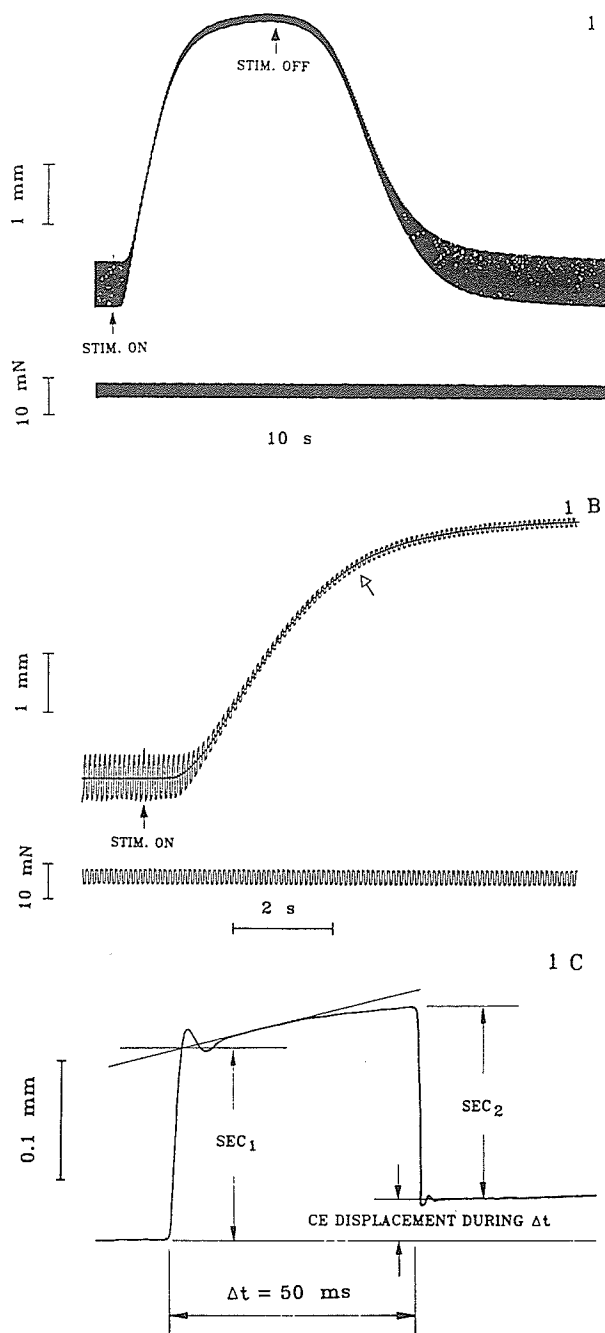stimulation. The duration of stimulation was 10 s, which

1 A

1 B

1 C

FIG. 1. A: Records of input force perturbations (*lower trace*) and resulting length perturbations (*upper trace*) during active shortening and relaxation of tracheal smooth muscle. Force perturbations were produced by rapidly (10 cycles/s) changing force level in lever from 0 to 4 mN repetitively (rectangular force wave). Amplitude of force wave was ~10% of P_o. Onset and termination of electrical stimulation are indicated on traces. Shortening is indicated in upward direction. B: portions of traces in A are here displayed at different time scale. Rectangular shape of force wave is visible here. Line through middle of *upper trace* was displacement curve of the muscle under a preload of 2 mN (mean value of force levels of rectangular force wave). C: magnification of a small portion of length perturbation trace around area indicated by *arrow* in B. SEC length was obtained by averaging lengths

was also the contraction time for the muscle. An equilibrium state was achieved when the muscle developed a steady tetanic tension under stimulation. The optimum muscle length (l_o) was obtained by varying the preload (and hence the length) of the muscle strip and measuring the isometric tetanic tension. The length that was associated with the development of maximum isometric tension (P_o) was identified as l_o. The preload associated with l_o was ~10% of P_o. Tension was normalized to the muscle's cross-sectional area. The area was determined by dividing the muscle volume (wet muscle density was assumed to be 1.0 g/cm^3) by its optimum length.

The instantaneous force and displacement produced by the muscle were recorded with the use of an electromagnetic lever system. The lever was fashioned from magnesium and was attached by epoxy cement to a coil suspended in a strong magnetic field provided by a permanent magnet. This system had a total compliance of 0.2 μm/g and a total equivalent moving mass of 225 mg. The equivalent mass of the lever was 40 mg. The frequency response of the lever system was 450 Hz. The apparatus was originally developed by Brutsaert et al. (2) for cardiac muscle. Signals from the lever system were digitized by an analog-to-digital (A/D) converter, and the digital signals were fed to an HP9836 computer that analyzed and plotted out data in both graphical and numerical forms. The maximum sampling frequency of the recording system was 4,000 Hz.

The compliance of the thread connecting the muscle strip to the lever was measured after each experiment. The muscle was removed, and the thread was fixed to the clamp in the bath. Load steps were applied to the thread, and the subsequent displacements were recorded. The thread compliance was not constant with respect to load. The whole stress-strain curve (exponential in shape) for the thread had to be obtained after each experiment and used to correct the experimental data.

Experimental procedure and data analysis. Continuous measurement of $\Delta P/\Delta L$ was made by applying ΔP to an isotonically contracting muscle and measuring the amplitude of the resulting displacement perturbations (ΔL). The force perturbation that the muscle subjected to was a train of rectangular force waves varying from 0 to ~4 mN (10% of P_o) with a frequency of 10 Hz. The length oscillation was critically damped. Examples of the experimental records are shown in Fig. 1. The reason square-wave force perturbation was used instead of a sinusoidal one (which is used by most investigators when they apply length perturbations to isometrically contracting muscle) was that the step change of force quick-released and stretched the muscle and thus revealed the corresponding quick length transient (the elastic response) that represented the change in the undamped SEC length (Fig. 1C). The force perturbation did not reduce the degree of activation of the muscle. This was concluded from experimental observations that the displacement curve of the muscle under a load of 2 mN superimposed the mean displacement curve of the same muscle under force per-

of SEC$_1$ and SEC$_2$ and subtracting compliance of thread and lever from averaged value. Data were recorded with a sampling frequency of 4,000 Hz to show details of trace. See text for definitions.

turbations changing from 0 to 4 mN at a perturbation frequency of 10 Hz (Fig. 1B). Also, the P_o after the perturbation was not reduced. However, if a force perturbation amplitude >20% of P_o was used, then the shortening ability of the muscle was reduced, probably due to disruption of the cross-bridge attachments by large force steps. Ideally, small amplitude of force perturbation should be used. However, if the amplitude was too small, then the resulting small length perturbation could not be accurately measured. In our experiments, an amplitude of 10% P_o was chosen. The force perturbation method enabled us to measure the stiffness continuously in a single isotonic contraction. A perturbation frequency of 10 Hz was chosen because at this frequency (or lower) the recording system was able to faithfully record the length perturbation curve with 50 digitized data points for each perturbation cycle of 100 ms that consisted of a quick length transient (elastic response) completed in <10 ms and a slower shortening phase due to the contraction of the contractile element (CE). The 10-Hz perturbation frequency enabled us to make measurements of $\Delta P/\Delta L$ 20 times/s. For smooth muscle, because of the relatively long time course of contraction, this perturbation frequency was adequate to give a "continuous" function of the SEC stiffness with respect to time. Stiffness of the SEC was obtained by dividing the ΔP by the corresponding ΔL. The compliance of the thread and the lever system was taken into account when measuring the SEC length. When the muscle was at or near l_o, the compliance of the measuring system was much less than that of the muscle itself (<8%). But as the muscle shortened, the stiffness increased and a relatively larger proportion of the measured compliance was from the measuring system. At the peak of contraction (Fig. 1A), about one-third of the ΔL was contributed by the measuring system. Therefore, it was very important that we accurately measured the compliance of the lever and the connecting thread after each experiment.

Our previous study (23) has shown that the SEC stiffness is time dependent. To eliminate the time variable and address oneself purely to the effect of length on stiffness, we obtained the stress-strain curve for SEC at four different muscle lengths. All the curves were obtained by quick releasing and quick stretching the muscle at 10 s after contraction (Fig. 2). In an isometric contraction of canine tracheal smooth muscle, it takes ~10 s for the muscle to reach P_o. The muscle length, just before the load clamps, was controlled by the isotonic load. A lighter load would allow the muscle to shorten more before the load clamp came on and vice versa. The length transients were critically damped. The damping was provided to the lever system electronically by differentiating and inverting the displacement signal and adding this negative velocity signal to the original displacement signal through an adjustable resistor that controlled the degree of damping. The amount of rapid elastic length response after quick release or quick stretch was taken as the change in the length of the undamped SEC. The SEC length was measured by drawing a tangent line over the displacement curve 100 ms after the onset of load clamps as shown in Fig. 2. The

SEC length under zero load was arbitrarily defined as zero. For quick release, the extension of the SEC under a given afterload was determined by subtracting the length of the elastic recoil under the afterload from that obtained with zero afterload. For quick stretch, the extension of the SEC under a given afterload was determined by adding the length of the elastic length transient under the afterload to the length of the elastic recoil obtained with zero afterload. The same method was used by Herlihy and Murphy (11), except that in their experiment quick stretch was not employed. The load clamp was controlled by a digital timer that triggered the release or stretch of the muscle at a preset time. The timer also controlled the onset and duration of stimulation of muscle.

The P_o was used to evaluate deterioration of the muscle during experiment. If P_o changed by >10% from beginning to end of experiment, then the experimental results were discarded. Data were obtained in random fashion with respect to load and muscle length.

Studies (1, 11, 23, 25, 31) including the present one have shown that stiffness of SEC is linearly related to load and can be conveniently represented by a linear equation

$$d\sigma/d\epsilon = E_o + A\sigma \qquad (1)$$

where σ is the stress in muscle, ϵ is the strain of the SEC (normalized to l_o), $d\sigma/d\epsilon$ is the stiffness, E_o is the initial elastic modulus, and A is the slope of the linear stiffness-stress curve. By arbitrarily defining that $\epsilon = 0$ when $\sigma = 0$, $Eq. 1$ can be integrated to give

$$\sigma = (E_o/A)(e^{A\epsilon} - 1) \qquad (2)$$

$Equation$ 2 describes the stress-strain relations of the SEC, and it was used in this study to fit the experimental data. The computer was used to perform the two-dimensional (A, E_o) search for the minimum deviation of the experimental data from the curve described by $Eq.$ 2. In our previous study (23), linear, parabolic, and exponential functions were used to fit the SEC stress-strain data. The exponential function ($Eq.$ 2) was chosen because it gave the best fit. In this study, the exponential equation was chosen for the same reason.

RESULTS

The experiments were divided into two groups. One measured the stiffness change during an isotonic contraction and relaxation using the force perturbation technique. The other measured the stiffness change with respect to muscle length by obtaining the stress-strain curves of the SEC at different muscle lengths 10 s after onset of stimulation. For the first group of data, the mean values ($n = 5$) of the muscle length and the SEC stiffness as functions of time are plotted in Figs. 3 and 4. Figure 3 shows the functions during contraction, whereas Fig. 4 shows the functions during relaxation. The data for displacement were obtained from raw data such as the ones shown in Fig. 1. Displacement of muscle at a particular point in time was taken as the mean value of the upper and lower limits of the amplitude of the length perturbation curve at that time. Muscle length
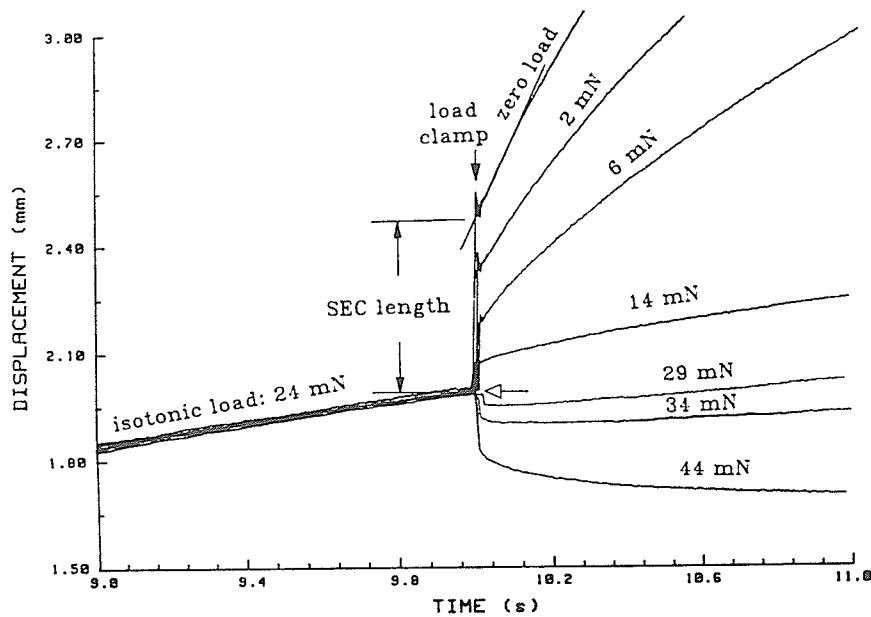
FIG. 2. Experimental records from which the SEC length of muscle under various afterloads were obtained. Apparent SEC length revealed by quickly releasing muscle from isotonic load (24 mN) to zero load was labeled on the curve as an example. Compliance of the measuring system (thread and lever) was subtracted from the apparent SEC length to give true SEC length of muscle. Muscle length just before onset of load clamping indicated by *arrow* was obtained by subtracting muscle displacement (read from y-axis) from l_o. Muscle length just before onset of load clamping (10 s) was controlled by isotonic load. See text for more details and definitions.
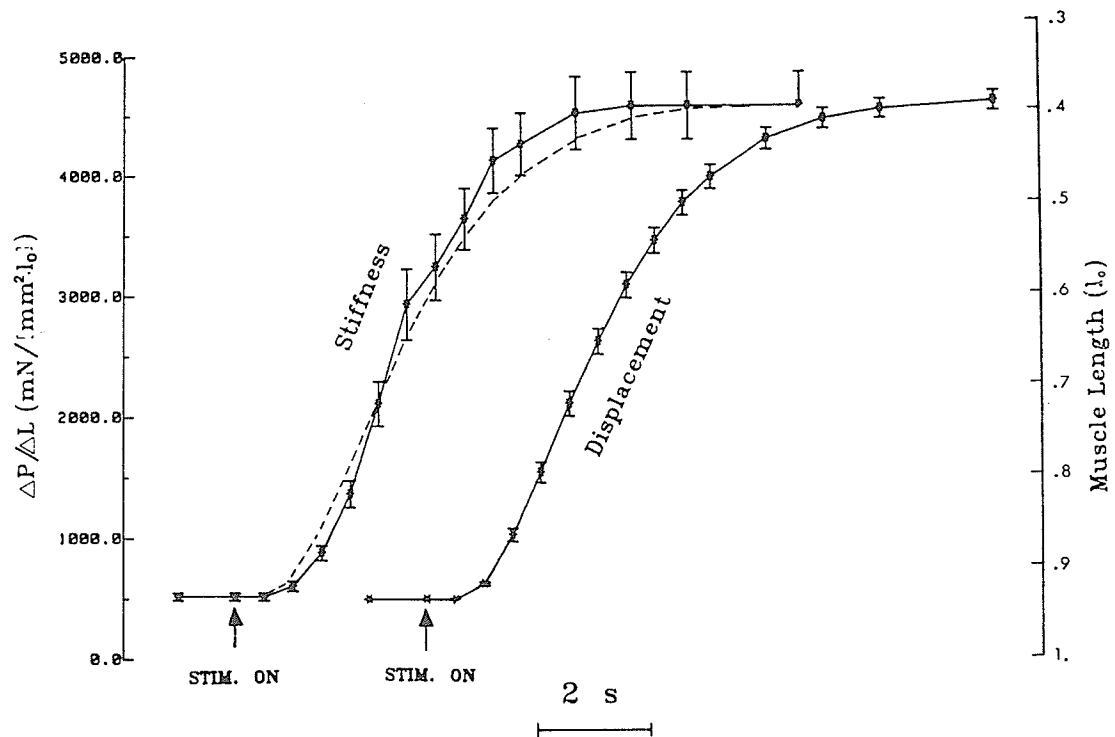

FIG. 3. Series elastic component (SEC) stiffness and displacement (shortening) of muscle as functions of time. Standard error bars are shown on curves ($n = 5$). If displacement curve was shifted so that time of onset of stimulation superimposes that of stiffness curve, displacement curve would occupy position indicated by dashed line. $\Delta P/\Delta L$, stiffness estimated by force perturbation method. Shortening is indicated in upward direction.

was calculated by subtracting the amount of displacement from l_o. Stiffness at a particular point in time was obtained by dividing the ΔP, which remained the same throughout contraction (Fig. 1), by the corresponding ΔL at that time. During contraction, stiffness increased as the muscle shortened (Fig. 3). During relaxation, the decrease in stiffness preceded that of muscle shortening and also stiffness decreased as the muscle lengthened (Fig. 4).

For the second group of data, the SEC stiffness was obtained by measuring the slope of the SECs stress-strain curves (Fig. 5). The curves were obtained from
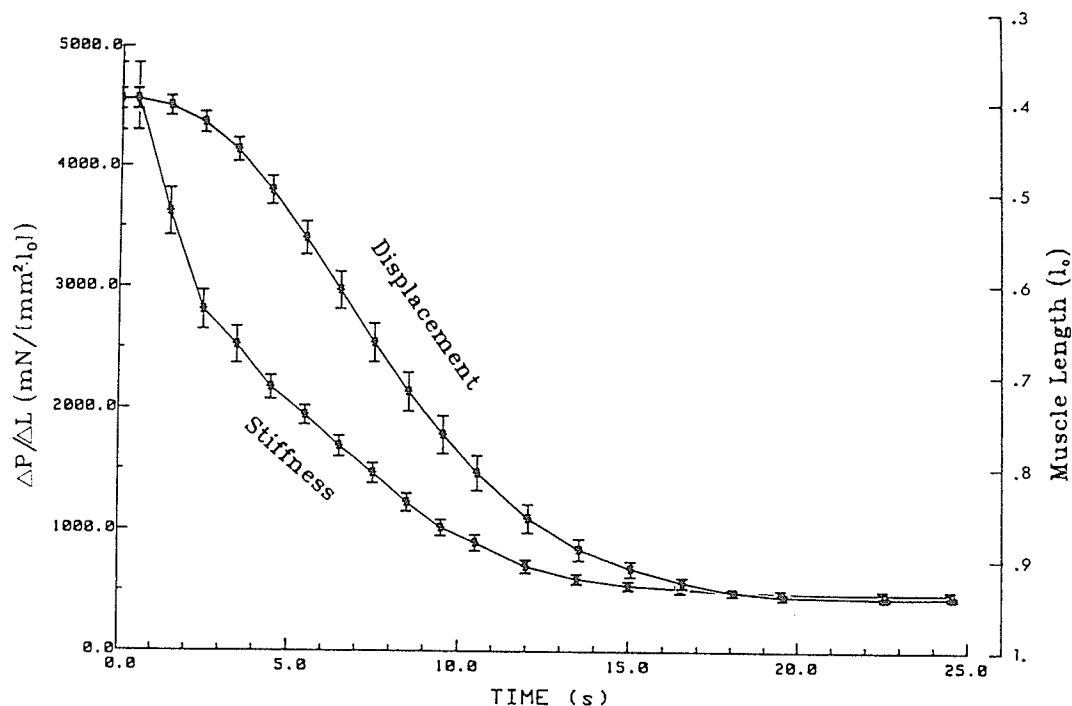
FIG. 4. SEC stiffness and displacement (lengthening) of muscle as functions of time. Termination of stimulation for both curves occurs at *time 0*. Standard error bars are shown ($n = 5$).

raw data such as the ones shown in Fig. 2. Because the stress-strain curves were not linear, the stiffness was stress (or strain) dependent. A stress level of 5% P_o was chosen for calculating the stiffness (Fig. 6) for the stiffness to be comparable to that in the first group of data.

In the first group, the stiffness was estimated by applying a force perturbation varying from 0 to 10% of P_o. Five percent P_o was the mean value of the force perturbation amplitude. The "constant-stress stiffness" shown in Fig. 6 (solid line) was calculated from *Eq. 1*. The constants A
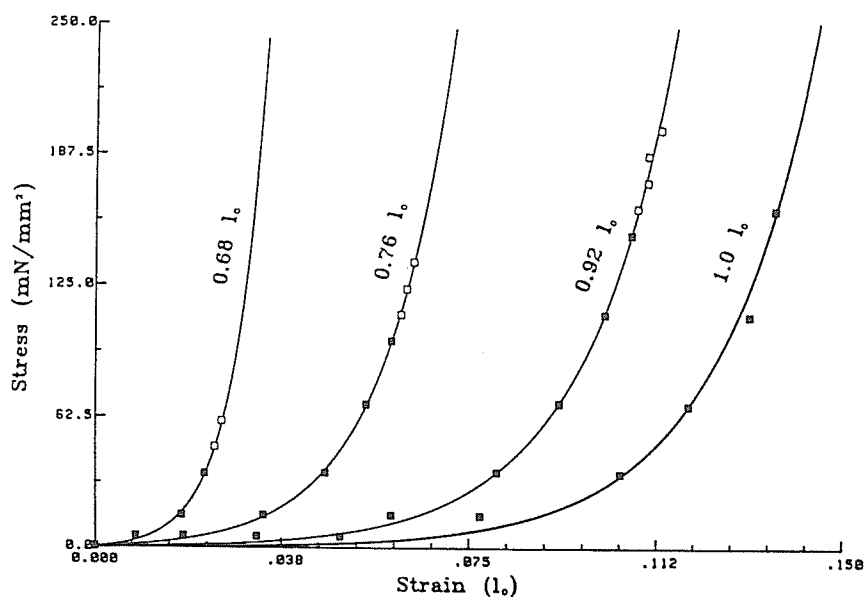
FIG. 5. Stress-strain curve from a single experiment (*expt 2* in Table 1). Muscle lengths at which curves were obtained were labeled on curves. ■, data obtained from quick releases. □, data obtained from quick stretches. Data were fitted by *Eq. 2*. l_o, optimum muscle length.
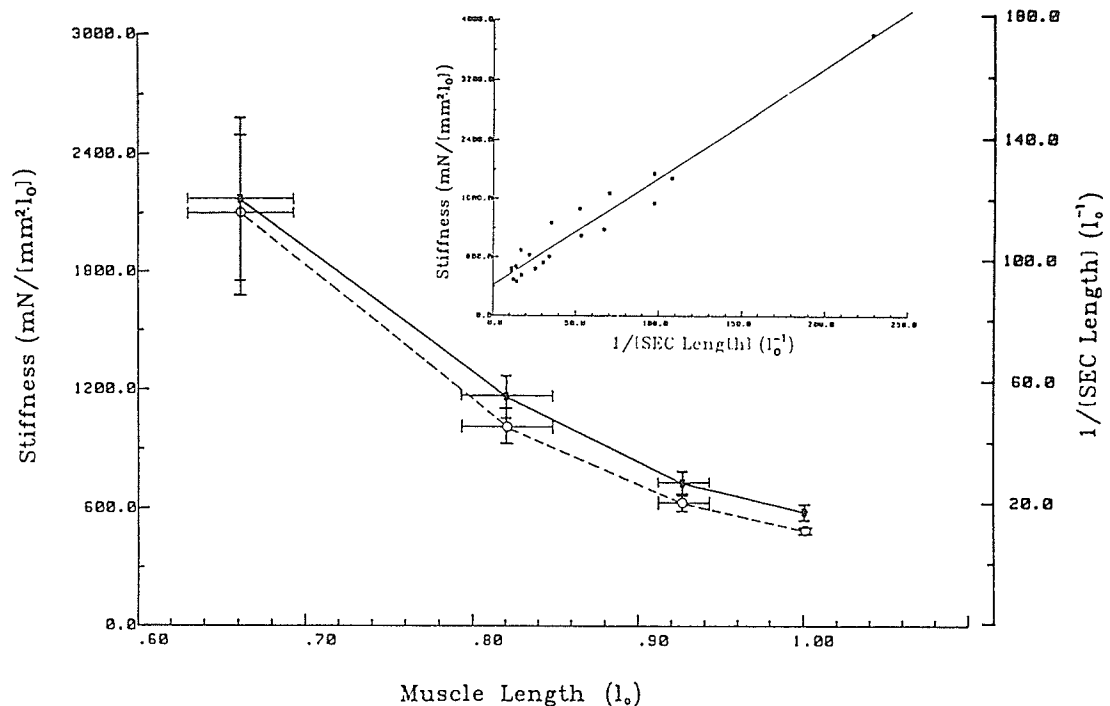
FIG. 6. Constant-stress stiffness (solid line) and 1/[SEC length] (dashed line) as functions of muscle length obtained 10 s after onset of stimulation. Correlation of stiffness and reciprocal of SEC length is shown in *inset.* Correlation coefficient (r) is 0.945. Standard error bars are shown ($n = 5$). See text for definitions.

and E_o were obtained by curve fitting. The σ was set to equal 5% P_o. If different values for σ were used to calculate the stiffness, the stiffness vs. length curve (Fig. 6) would remain basically the same shape but shift up or down (without rotation) depending on the value of σ used. The constant-stress stiffness could also be obtained by drawing a tangent line over the stress-strain curve at the 5% P_o stress level and measuring the slope of the tangent line.

The relationship between constant-stress stiffness and the SEC length (L) was examined by plotting the reciprocal of the SEC length against the stiffness. The SEC lengths were obtained by measuring the amount of strain at 5% P_o from data such as the ones shown in Fig. 5. Assuming that the increase in SEC stiffness at short muscle length was due to a decrease in the SEC length itself, then, when other variables such as stress and time were held constant, the reduction of the SEC length during shortening should linearly relate to the increase in the apparent stiffness. In other words, $d\sigma/d\epsilon$ is inversely proportional to L. Figure 6, *inset,* shows that stiffness and $1/L$ (1/[SEC length]) are linearly related. The reciprocal of SEC length was also plotted as a function of muscle length (l) in Fig. 6 (dashed line). Values of stiffness and $1/L$ varied with muscle length in a very similar fashion.

Figure 7 shows the change in stiffness during isotonic contraction and relaxation, as a function of muscle length (solid line). The curves were obtained from data shown in Figs. 3 and 4. Note that the time variable was not held constant. Therefore, part of the changes in stiffness was due to time variation, which could be related to the

variation of the number of attached cross bridges. The stiffness vs. muscle length curve shown in Fig. 6 was redrawn in Fig. 7 (dashed line) for purpose of comparison. Note that the dashed line was obtained with time variable held constant.

Table 1 summarizes the results from the second group of data. It lists, for each experiment, the values of P_o, muscle lengths, and the corresponding SEC lengths (at 5% P_o), constants A, E_o (from *Eq. 1*), and the coefficients of determination (r^2) for curve fitting (for obtaining A and E_o), the correlation coefficients for E_o and 1/[SEC length] values. The values of A and E_o associated with each of the four muscle lengths were significantly different from one another ($P < 0.05$) according to the paired t test.

DISCUSSION

The main finding in this study was that the SEC stiffness of canine tracheal smooth muscle increased as muscle length decreased. The increase in stiffness was not likely due to an increase in the number of attached cross bridges because no evidence has been found in either smooth or striated muscle to indicate that the number of attached cross bridges increased as muscle shortens below l_o. On the contrary, evidences gathered from length-tension studies (4, 7, 21, 26) indicated that tension decreased at short muscle lengths, suggesting that the number of attached cross bridges decreased when muscle shortened below its optimum length.

One possible explanation for the observed increase in stiffness at short lengths is that the part of the muscle
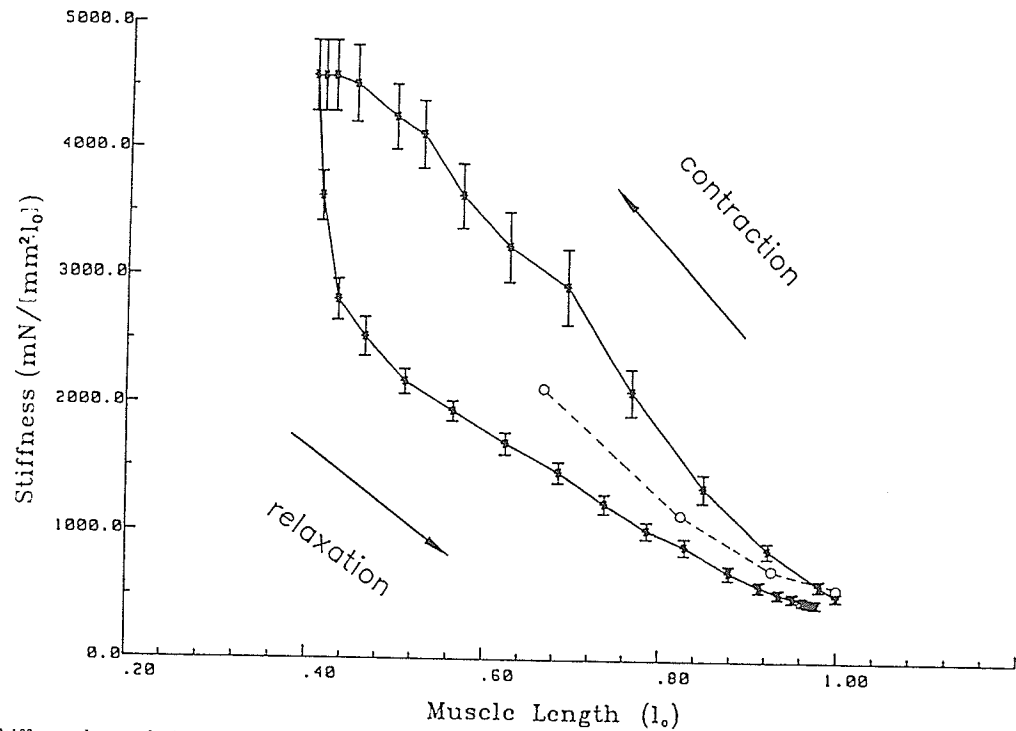
FIG. 7. Stiffness change during isotonic contraction and relaxation as a function of muscle length (solid line). *Upper curve* was obtained during contraction, and *lower curve* was obtained during relaxation. Standard error bars are shown ($n = 5$). Dashed line is stiffness vs. muscle length curve redrawn from Fig. 6 for purpose of comparison. Note that dashed line was obtained with time variable held constant.

TABLE 1. *Stress-strain relations of SEC obtained by quick releasing and quick stretching muscle at four different muscle lengths*

	Expt					Mean±SE
	1	*2*	*3*	*4*	*5*	
P_o, mN/mm^2	223	181	235	197	208	208±9.5
l_{muscle}, l_o	0.54	0.682	0.67	0.706	0.709	0.661±0.031
l_{SEC}, l_o	0.0093	0.0103	0.0044	0.0143	0.0103	0.0097±0.0016
A, l_o^{-1}	104	122	175	150	145	139.2±12.2
E_o, mN/mm$^{-2}\cdot l_o$	707.2	439.2	1750	195.0	435.0	705±273.5
r^2	0.9920	0.9990	0.9608	0.9978	0.9944	0.9888±0.0071
l_{muscle}, l_o	0.747	0.76	0.847	0.873	0.875	0.820±0.028
l_{SEC}, l_o	0.0191	0.0150	0.0282	0.0291	0.0188	0.0220±0.0028
A, l_o^{-1}	115	98	102	71.5	82.5	93.8±7.6
E_o, mN$\cdot$mm$^{-2}\cdot l_o^{-1}$	161	264.16	71.4	100.1	231.0	165.6±36.9
r^2	0.9988	0.9916	0.9676	0.9988	0.9984	0.9910±0.0060
l_{muscle}, l_o	0.87	0.92	0.94	0.94	0.96	0.926±0.015
l_{SEC}, l_o	0.0450	0.0386	0.0583	0.0572	0.0326	0.0463±0.0051
A, l_o^{-1}	70	65	75	53	59.5	64.5±3.86
E_o, mN$\cdot$mm$^{-2}\cdot l_o^{-1}$	35	52	11.3	26.5	104.1	45.8±16.0
r^2	0.9888	0.9966	0.9948	0.9976	0.9984	0.9952±0.0017
l_{muscle}, l_o	1.0	1.0	1.0	1.0	1.0	1.0±0.0
l_{SEC}, l_o	0.0875	0.0688	0.0874	0.0799	0.0715	0.0790±0.004
A, l_o^{-1}	54	50	54.5	49	50	51.5±1.1
E_o, mN$\cdot$mm$^{-1}\cdot l_o^{-1}$	5.4	15	5.5	9.8	15	10.1±2.1
r^2	0.9996	0.9988	0.9896	0.9928	0.9982	0.9958±0.0020
r (E_o, $1/l_{SEC}$)	0.9786	0.9984	0.9979	0.9932	0.9989	0.9934±0.0040

P_o, maximum isometric tension; l_o, optimum muscle length; l_{muscle}, muscle length measured in l_o; l_{SEC}, series elastic component (SEC) length measured in l_o; A and E_o, constants from fitting stress-strain curve of SEC (*Eq. 2*), measured in l_o^{-1} and mN$\cdot$mm$^{-1}\cdot l_o^{-1}$, respectively; r^2, coefficient of determination for fitting SEC stress-strain curve (for obtaining A, E_o values); r (E_o, $1/l_{SEC}$), correlation coefficient of E_o and $1/l_{SEC}$ values.

structure that constitutes the SEC becomes shorter when muscle shortens. The ultrastructure of smooth muscle is not as well revealed as that for skeletal muscle. However, it is generally believed that the sliding filament mechanism also is responsible for smooth muscle contraction (24). This implies the existence of overlap (between thick and thin filaments) and nonoverlap zones in smooth muscle. Could this nonoverlap be part of the SEC in smooth muscle? Compared with smooth muscle, the nonoverlap zones in skeletal muscle seem to contribute little to the series compliance (1, 9, 15). The SEC of skeletal muscle is also stiffer than that of smooth muscle. The SEC length at P_o for various types of smooth muscle varies somewhere from 7 to 20% of the l_o (11, 14, 18), whereas in skeletal muscle, it is <1% (29, 32). Also the thin-to-thick filament ratio for smooth muscle is much greater than that for skeletal muscle (24, 32). For example, the ratio is ~15:1 in rabbit portal vein compared with the ratio of 2:1 in frog sartorius. It is possible that a significant part of the series compliance in smooth muscle is of noncross-bridge origin, unlike that in skeletal muscle.

Theoretical relationship between the various sources of series compliance and the apparent muscle stiffness was well described by Ford et al. (9) for striated muscle. The description is probably valid for smooth muscle if one insists that the sliding-filament, cycling-cross-bridge mechanism is responsible for smooth muscle contraction. At $l < l_o$, the extensibility of the thin filament is critical in determining the behavior of the apparent muscle stiffness with respect to length. If we assume that the nonoverlap portion of the thin filaments contributes to the series compliance of the muscle, then as the muscle shortens, an apparent increase in muscle stiffness would be observed due to the diminution of the nonoverlap portion. A shorter SEC will produce a smaller length response when it is subjected to a constant load step. In other words, the ΔL due to a constant load step is directly proportional to the L itself. It follows that muscle stiffness must be inversely proportional to the SEC length. Our experiments (Fig. 6) showed that indeed stiffness and 1/[SEC length] are highly correlated ($r = 0.945$). This suggests that in canine trachealis, the increase in SEC stiffness may be due to a decrease in SEC length itself, and the decrease in SEC length may be associated with the diminution of the nonoverlap zones during contraction.

Additional evidence supporting the notion that the increase in muscle stiffness was due to the nonoverlap portion of the thin filaments comes from the observation that the E_o increased as the muscle length decreased or as the nonoverlap portion diminished. Table 1 shows that E_o and $1/L$ values have a very high correlation coefficient ($r = 0.9934$). Theoretically, spring stiffness (k) at different spring lengths (under a constant tension) can be expressed as $k(L_o/L)$, where L_o is a reference length at which the k value is obtained, and L is any given length. For example, if $L = 0.5 L_o$, then the spring will appear to be twice as stiff as the spring with length L_o. The muscle's SEC can be regarded as a spring with stiffness characteristics described by Eq. 1 ($k = E_o + A\sigma$). If we assume that the SEC length becomes shorter

as the muscle shortens, as it would in the case when the nonoverlap portion of the thin filaments contribute to series compliance, then the SEC stiffness at different SEC lengths can be expressed as $(E_o + A\sigma)(L_o/L)$, where L_o is defined as the SEC length when the muscle length is l_o, and L is any given SEC length. From the above expression, the initial elastic modulus at short SEC length ($L < L_o$) is: $(E_o)(L_o/L)$. Therefore, if the above assumption regarding the source of the series compliance is true, then the initial elastic modulus should be inversely proportional to the SEC length (L). Our experimental data (Table 1) show that E_o values obtained at different Ls correlates very closely to the $1/L$ values, supporting the above assumption that the nonoverlap portion of the thin filaments constitute part of the muscle's SEC and the SEC length decreases as muscle shortens. Our previous study (23) showed that if muscle length was held constant, then the E_o value stayed constant throughout contraction, although the overall SEC stiffness changed with time during contraction.

Stiffness change during an isotonic contraction can be attributed to at least two variables: time and length. The time effect on stiffness while muscle length and stress were held constant was examined in our previous study (23). Zero load (or near zero load) shortening velocity of smooth muscle (an index of cross-bridge cycling rate) has been shown to vary with time (6, 22). Dillon et al. (6) showed that in vascular smooth muscle, shortening velocity and myosin light chain (LC 20) phosphorylation varied in a similar manner during an isometric contraction. Kamm and Stull (17) showed that stiffness also varied with myosin light-chain phosphorylation during the initial phase of contraction in smooth muscle. These evidences suggest that the number of active cross bridges could vary during the time course of smooth muscle contraction and give rise to the observed change in stiffness (23). The difference between the stiffness vs. length curves shown in Figs. 6 and 7 is that the former was obtained when time variable was fixed, whereas the latter was obtained during an isotonic contraction in which both time and muscle length changed. The difference in values between the two curves can be attributed to the time variable, which could be associated with the variation of the number of attached cross bridges during contraction. Comparing the curves in Figs. 6 and 7, it can be seen that stiffness (at any given length) was greater early in contraction than that at the plateau of contraction (10 s). This is in agreement with our previous finding (23) that stiffness (at a specific stress and muscle length) increased rapidly during contraction, reached the peak in ~2 s after onset of contraction, and then gradually decreased as contraction proceeded. During relaxation, there was a rapid decrease in muscle stiffness shortly after the termination of stimulus, followed by a gradual decrease in stiffness as the muscle lengthened (Fig. 7). Stiffness (at any length) at the plateau of contraction was greater than that during relaxation. This suggests that the number of attached cross bridges was less in a relaxing muscle.

Inactivation is another phenomenon that is associated with muscle shortening (13, 27, 30). Taylor and Rudel (30) observed that myofibrils in the core of frog semiten-

dinosus fibers became "wavy" at short muscle lengths during active shortening and appeared not to contribute to the generation of active tension. Inactivation at short lengths was also observed in tracheal smooth muscle (27). Inactivation is always associated with decrease in isometric tension, which has a positive correlation with stiffness. Therefore, it is highly unlikely that the increase in stiffness at short muscle lengths observed in our experiments (Figs. 6 and 7) could be due to shortening inactivation.

The values of the SEC stiffness measured by the two methods, namely the force perturbation and load clamp methods, are comparable. The force perturbation method measures the stiffness at a single stress level, whereas the load clamp gives the whole stress-strain characteristics of the SEC. The force perturbation only provides a means of estimating the $\Delta P/\Delta L$. By definition, stiffness is the limit of $\Delta P/\Delta L$ when ΔL is infinitesimally small. But, for purposes of this study, stiffness estimated by $\Delta P/\Delta L$ (with a finite ΔL) is accurate enough. In fact, it showed no statistical difference when compared with the stiffness calculated from quick-release method under the same experimental conditions (time, stress) (23).

For the load clamp method, data obtained by quick release and those obtained by quick stretch fall onto the same curve that characterizes the stress-strain relations of the SEC (Fig. 5). The continuity of the data suggest that the behavior of the SEC is independent of the direction of the force applied to it. However, we observed in the experiments that if the afterload was too large when stretching, then the muscle's stiffness would suddenly appear to decrease and the data would start to deviate from the curve. The "yield point" of the SEC occurred when the afterload was about twice as large as the load on muscle before the load clamp. In our experiments, large afterloads were avoided when stretching the muscle. Because large loads could potentially break the cross bridges and cause sliding of the thick and thin filaments in the direction opposite to contraction. Under such circumstance, if the observed "elastic length transient" were taken as the length change of the SEC, then the SEC compliance would be overestimated.

A viscoelastic multisegment model similar to the one used by Sugi and Kobayashi (29) is worth mentioning here. Although the model was developed for skeletal muscle, it was never very popular in the field of skeletal muscle mechanics. This was due to the findings that the cross bridges were the major source of series compliance in skeletal muscle (1, 9, 12). Julian and Morgan (15), however, found that by assuming a small filament compliance, a better fit between the experimental data and the theoretical calculations could be obtained. The usefulness of the model is that it relates the SEC to subcellular structures of the muscle. The model is basically a Voigt model with a length dependent SEC. A Maxwell model can also be used. In using either model, one has to accept that stiffness of the SEC is nonlinear (stress dependent) and, as this study indicated, the SEC was also length dependent for tracheal smooth muscle. The length dependency of the SEC in vascular smooth muscle was also found by Cox (5).

In conclusion, the SEC stiffness of tracheal smooth

muscle increased as muscle length decreased. The increase in SEC stiffness correlated very closely to the decrease in the SEC length itself. This suggested that the diminution of the length of SEC is the cause of the apparent increase in the SEC stiffness.

REFERENCES

1. BRESSLER, B. H., AND N. F. CLINCH. Crossbridges as the major source of compliance in contracting skeletal muscle. *Nature Lond.* 250: 221–222, 1975.
2. BRUTSAERT, D. L., AND V. A. CLAES. Onset of mechanical activation of mammalian heart muscle in calcium and strontium containing solution. *Circ. Res.* 35: 345–347, 1974.
3. CECCHI, G., P. J. GRIFFITHS, AND S. TAYLOR. Muscular contraction: kinetics of crossbridge attachment studied by high frequency stiffness measurements. *Science Wash. DC* 217: 70–72, 1982.
4. CLOSE, R. I. The relations between sarcomere length and characteristics of isometric twitch contractions of frog sartorius muscle. *J. Physiol. Lond.* 220: 745–761, 1972.
5. COX, R. H. Influence of muscle length on series elasticity in arterial smooth muscle. *Am. J. Physiol.* 234 (*Cell Physiol.* 3): C146–C154, 1978.
6. DILLON, P. F., M. O. AKSOY, S. P. DRISKA, AND R. A. MURPHY. Myosin phosphorylation and the crossbridge cycle in arterial smooth muscle. *Science Wash. DC* 211: 495–497, 1981.
7. EDMAN, K. A. P. The relation between sarcomere length and active tension in isolated semitendinosus fibres of the frog. *J. Physiol. Lond.* 183: 407–417, 1966.
8. FORD, L. E., A. F. HUXLEY, AND R. M. SIMMONS. Tension transients during the rise of tetanic tension in frog muscle fibre. *J. Physiol. Lond.* 372: 595–609, 1986.
9. FORD, L. E., A. F. HUXLEY, AND R. M. SIMMONS. The relation between stiffness and filament overlap in stimulated frog muscle fibres. *J. Physiol. Lond.* 311: 219–249, 1981.
10. HELLSTRAND, P., AND B. JOHANSSON. Analysis and the length response to a force step in smooth muscle from rabbit urinary bladder. *Acta Physiol. Scand.* 106: 219–249, 1979.
11. HERLIHY, J. T., AND R. A. MURPHY. Force-velocity and series elastic characteristics of smooth muscle from the hog carotid artery. *Circ. Res.* 34: 461–466, 1974.
12. HUXLEY, A. F., AND R. A. SIMMONS. Mechanical properties of the crossbridges of frog striated muscle. *J. Physiol. Lond.* 218: 59–60P, 1971.
13. JEWELL, B. R., AND J. R. BLINKS. Drugs and the mechanical properties of heart muscle. *Annu. Rev. Pharmacol.* 8: 113–130, 1968.
14. JOHANSSON, B. Active state in the smooth muscle of the rat portal vein in relation to electrical activity and isometric force. *Circ. Res.* 32: 246–257, 1973.
15. JULIAN, F. J., AND D. L. MORGAN. Tension, stiffness, unloaded shortening speed and potentiation of frog muscle fibres at sarcomere lengths below optimum. *J. Physiol. Lond.* 319: 205–217, 1981.
16. JULIAN, F. J., AND M. R. SOLLINS. Variation of muscle stiffness with force at increasing speeds of shortening. *J. Gen. Physiol.* 66: 287–302, 1975.
17. KAMM, E. K., AND J. T. STULL. Activation of smooth muscle contraction: relation between myosin phosphorylation and stiffness. *Science Wash. DC* 232: 80–82, 1986.
18. LUNDHOLM, L., AND E. MOHME-LUNDHOLM. Length at inactivated contractile elements, length-tension diagram, active state and tone of vascular smooth muscle. *Acta Physiol. Scand.* 68: 347–359, 1966.
19. MEISS, R. A. Dynamic stiffness of rabbit mesotubarium smooth muscle: effect of isometric length. *Am. J. Physiol.* 234 (*Cell Physiol.* 3): C14–C26, 1978.
20. MULVANY, M. J., AND D. M. WARSHAW. The anatomical location of the series elastic component in rat vascular smooth muscle. *J. Physiol. Lond.* 314: 321–330, 1981.

21. RAMSEY, R. W., AND S. F. STREET. The isometric length-tension diagram of isolated skeletal fibres of the frog. *J. Cell Comp. Physiol.* 15: 11–34, 1940.

22. SEOW, C. Y., AND N. L. STEPHENS. Force-velocity curves for smooth muscle: analysis of internal factors reducing velocity. *Am. J. Physiol.* 251 (*Cell Physiol.* 20): C362–C368, 1986.

23. SEOW, C. Y., AND N. L. STEPHENS. Time dependence of series elasticity in tracheal smooth muscle. *J. Appl. Physiol.* 62: 1556–1561, 1987.

24. SOMLYO, A. V., M. BOND, P. F. BERNER, F. T. ASHTON, H. HOLTZER, AND A. P. SOMLYO. The contractile apparatus of smooth muscle: an update. In: *Smooth Muscle Contraction*, edited by N. L. Stephens. New York: Dekker, 1984, p. 1–20.

25. STEPHENS, N. L., E. A. KROEGER, AND J. A. MEHTA. Force-velocity characterization of respiratory airway smooth muscle. *J. Appl. Physiol.* 26: 685–692, 1969.

26. STEPHENS, N. L., AND U. KROMER. Series elastic component of tracheal smooth muscle. *Am. J. Physiol.* 220: 1890–1895, 1971.

27. STEPHENS, N. L., R. W. MITCHELL, AND D. L. BRUTSAERT. Shortening inactivation, maximum force potential, relaxation, contractility. In: *Smooth Muscle Contraction*, edited by N. L. Stephens. New York: Dekker, 1984, p. 91–112.

28. SUGI, H., AND T. KOBAYASHI. Sarcomere length and force changes in single tetanized frog muscle fibres following quick changes in fibre length. In: *Contractile Mechanisms in Muscle*, edited by G. H. Pollack and H. Sugi. New York: Plenum, 1984, p. 623–635.

29. SUGI, H., AND S. SUZUKI. Extensibility of the myofilaments in vertebrate skeletal muscle as studied by stretching rigor muscle fibres. *Proc. Jpn. Acad.* B56: 290–293, 1980.

30. TAYLOR, S. R., AND R. RUDEL. Striated muscle fibres: inactivation of contraction induced by shortening. *Science Wash. DC* 167: 882–884, 1970.

31. WARSHAW, D. J., AND F. S. FAY. Crossbridge elasticity in single smooth muscle cells. *J. Gen. Physiol.* 82: 157–199, 1983.

32. WOLEDGE, R. C., N. A. CURTIN, AND E. HOMSHER. *Energetic Aspects of Muscle Contraction.* London: Academic, 1985, p. 1–26.

THE UNIVERSITY OF MANITOBA

FACULTY OF MEDICINE
Department of Physiology

770 Bannatyne Avenue
Winnipeg, Manitoba
Canada R3E 0W3

Tel: (204) 788-6696
FAX: (204) 774-9517

**Ph# (204) 788-6526
FAX (204) 783-2788**

February 28, 1991

Ms Helen Agar
500K University Center

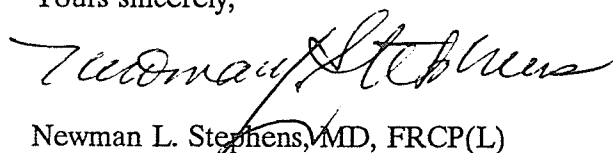<u>re: PhD (Physiology) Thesis of Dr. Chun Y Seow</u>

Dear Ms Agar:

This is written to permit Dr. Seow to use in his thesis papers published under our cojoint authorship. These are as follows:

1. Antonissen LA, RW Mitchell, EA Kroeger, W Kepron, KS Tse and NL Stephens. J Appl Physiol 46:681-687,1979.

2. Kroeger EA and NL Stephens. Am J Physiol 228(2): 633-636, 1975.

3. Packer CS and NL Stephens. Can J Physiol Pharmacol 63: 669-674, 1985.

4. Seow CY and NL Stephens. AM J Physiol 251 (Cell Physiol 20): C362-368, 1986.

5. Seow CY and NL Stephens. J Appl Physiol 62(4):1556-1561,1987.

6. Seow CY and NL Stephens. J Appl Physiol 64(5): 2053-2057, 1988.

7. Seow CY and NL Stephens. Am J Physiol 256 (Cell Physiol 25):C341-C350,1989.

8. NL Stephens. In: <u>Airway Dynamics: Physiology and Pharmacology.</u> Ed. A Boritruys, Springfield, IL: Thomas, 191-208, 1970.

9. Stephens Nl, U Kromer. Am J Physiol 220:1890-1895, 1971.

...2

10. Stephens NL, EA Kroeger, U Kromer. Am J Physiol 228(2):628-632, 1975.

11. Stephens NL, EA Kroeger, JA Mehta. J Appl Physiol 26:685-692, 1969.

12. Stephens NL, RW Mitchell, DL Brutsaert. In: Smooth Muscle Contraction. Ed: NL Stephens, Publ. M. Dekker, NY, pp 91-112, 1984.

13. Stephens NL and CM Skoog. Am J Physiol 226:1462-1467, 1974.

Yours sincerely,

Newman L. Stephens, MD, FRCP(L)
Professor

NLS/jo